

2

FINAL COPY

NPS-MR-91-001

# NAVAL POSTGRADUATE SCHOOL

Monterey, California

DTIC  
ELECTE  
JAN 17 1991



AD-A231 152

ONR TROPICAL CYCLONE MOTION  
RESEARCH INITIATIVE:  
FIELD EXPERIMENT SUMMARY

Russell L. Elsberry  
B. C. Diehl, J. C.-L. Chan, P. A. Harr,  
G. J. Holland, M. Lander, T. Neta, & D. Thom

November 1990

Interim Report for Period  
October 1989 - September 1990

Approved for public release; distribution is unlimited.

Prepared for:  
Naval Postgraduate School  
Monterey, CA 93943

Chief of Naval Research (Code 1122MM)  
Arlington, VA 22217

Naval Postgraduate School  
Monterey, California 93943-5000

Rear Admiral R. W. West  
Superintendent

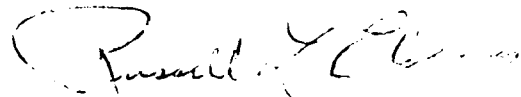
H. Shull  
Provost

The work reported herein was in support of the Accelerated Research Initiative on Tropical Cyclone Motion of the Office of Naval Research (Marine Meteorology). The Chief of Naval Research provided some travel funds to support the attendance of a few participants.

Funding for preparation of the report was provided by the Naval Postgraduate School

Reproduction of all or part of the report is authorized.

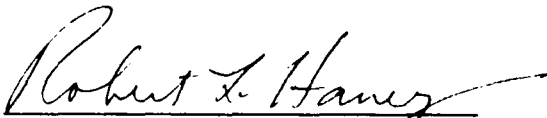
This report was prepared by:



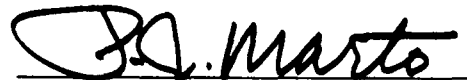
Russell L. Elsberry  
Professor of Meteorology

Reviewed by:

Released by:



Robert L. Haney, Chairman  
Department of Meteorology



Paul J. Marto  
Dean of Research

REPORT DOCUMENTATION PAGE				Form Approved OAI No 0704 0188			
1a REPORT SECURITY CLASSIFICATION UNCLASSIFIED			1b RESTRICTIVE MARKINGS				
2a SECURITY CLASSIFICATION AUTHORITY			3 DISTRIBUTION/AVAILABILITY OF REPORT Approved for public release; distribution is unlimited.				
2b DECLASSIFICATION/DOWNGRADING SCHEDULE							
4 PERFORMING ORGANIZATION REPORT NUMBER(S) NPS-MR-91-001			5 MONITORING ORGANIZATION REPORT NUMBER(S)				
6a NAME OF PERFORMING ORGANIZATION Naval Postgraduate School		6b OFFICE SYMBOL (If applicable) MR		7a NAME OF MONITORING ORGANIZATION Office of Naval Research (Code 1122MM)			
6c ADDRESS (City, State, and ZIP Code) Monterey, CA 93943-5000			7b ADDRESS (City, State, and ZIP Code) Arlington, VA 22217-5000				
8a NAME OF FUNDING/SPONSORING ORGANIZATION Naval Postgraduate School		8b OFFICE SYMBOL (If applicable)		9 PROCUREMENT INSTRUMENT IDENTIFICATION NUMBER O&MN, Direct Funding N0001490WR24005			
8c ADDRESS (City, State, and ZIP Code) Monterey, CA 93943-5000			10 SOURCE OF FUNDING NUMBERS				
			PROGRAM ELEMENT NO 0601153N	PROJECT NO RR033-03-0B	TASK NO	WORK UNIT ACCESSION NO	
11 TITLE (Include Security Classification) ONR TROPICAL CYCLONE MOTION RESEARCH INITIATIVE; FIELD EXPERIMENT SUMMARY (U)							
12 PERSONAL AUTHOR(S) Russell L. Elsberry, B. C. Diehl, J. C.-L. Chan, P. A. Harr, G. J. Holland, M. Lander, T. Neta and D. Thom							
13a TYPE OF REPORT Interim		13b TIME COVERED FROM 89/10 TO 90/09		14 DATE OF REPORT (Year, Month, Day) 1990, November		15 PAGE COUNT 106	
16 SUPPLEMENTARY NOTATION							
17 COSATI CODES			18 SUBJECT TERMS (Continue on reverse if necessary and identify by block number)				
FIELD	GROUP	SUB-GROUP					
19 ABSTRACT (Continue on reverse if necessary and identify by block number) <p>The Office of Naval Research Tropical Cyclone Motion initiative is a five-year program to improve basic understanding of tropical cyclone motion. The Tropical Cyclone Motion (TCM-90) field experiment was carried out during August and September 1990. The first section of this report describes the data management plan for TCM-90, and includes descriptions of the observational systems that provided data in real-time and on a delayed basis. The second section of this report summarizes the seven Intensive Observation Periods during TCM-90. A summary of the real-time data collection also is provided to aid the reader in selecting cases for study. A more complete listing that includes delayed data will be provided about April 1991, when the production of the final analyses will begin.</p>							
20 DISTRIBUTION/AVAILABILITY OF ABSTRACT <input checked="" type="checkbox"/> UNCLASSIFIED/UNLIMITED <input type="checkbox"/> SAME AS RPT <input type="checkbox"/> DTIC USERS				21 ABSTRACT SECURITY CLASSIFICATION UNCLASSIFIED			
22a NAME OF RESPONSIBLE INDIVIDUAL Russell L. Elsberry			22b TELEPHONE (Include Area Code) (408) 646-2373		22c OFFICE SYMBOL MR		

## Table of Contents

Introduction	1
I. Data Management Plan	3
1.1 Data Management Strategy	3
1.2 Real-time Data Management	5
1.2.1 Real-time Data Collection	5
1.2.2 Delayed Data Collection	5
1.3 Data Collections, Quality Assurance, Archival and Distribution	8
a. SPECTRUM-90	8
b. TYPHOON-90	8
c. TCM-90	8
d. Final Analyses	9
e. Data Exchanges	10
1.4 Data Programs	10
1.4.1 Aircraft Data Program	10
1.4.2 Rawinsonde Program	10
a. Regular Sites	11
b. Special Sites	11
c. Aircraft	11
1.4.3 Radar Wind Profilers	16
1.4.4 Buoys	16
1.4.5 Doppler Radar	16
1.4.6 Satellites	20
1.5 Data Streams	20
1.6 Data Sets and Products	20
1.6.1 Experiment Operations Center Products	27
1.6.2 Data Users Guide	27
1.7 Data Users/Organizations	27
II. Intensive Observation Period (IOP) Summaries	29
IOP 1 Typhoon Winona	32
IOP 2 and IOP 3 Typhoon Yancy	45
IOP 3 Typhoon Zola	56
IOP 4 Typhoon Dot	63
IOP 5 Typhoon Ed	76
IOP 5, 6 and 7 Typhoon Flo	91
References	106
Distribution List	107

Approved For	↓
DATE	
BY	
TITLE	
B.	
D. T. NO.	
A-1	

## List of Figures

- Figure 1.1 Data management plan for the TCM-90 experiment.
- Figure 1.2 Real-time and delayed data collection for TCM-90. The acronyms beginning with ADPxxx refer to specific data files at Fleet Numerical Oceanography Center. Programs at FNOC are separated according to whether they are executed on the vector processor (CYBER 205) or the front-end computers that provide input or receive outputs from the CYBER 205.
- Figure 1.3 Upper-air network of TCM-90 and concurrent experiments. Regular rawinsonde stations with 12-hourly soundings are indicated by small circles. The large circles, squares and triangles represent the special rawinsonde stations with soundings at 06 and 18 UTC for SPECTRUM, U.S. and Taiwan stations, respectively. The ship symbols show the fixed positions of the participating ships.
- Figure 1.4 Aircraft data stream.
- Figure 1.5 Regular and special site upper-air data stream.
- Figure 1.6 Radar wind profiler data stream.
- Figure 1.7 Drifting buoy data stream.
- Figure 1.8 Satellite data stream.
- Figure 1.9 TCM-90 project operations overview.
- Figure 2.1 Working best track of Typhoon Winona (12W) from 00 UTC 4 August to 18 UTC 11 August 1990. Positions at 6-h intervals are shown for the tropical depression (circles), tropical storm (open cyclone symbols) and typhoon (closed cyclone symbols). The labels indicate day and hour (Z), the translation speed (kt) and maximum wind speed (kt).
- Figure 2.2 Streamlines at 200 mb at 00 UTC 7 August with TD 12W (Winona) near 27°N, 134°E and TS Vernon 34°N, 144°E.
- Figure 2.3 FNOC 500 mb wind (kt) and height (5xxx m) analysis at 00 UTC 7 August.
- Figure 2.4 500 mb wind and height analysis at 00 UTC 8 August with TS Winona near 26°N, 137°E.
- Figure 2.5 Streamline analysis at 200 mb at 00 UTC 8 August.
- Figure 2.6 500 mb wind and height analysis at 00 UTC 9 August with severe TS Winona near 30°N, 137°E.
- Figure 2.7 Coverage of upper-air soundings during a regular synoptic time of 00 UTC 9 August.

Figure 2.8 Coverage of upper-air soundings during an off-time period of 06 UTC 9 August.

Figure 3.1 Working best track of Typhoon Yancy from 00 UTC 11 August to 00 UTC 22 August. Symbols are the same as in Figure 2.1.

Figure 3.2a Streamline analyses for 00 UTC 14 August at the gradient level. Winds of greater than  $15 \text{ m s}^{-1}$  are stippled.

Figure 3.2b Streamline analyses for 00 UTC 14 August at 200 mb.

Figure 3.3 Mean sea level pressure (mb) analysis by M. Lander for 00 UTC 19 August that indicates the large horizontal extent of Typhoon Yancy and the trailing circulation that would become Typhoon Zola.

Figure 3.4 NOGAPS 500 mb analysis for 12 UTC 16 August that indicates the midlatitude short-wave trough and the break in the subtropical ridge. Heights are in decameters and each full wind barb is  $10 \text{ kt}$  ( $5 \text{ m s}^{-1}$ ).

Figure 4.1 Working best track of Typhoon Zola between 06 UTC 15 August and 00 UTC 23 August. Symbols are the same as in Figure 2.1.

Figure 5.1 Working best track of typhoon Dot between 12 UTC 2 September and 18 UTC 7 September. Symbols are the same as in Figure 2.1.

Figure 5.2a Streamline analyses for 00 UTC 3 September at the gradient level. Winds of greater than  $15 \text{ m s}^{-1}$  are stippled.

Figure 5.2b Streamline analysis for 00 UTC 3 September at 200 mb.

Figure 5.3a Streamline analyses for 00 UTC 7 September at the gradient level. Winds of greater than  $15 \text{ m s}^{-1}$  are stippled.

Figure 5.3b Streamline analysis for 00 UTC 7 September at 200 mb.

Figure 5.4a Analysis of the 500 mb winds and geopotential height fields (88 represents 5880 m) for 00 UTC on 3 September.

Figure 5.4b Analysis at 500 mb and geopotential height fields (88 represents 5880 m) for 00 UTC 5 September.

Figure 5.4c Analysis of 500 mb and geopotential height fields (88 represents 5880 m) for 00 UTC 7 September.

Figure 6.1 Working best track of Typhoon Ed between 12 UTC 6 September and 00 UTC 20 September. Symbols are the same as in Figure 2.1.

Figure 6.2 Schematic of the evolution of a supercluster of mesoscale convective systems (panel A), the subsequent collapse 24 h later (panel B) and the area of convection that was to become Typhoon Ed (panel C).

Figure 6.3 Schematic illustration of the wind flow (arrows) and Cb elements relative to the surface low pressure center in the early stages (10 September) of Typhoon Ed.

Figure 6.4 Low-level cloud arcs in visible satellite imagery on 11 September. Displacements of these arcs between images are an indication of the wind speeds.

Figure 6.5 Visible satellite imagery at 2332 UTC 13 September with ragged banding around formative eye of Tropical Storm Ed.

Figure 6.6 Schematic of surface pressure (thin lines) features when Typhoon Ed, TD 20 (pre-Flo) and a monsoon depression co-existed within a large monsoon trough with monsoon gales along the southern boundary (long arrow). The subtropical ridge (zig-zag line) extended to the west during this period.

Figure 6.7 (a) Relative motion of tropical cyclones Ed and Flo with respect to the midpoint between the cyclones. Large dots indicate 00 UTC positions and small dots indicate intermediate 6-h intervals. (b) Orbital rate at rotation (degrees per h) with respect to the midpoint.

Figure 7.1 Working best track of Supertyphoon Flo between 12 UTC 10 September and 06 UTC 20 September. Symbols are the same as in Fig. 2.1.

Figure 7.2a Streamline analyses for 00 UTC 12 September at the gradient level. Winds of greater than  $15 \text{ m s}^{-1}$  are stippled.

Figure 7.2b Streamline analysis for 00 UTC 12 September at 200 mb.

Figure 7.3 Composite analysis for the 36 h beginning at 12 UTC 13 September. Gradient-level winds greater than  $15 \text{ m s}^{-1}$  are stippled and those greater than  $25 \text{ m s}^{-1}$  are hatched.

Figure 7.4a Streamline analyses for 00 UTC 17 September at the gradient level. Winds of greater than  $15 \text{ m s}^{-1}$  are stippled.

Figure 7.4b Streamline analysis for 00 UTC 17 September at 200 mb.

## List of Tables

Table 1.1 TCM-90 aircraft, dropwindsondes and responsible agencies.

Table 1.2 Frequency of upper-air soundings transmitted by each of the instrument platforms for non-IOP and IOP periods.

Table 1.3 Upper-air sounding sites with special 06 and 18 UTC soundings during Intensive Observing Periods of one of the international field experiments.

Table 1.4 Radar wind profiler data sources during the international field experiments.

Table 1.5 Latitude and longitude positions for the drifting and fixed buoys available during the TCM-90 experiment.

Table 1.6 Characteristics of the MRI Doppler radar on Okinawa.

Table 1.7 Characteristics of the Taiwan Doppler radar.

Table 1.8 TCM-90 participant requested observations

Table 2.1 Upper-air soundings during IOP 1.

Table 3.1 Upper-air soundings during IOP 2.

Table 4.1 Upper-air soundings during IOP 3.

Table 5.1 Upper-air soundings during IOP 4.

Table 6.1 Upper-air soundings during IOP 5.

Table 7.1 Upper-air soundings during IOP 6.

Table 7.2 Upper-air soundings during IOP 7.



## ACKNOWLEDGEMENTS

Sincere thanks and a "well done" are extended to everyone who contributed to TCM-90 and the three coincident field experiments. The success is due ultimately to all the people on tropical islands, ships, airplanes, etc. who made the observations. The supporting staffs who communicated the data, operated the satellites and computers also contributed. The data collection, processing analysis and display of the observations also involved a large number of individuals. Special mention must be made of all the Fleet Numerical Oceanography Center (FNOC) personnel who assisted in the real-time data collection, but especially Commanding Officer CAPT J. Jensen, Leo Clarke, Howard Lewit, Bill Clune and Gail Brown. Nancy Baker and Jim Goerss of the Naval Oceanographic and Atmospheric Research Lab assisted in the preparations for the real-time data collection. The dedicated efforts of Pat Harr, whose knowledge of FNOC operations was critical, and Tamar Neta are specially acknowledged.

The real-time data collection and display at the Experimental Operations Center in Guam was successful due to the efforts of all the Naval Oceanography Command Center (NOCC) personnel who took a sincere interest in TCM-90. A long list of NOCC personnel under CAPT R. Plante made all the pre-experiment arrangements, and then carried them out in a "can-do" manner under the leadership of CAPT D. Rudolph. Tremendous support was provided by the Joint Typhoon Warning Center personnel under LCOL C. P. Guard, who served as the local host of TCM-90 and taught us so much about typhoons and tropical meteorology. Special mention is made of the liaison efforts of LCDR L. Carr III who made so many arrangements that helped the experiment go smoothly, and Frank Wells who participated in the planning of TCM-90 and also freely shared his knowledge.

Special observations for TCM-90 were provided by many organizations. The National Weather Service made special rawinsonde launches. A Monash University team under D. Paice was very dedicated in making observations at Saipan. Outstanding support was provided to make rawinsonde observations at Clark AB and Cubi Point and at Iwo Jima. The successful profiler installation at Saipan was arranged by NOAA Aeronomy Lab personnel, who also upgraded the profiler at Ponnpei. A long, dedicated effort by 20th Weather Squadron personnel under LCOL S. Horn and LCOL R. Kandler was required to get approval for the profiler at Okinawa. Local support at Kadena AB was provided by Detachment 8 personnel under LCOL K. Nash and then LCOL A. Simoncic. An outstanding effort by Dick Lind and Paul Dobos of the Naval Postgraduate School was required to accomplish the installation. Keith Jones also contributed to the successful operation.

The NASA DC-8 team provided some exciting observations. The extra efforts of all personnel involved, and especially LCDR G. Dunnavan, are acknowledged.

All the contributions by TCM-90 participants can not be described here. A special acknowledgement is made to Greg Holland who participated throughout the planning and execution of TCM-90. Of course, the entire project would not have occurred without the sponsorship of the Office of Naval Research Marine Meteorology Program. Dr. R. F. Abbey magically arranged financial support. The Naval Postgraduate School Direct Research Fund also made significant contributions to finance TCM-90. Special assistance by Dr. Gil Howard is acknowledged.

A heartfelt thank you is extended to the faculty and staff of the Department of Meteorology at the Naval Postgraduate School. Their consistent and outstanding support throughout the TCM-90 planning and execution is gratefully acknowledged. Special thanks are given to Penny Jones who carefully typed this report and lots of other letters, reports, etc. Pat Harr and George Dunnavan reviewed drafts of this report.

A personal acknowledgement is given to the spouses of all the TCM-90 participants, who, like my wife Linda, provided support and encouragement to successfully complete an outstanding experiment.

## Introduction

The Tropical Cyclone Motion (TC-90) field experiment was conducted in the western North Pacific during August and September 1990. This field experiment was the culmination of a five-year Tropical Cyclone Motion research initiative of the Office of Naval Research Marine Meteorology Program. This report is being circulated as soon as possible after the field experiment to facilitate research with the data. Descriptions of the data sets thus will be based primarily on the observations received in real-time, which probably represents 90% of the upper-air soundings. Efforts are in progress to determine whether the missing observations were not made (probably 5%) or whether they will be available in a delayed mode (probably 5%). Although a more complete data summary could have been provided in several months, the choice was made to issue this preliminary report. The merging of the real-time and delayed data sets is expected to be completed by April 1991, and this set of raw observations will be distributed to participants. A final summary of all data collected will be provided as a byproduct of the quality control steps in the objective analysis and data assimilation to produce the final analysis fields at the National Meteorological Center.

This report contains two sections. The first section describes a data management plan for TCM-90 that was prepared prior to the beginning of the field experiment. It contains a section on the data programs that also serves as a general description of the observations. The collection of these data streams is then described.

The second section provides a preliminary description of each Intensive Observing Period (IOP). A synoptic summary of the formation and motion of the storm is provided for guidance in selecting cases for study. An indication of the hypotheses that might be studied with the data from that IOP is provided. These hypotheses are:

### **Hypothesis I**

Interactions between large intense tropical cyclones and subtropical ridge will modify both circulations and cause significant departures in the tropical cyclone track compared to an unmodified ridge-cyclone situation.

### **Hypothesis II**

Significant turns in the tropical cyclone occur when the interaction with transient synoptic-scale features, such as midlatitude troughs or TUTT cells, causes a response that extends the effects over a deep layer.

### **Hypothesis III**

A limited set of propagation vectors, which are the departures of the storm motion from a specifically defined steering flow, may be defined for particular cyclone characteristics and environmental configurations.

It is hoped that this preliminary description will be adequate to initiate research studies. Quick-look analyses based on real-time observations are available, as are some selected objective analyses prepared at the Experiment Operations Center. Other special data sets such as the NASA DC-8 flight-level observations and the dropwindsondes from the National Center of Atmospheric Research are expected to be available in November 1990. Hopefully, interpretations of these and other special data sets such as from the radar wind profilers can proceed while the final analyses are being produced.

I. Data Management Plan for TCM-90  
(B. C. Diehl and R. L. Elsberry, principal authors)

This Data Management Plan addresses the data collection, processing and archiving for TCM-90. However, it must also address observations from three concurrent tropical cyclone field experiments: (i) ESCAP/WMO Typhoon Committee Special Experiment Concerning Typhoon Recurvature and Unusual Movement (**SPECTRUM**); (ii) USSR **TYPHOON-90** expedition; and (iii) Taiwan Area Typhoon Experiment (**TATEX**). Although each of the experiments has specific objectives and different organizational structures and procedures, the Data Management Plan will provide a framework for a comprehensive data set that will incorporate the individual objectives and concurrent experiments.

The components of the Data Management Plan include the Data Management Strategy (Section 1.1), a description of the Real-time Data Management (Section 1.2), the various Data Programs (Section 1.3) and Data Streams (Section 1.4), the Data Sets and Products (Section 1.5) and the Data Users and Organizations (Section 1.6).

### 1.1 Data Management Strategy

The data management strategy for the TCM-90 experiments is summarized in Fig. 1.1. The ultimate goal of the data management is to produce final analyses at gridpoints to be used by researchers to understand tropical cyclone motion. These final analyses may be used for diagnostic studies or as initial fields for numerical model studies. A byproduct of the four-dimensional data assimilation system that will produce the final analyses is a quality controlled listing of all observations collected in the final experiment. As indicated in Fig. 1.1, interim (or raw) observation sets will be available for researchers who want to do subjective analyses or who will do their own objective analysis or data assimilation to derive gridpoint values.

A similar comprehensive data collection and analysis procedure does not exist for other experiments. **TYPHOON-90** is really self-contained relative to data collection efforts (see Section 1.3). The primary data collection effort for **SPECTRUM-90** will be in real-time via the Global Telecommunication System (GTS), which is also the major component of the real-time data collection effort for TCM-90. Details of the Taiwan data management plan are not available.

To produce a comprehensive data set that best depicts the state of the atmosphere during the IOP's, real-time data management of all the observations made during the experiment is crucial. This includes data that are delayed due to failure in transmission or being lost in the communication network. A more detailed strategy for the real-time and delayed data collection for TCM-90 is presented in Fig. 1.2. A more thorough discussion of these strategies can be found in the following section.

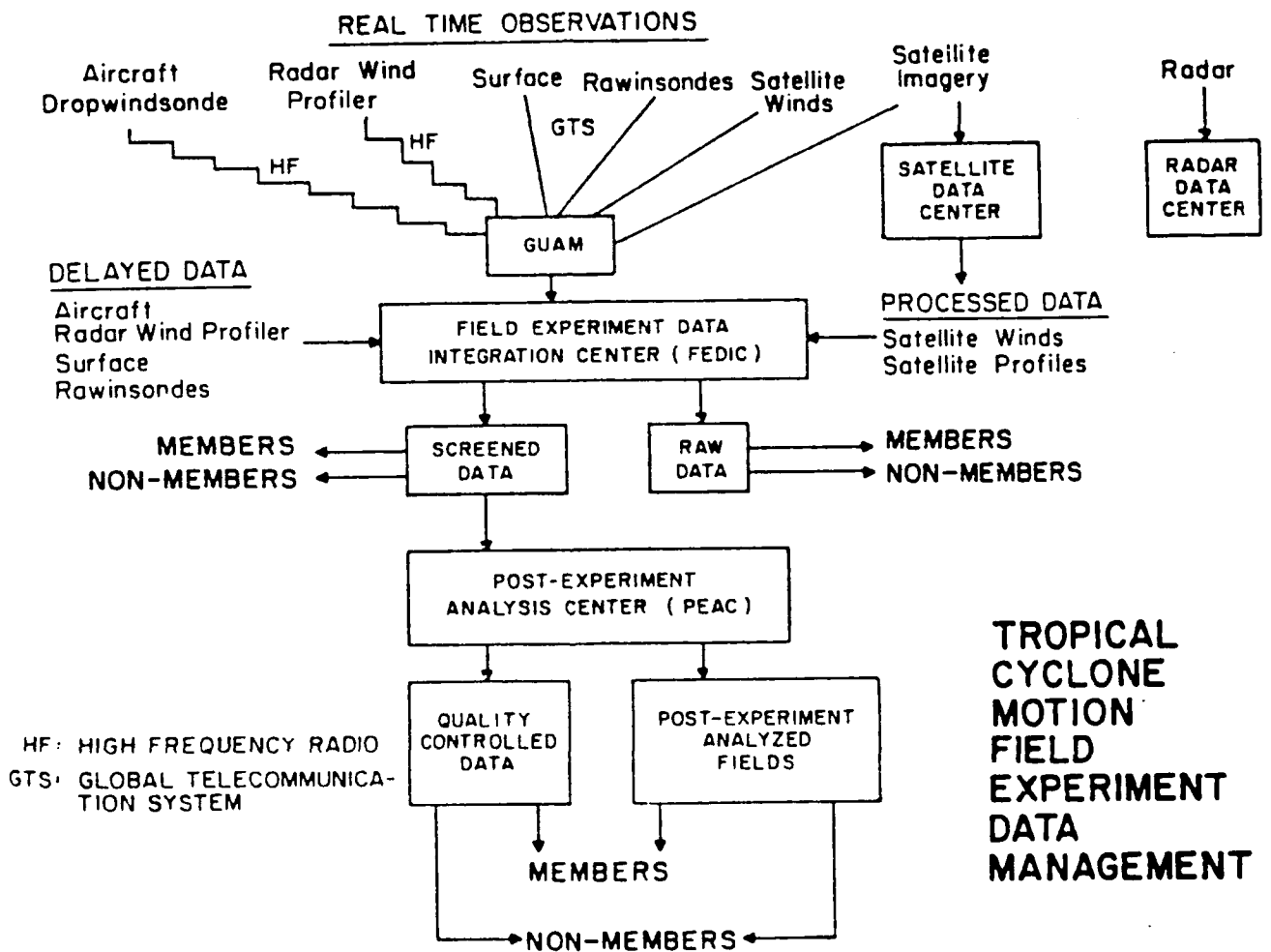


Figure 1.1 Data management plan for the TCM-90 experiment.

## 1.2 Real-time Data Management

### 1.2.1 Real-time Data Collection

Arrangements have been made to receive the data at the TCM-90 Operations Center in Guam via a node on the Automated Weather Network (AWN). These arrangements are being coordinated with the Joint Typhoon Warning Center (JTWC) personnel. Collection of complementary or auxiliary real-time data such as storm fixes and warnings, JTWC or Experiment Forecast Center analyses and forecasts, etc. will be arranged at JTWC.

Plans for the TCM-90 data collection effort are illustrated in Fig. 1.2. The real-time observations are received at the Fleet Numerical Oceanography Center (FNOC) in the standard WMO codes via the GTS and are decoded and stored in a special FNOC packed binary format to save space. As part of the Global analysis and forecast cycle at FNOC, a two-step procedure is executed each six hours to prepare the data on a regular grid for the numerical weather prediction model. The QUALITY CONTROL step has been developed by Nancy Baker of the Naval Oceanographic and Atmospheric Research Lab (NOARL), who followed the procedures used at the European Center for Medium-range Weather Forecasts (ECMWF). Among the procedures in this step is the conversion of all observations into the FGGE II format and various gross-error, vertical consistency and hydrostatic checks, etc. All observations are "flagged" as to their likely correctness, especially those observations that are changed. However, the most serious aspect in this step is that procedures are included to detect near-duplicate observations and delete the most suspect of the duplicates. Consequently, some of the data are lost in this step. As the OPTIMUM INTERPOLATION step in Fig. 1.2 is the combination of the screened observations onto the Global grid, this step is not of particular concern here. Additional flags as to the likely reliability of each observation in relation to the first-guess fields from the numerical model, or in comparison with other observations, are set in this step.

It is most convenient to archive the real-time data from the ADPFGGE file at FNOC (Fig. 1.2) that includes the quality control and optimum interpolation flags. Except for the discarded duplicate observations, all the other real-time observations can be reconstructed by ignoring the corrections and the flags. On the other hand, this file constitutes a "screened" data set that should be useful to many users who desire the TCM-90 observations.

### 1.2.2 Delayed Data Collection

During the experiment, some of the upper air observations will be missing due to failure to make the sounding, failure to transmit the observations within a specified time, or due to loss in the communication network. In addition, much of the radar wind profiler data will not be transmitted in real-time

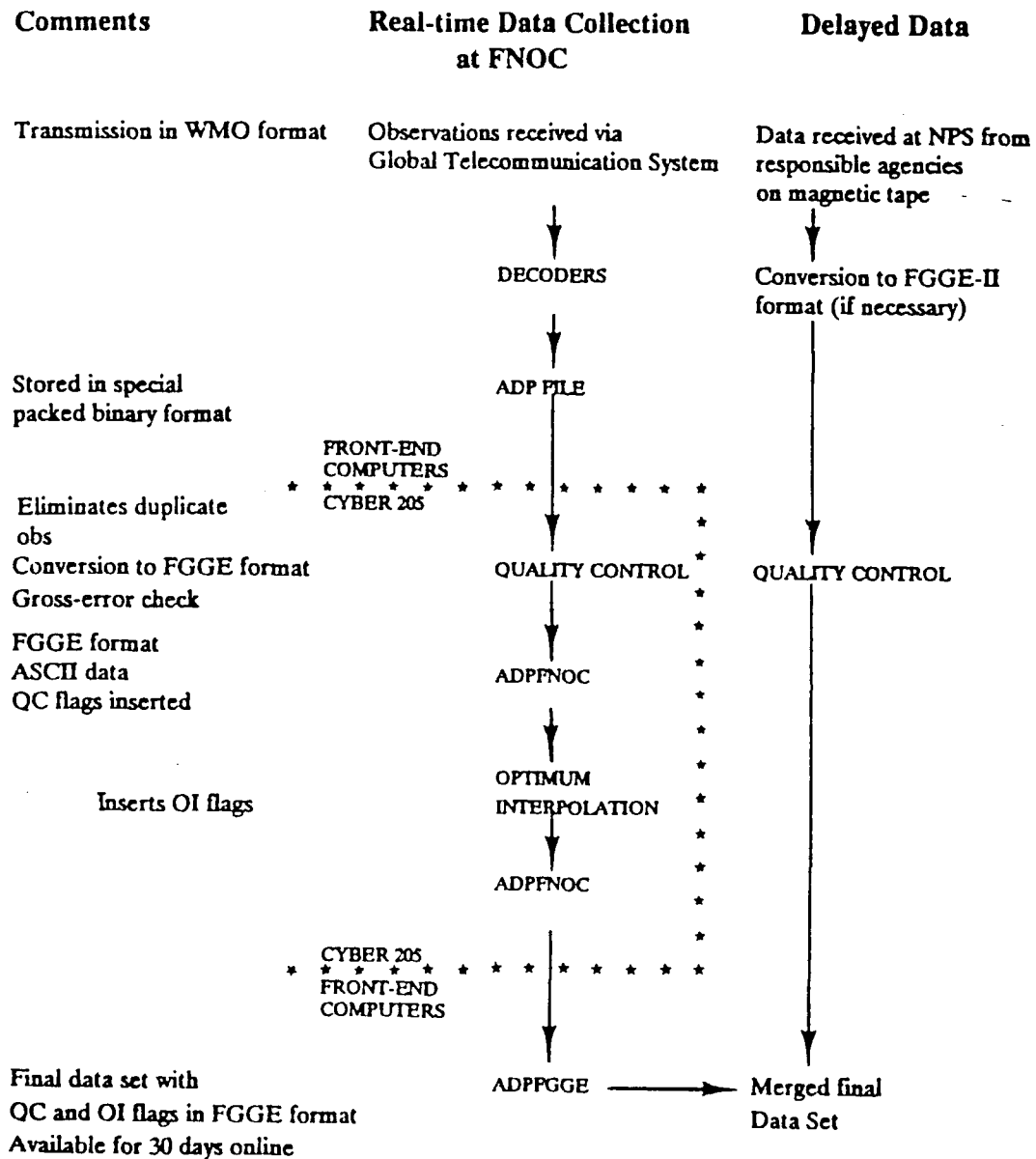


Figure 1.2 Real-time and delayed data collection for TCM-90. The acronyms beginning with ADPxxxx refer to specific data files at Fleet Numerical Oceanography Center. Programs at FNOC are separated according to whether they are executed on the vector processor (CYBER 205) or the front-end computers that provide input or receive outputs from the CYBER 205.



(especially the hourly radar wind profiler observations if only 6 h observations are transmitted on the GTS). Similarly, some of the special experimental observations will not be available in real-time.

To produce the best possible description of the atmosphere during the IOP's, it is essential that every effort be made to collect all observations made within the experimental domain. Procedures and displays have been developed to detect when expected observations are not received at FNOC. Summaries will be prepared for each IOP and for the entire experiment of the data missed in real-time collection. Procedures for acquiring delayed or post-processed data within three months after the end of the field experiment (by 31 December 1990) have been developed. Examples of the post-processed data include: (i) checked rawinsondes from the ships (also from land stations?); (ii) reprocessed satellite cloud-drift winds and profiles from the Satellite Data Center; (iii) checked flight-level data from the Aircraft Data Center; (iv) recalculated soundings from the Dropwindsonde Processing Center; (v) radar wind profiler observations that are reprocessed, etc. Special efforts will be made to collect the ship surface observations from centers that regularly search for such data from ship logs.

As shown in Fig. 1.2, the delayed data are to be collected at the Naval Postgraduate School. After conversion to the FGGE II format, some quality control of the observations may be done or the delayed data may simply be flagged as a special set. A merged final data set will be produced from the real-time and delayed data sets.

The product of the above tasks is to be a complete data set for the field experiment. If all delayed data are collected within three months following the field experiment, the goal is to have the raw and screened data available for transmittal to the National Meteorological Center (NMC) within five months after the experiment. Distribution to the Members of the field experiment team (including cooperating national centers) of the raw and screened data should occur by 6 months after the end of the field experiment, and to non-members by 12 months. Since these requests will come from a variety of locations with different needs, the task is to establish a data management system that has flexibility and is convenient to fulfill these requests. These data must be provided in a generic, easy to use format for the broadest range of users.

The final task is related to the receipt, archiving and distribution of the final analyses from NMC. These gridpoint fields on the inner analysis grid (Fig. 1, Elsberry 1989a) will include the basic meteorological variables of wind, pressure, temperature and moisture. In addition, derived or diagnostic fields such as vertical fluxes, latent heat release by convective or large-scale precipitation, etc. will be provided by NMC. These fields should be received 11 months following the end of

the experiment. Distribution to Members should occur by 12 months after the experiment and to non-members after 18 months. Provision of the data in an easy to read format is again a high priority.

### 1.3 Data Collections, Quality Assurance, Archival, Distribution

As stated in the introduction, the TCM-90, SPECTRUM and TYPHOON-90 experiments have different objectives, but the Data Management Plan will ensure that the different data programs for each of the experiments will follow the same procedures. The procedures include data collection, quality control, archival and distribution procedures outlined below.

Although more detailed descriptions of data collection were provided in Section 1.2, several important differences in data collection, quality control, archival and distribution procedures for the different experiments should be pointed out.

#### a. SPECTRUM

The SPECTRUM is an experiment to improve tropical cyclone track prediction. Thus, the primary data collection effort will be in real-time via the GTS. All Typhoon Committee Members will prepare a catalog of their data sets, and the JMA will compile an overall catalog based on information provided by Members. This catalog is expected to be distributed by December 1990. In addition, the JMA is expected to produce a "quick-look" data set based on real-time data transmitted to the RSMC via GTS. Copies of the quick-look data set on magnetic tape will be made available to Typhoon Committee Members.

#### b: TYPHOON-90

This USSR expedition is also self-contained relative to data collection efforts. The flag ship has a computer center for archiving the observations. All types of standard ship observations are transmitted in real-time to the flagship and to the Hydrometeorological Center in Vladivostok (and Tokyo). All of the information is collected on the flagship and stored on magnetic tapes in a format suitable for international exchanges. A special group on the flagship is responsible for the preparation and quality controlling of this information.

#### c. TCM-90

Data management for the TCM-90 is indicated in Fig. 1.1. To the maximum extent possible, the experimental data will be transmitted in real-time so that they may be used by the Experimental Forecast Group and by the Experiment Operations Team. However, it is anticipated that some observations will be delayed, lost in communication, or will be made by research groups that do not have access to the GTS. Because the focus of TCM-90 is to improve basic understanding of tropical cyclone

motion, a maximum effort will be made to collect all delayed data or non-transmitted experimental data. In addition, post-experiment processing of the satellite cloud-drift winds, research aircraft observations, dropwindsondes, etc. is planned. These data will be combined with the real-time data at the Data Integration Center (Fig. 1.1) at the Naval Postgraduate School under the direction of Tamar Neta and Patrick Harr. The "raw" data are the real-time, delayed and post-experiment data from the instrument operators and specialized centers, or from cooperating experiments. A first-level quality control to remove transmission glitches or illogical records will be performed. Further data processing may include removal of duplicates, and a more detailed quality control (details not determined). These screened data in the so-called FGGE Level II format are expected to be available about six months after the experiment.

#### d. Final Analyses

For many users, the raw or screened data will be adequate for research or prediction studies. However, other users may desire "final analyses" that are based on all of the real-time and delayed data from the experiment. A workshop (Elsberry 1989b) considered the data assimilation systems that presently exist for preparing the final analyses. A consensus was obtained on the essential characteristics for the data handling preparations, objective analysis, data assimilation system, initialization technique and other related aspects for preparing the final analyses. The inner analysis domain will be between  $5^{\circ}$  N and  $40^{\circ}$  N,  $105^{\circ}$  E and  $150^{\circ}$  E. As the desired horizontal resolution is 50 km, the grid will be about 75 points in the zonal direction. About 20 levels will be used in the vertical. Since all upper air stations are expected to launch rawinsondes each 6 h during an IOP, the plan is to produce 6-h analyses during an IOP. During the intervals between IOP's, standard 12 h synoptic times generally will be adequate. If a 6-h update cycle is utilized throughout the two-month period, there maybe some interest in the 6-h fields in the intervals between IOP's as well.

The U.S. National Meteorological Center will prepare the final analyses under the leadership of S. Lord. A multivariate objective analysis will be used for the wind and mass fields. A gradual decoupling with the mass field as the Equator is approached will be used to maintain the divergent, ageostrophic wind components in the tropical circulations. The analysis of the moisture field will be univariate. Methods of including bogus moisture profiles based on satellite-observed cloud patterns, tops, etc. will be explored. Some provision for manual inspection of the flagged observations during the data assimilation cycle will be maintained, and the analyzed data fields will be extensively checked versus observations known to be good. A minimum bogus of the tropical cyclone position and inner core structure will be used to avoid contamination for the outer wind structure that will be resolved by observations.

Other details of the data assimilation and initialization procedures will be published later. The final analyses will be archived in the GRIdded Binary (GRIB) format. The present plan is to have these analyses available about one year after the field experiment.

#### e. Data Exchanges

The final analyses described in Section d above will be most accurate if all the observations made during the field experiments are shared in real-time or on a delayed basis. Thus, negotiations are in progress to arrange data exchanges. Complete data sets will be made available first to researchers who participated in the planning and execution of the field experiments, and to other researchers on a delayed basis. Similarly, the final analyses will be distributed by the data center at the Naval Postgraduate School first to the experiment participants.

### 1.4 Data Programs

Extensive data programs are necessary to achieve the objectives of TCM-90 and the concurrent experiments. These include aircraft, soundings, radar wind profiler, buoy, Doppler radar and satellite data programs, each of which are outlined below.

#### 1.4.1 Aircraft Data Program

The goal of the TCM-90 Aircraft Data Program is to provide researchers with three-dimensional observations of the zones of interaction between tropical cyclones and the adjacent synoptic circulations. The aircraft data will also describe the structure and structure changes of this interaction zone and will help to determine tropical cyclone positions and for track and track change calculations. Unfortunately, late decisions as to participation of other U.S. (and USSR) aircraft restricted this component of TCM-90. The participating aircraft, type of dropwindsonde, real-time data transmission capability and responsible agency can be found in Table 1.1. More detailed information about the aircraft mission capabilities, sensors, etc. can be found in the TCM-90 Operations Plan for the aircraft.

#### 1.4.2 Rawinsonde Program

The rawinsondes from the TCM-90, SPECTRUM, TYPHOON-90 and Taiwan are important to test several of the experiment hypotheses. For example, a proper definition of the structure and location of the subtropical ridge requires an extensive array of upper-air soundings using a variety of platforms. Soundings are provided by a variety of observing aircraft, satellites and radar wind profilers. The data assimilation program that will be used to prepare the final analyses also depends on the rawinsondes for the vertical coupling between levels.

In addition to a variety of platforms to make the soundings, there will also be a variety of times when the soundings are made. The sounding frequency depends on whether or not the observing period is an IOP period and the type of platform. The frequency of upper-air soundings for the instrument platforms for IOP and non-IOP periods is summarized in Table 1.2.

In the discussion of the data management for the land-based soundings, they will be divided into two categories: Regular Sites (for regular synoptic soundings at 00 and 12 UTC) and Special Sites (for asynoptic soundings during an IOP at 06 and 18 UTC).

a. Regular Sites

The geographical distribution of synoptic sites that will launch additional rawinsondes at 06 and 18 UTC during SPECTRUM or TCM-90 IOP's is shown in Fig. 1.3. In addition, regular synoptic sites south of and including 40°N to the equator and from 100°E to 155°E should be included, which can be found from current World Meteorological Organization lists of regular upper-air synoptic stations. The Regular Site 06 and 18 UTC soundings will be transmitted real-time to the analysis and forecast centers via the GTS.

b. Special Sites

The special land and shipboard sites for the 06 UTC and 18 UTC soundings during the IOP's are listed in Table 1.3. The spatial distribution is shown in Fig. 1.3. Most of the stations in Table 1.3 were able to transmit the observations in real-time to the analysis and forecast centers via the GTS circuit. The remainder of the Special Site soundings will be considered delayed data and processed appropriately.

c. Aircraft

The frequency and real-time transmission capability of the dropwindsonde data and archival capabilities for the DC-8 aircraft in the TCM-90 experiment are listed in Table 1.2. The aircraft will use the regular Drop Code format for the dropwindsondes. For the flight-level winds, the RECCO code is used. All the flight-level winds and dropwindsonde data will be transmitted as delayed data.

Table 1.1 Aircraft, dropwindsondes and responsible agencies

Aircraft			
Type	Base	Real-time	Responsible Agency
DC-8	Okinawa	No	Nat'l Aero. and Space Administration (USA)
Dropwindsondes			
Type	Aircraft	Real-time	Responsible Agency
LORAN	DC-8	No	Nat'l Center for Atmos. Research

Platform	Observation Period	
	non-IOP	IOP
land	12 hourly	6 hourly; at 06 & 18 UTC
ship	12 hourly	6 hourly; at 06 & 18 UTC
satellite	no special processing	special processing 6 hourly cloud drift winds
Aircraft (DC-8)	no flights	onboard archival; selected 500 mb values transmitted by HF radio
radar wind profiler	if possible, 6-hourly	if possible, 6-hourly

Table 1.2 Frequency of upper-air soundings transmitted by each of the instrument platforms for non-IOP and IOP periods.

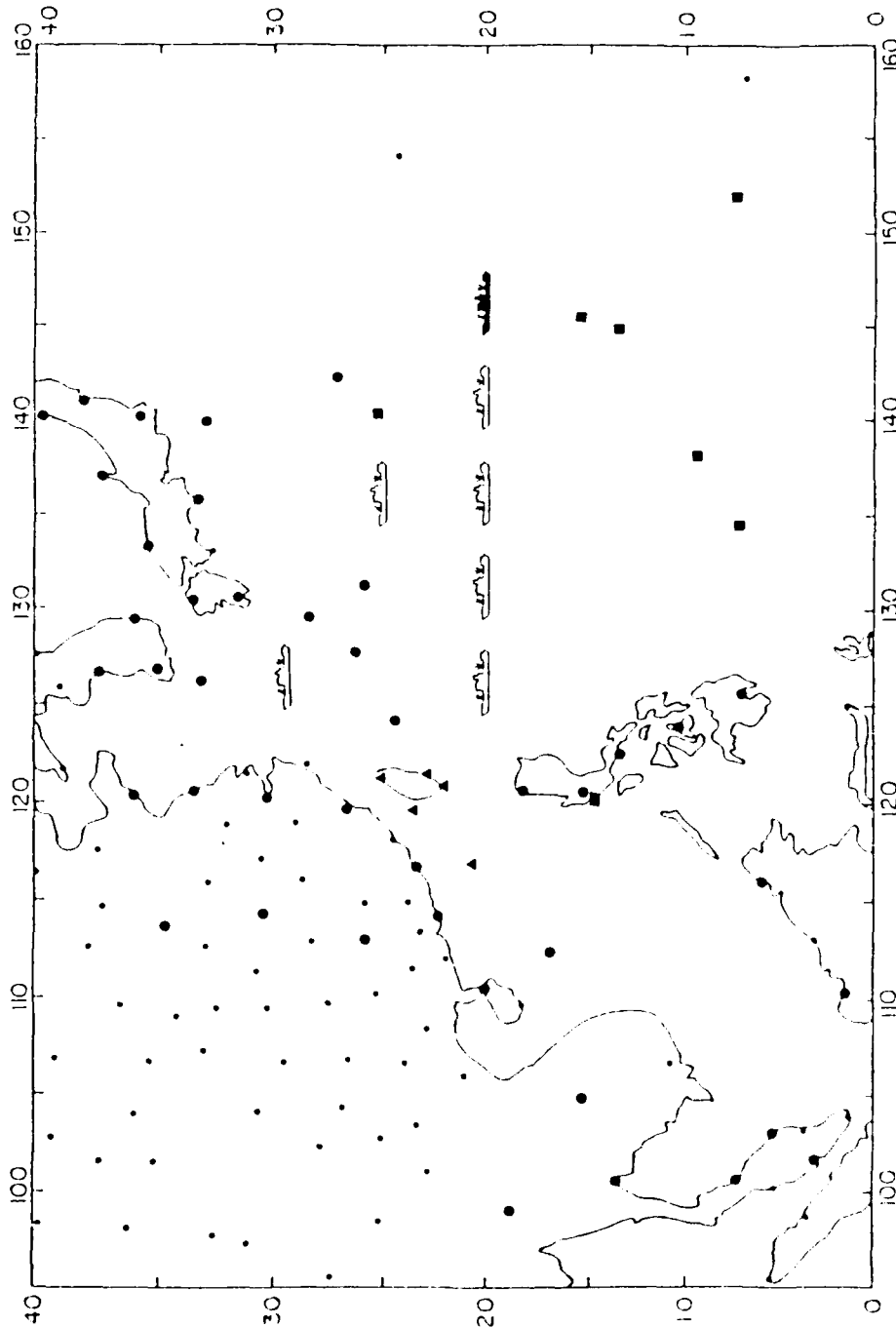


Figure 1.3 Upper-air network for TCM-90 and concurrent experiments. Regular rawinsonde stations with 12-hourly soundings are indicated by small circles. The large circles, squares and triangles represent the special rawinsonde stations with soundings at 06 and 18 UTC for SPECTRUM, U.S. and Taiwan stations, respectively. The ship symbols show the fixed positions of the participating ships.



Table 1.3 Upper-air sounding sites with special 06 and 18 UTC soundings during Intensive Observing Periods of one of the international field experiments.

Country/WMO Station Numbers	SPECTRUM	Responsible Agency
Japan	47582; 47590; 47600; 47678; 47744; 47778; 47807; 47827; 47909; 47918; 47936; 47945; 47971; 47991 (ships) Keifu-Maru; Chofu-Maru	Japan Met. Agency
Korea	47122; 47138; 47158; 47185	Korea Met. Agency
PRC	54857; 57083; 57494; 57972; 58150; 58457; 58847; 59316; 59758; 59981	State Met. Agency
Hong Kong	45004	Royal Observatory
Philippines	98223; 98444; 98646	PAGASA
(Clark AB)	98327	PAGASA - USAF
Thailand	48327; 48407; 48455; 48568	Thailand Met. Serv.
Malaysia	48615; 48648; 96413; 96471	Malaysia Met. Serv.
TCM-90		
U.S.	91217; 91334; 91408; 91413	Nat'l. Wea. Serv.
Cubi Point	98426	TCM-90
Saipan	91232	Monash Univeristy/ Bureau of Met.
Iwo Jima	(ship code)	U.S. Navy
(ships)	US Williams plus transiting ships	U.S. Navy
TYPHOON-90		
USSR		
(ships)	Academik Korolyov; Admiral Shirshov; OWS Okean; OWS Priboi	Inst. of Exper. Meteorology
TATEX		
Taiwan	46692; 46699; 46734; 46747; 46810	Central Wea Bureau and Nat'l. Science Council

#### 1.4.3 Radar Wind Profilers

The radar wind profiler sites in the experiment domain, real-time data transmission capabilities and the responsible agencies are listed in Table 1.4. The stations that transmit in real-time will provide hourly averaged winds transmitted over the GTS in PIBAL format at six hourly intervals during an IOP. The radar wind profiler data will be archived with higher vertical resolution as delayed data.

#### 1.4.4 Buoys

Both drifting and fixed buoys are available in the western North Pacific and East China Sea for the concurrent experiments. The U.S. deployed 12 drifting buoys in an array to complement the surface observations from the USSR ships. JMA has provided four fixed buoys for SPECTRUM and one fixed buoy will be supplied by Korea. Table 1.5 gives the latitude, longitude and responsible agency for each buoy.

The 12 drifting buoys were interspersed with the USSR ships and the stations along  $25^{\circ}\text{N}$  to establish a surface array through the subtropical ridge. The longitudinal positions are  $133$ ,  $138$ , and  $143^{\circ}\text{E}$  along latitudes of  $12.5$ ,  $15$ ,  $17.5$  and  $22.5^{\circ}\text{N}$  (see Table 1.5). Note that the gap at  $20^{\circ}\text{N}$  will be filled when the USSR ships are present. Although the southernmost line is less desirable for motion prediction, it provides an array that extends toward Yap and Koror. Such an array provides ground truth for satellite retrievals across the entire Philippine Sea, and increases the number of surface pressure reports for the surface analysis. These 12 buoys will report surface pressure, surface air temperature and sea temperature. Transmission will be hourly via Service ARGOS onto the GTS, or via the Local Users Terminal (LUT) on Guam. Expected lifetime for the buoys is 90-120 days.

The four fixed buoys of the JMA make a complete surface report of all meteorological parameters in addition to the sea temperature. The single Korean buoy records the surface winds, pressure and sea temperature. Observations will be transmitted every 3 hours via the Japanese satellite to GTS.

#### 1.4.5 Doppler Radar

Doppler radar coverage for the concurrent experiments will be supplied by three sources: the Japanese Meteorological Research Institute (MRI), National Taiwan University and by the Soviet flagship.

The MRI Doppler radar is a 3 cm Doppler radar on Okinawa. The radar characteristics are indicated in Table 1.6. The National Taiwan University radar is operated on the north end of Taiwan under the direction of the Air Navigation and Weather

Table 1.4 Radar wind profiler data sources during the international field experiment

Location	Lat/Long	Data	Agency
Saipan	15°N, 146°E	Real-time	Aeronomy Lab & Bureau of Met.
Kadena AB	26°N, 128°E	Real-time	Naval Postgrad. School
Tsukuba	35°N, 140°E	Delayed	Met. Res. Ins.
Kyoto	35°N, 136°E	Delayed	Univ. of Kyoto
Ponape	7°N, 158°E	Real-time	Aeronomy Lab
Taipei	25°N, 121°E	Delayed	Nat'l Science Council (Taiwan)

Table 1.5 Latitude and longitude positions for the drifting and fixed buoys available during the TCM-90 experiment.

12 drifting buoys in array

(1)	133°E	12.5°N	
(2)	133°E	15.0°N	
(3)	133°E	17.5°N	
(4)	133°E	22.5°N	
(5)	138°E	12.5°N	
(6)	138°E	15.0°N	
(7)	138°E	17.5°N	
(8)	138°E	22.5°N	(failed on deployment)
(9)	143°E	12.5°N	
(10)	143°E	15.0°N	
(11)	143°E	17.5°N	
(12)	143°E	22.5°N	

4 fixed buoys from Japanese Meteorological Agency

(1)	36°40'N	145°40'E
(2)	37°54'N	134°33'E
(3)	29°00'N	135°00'E
(4)	28°10'N	126°20'E

1 Korean buoy (deployment location not defined)

Table 1.6 Characteristics of the MRI Doppler radar on Okinawa

Wavelength:	3.06 cm
Pulse Length:	1.0 Microseconds
Peak Power:	50 kw
Half-Power Beam Width:	1.0 Deg.
Detectable Min. Signal:	-105 dBm
Pulse Repetition Freq.:	2000 Hz
Nyquist Velocity:	15.3 m/sec
Max Range of Process. Doppler Velocity:	64 km
Range Gate Width:	250 m

Table 1.7 Characteristics of the Taiwan Doppler radar

Frequency:	5.61 GHz
PRF:	900/1200 Hz
Pulse Width:	0.5 microseconds
Peak Power:	262 KW
Antenna Az. Rotation Rate:	2 rpm
Antenna Elevation:	-1 to 90 deg.
Dynamic Range:	> 85 dBm
Range Coverage:	120 km
Range Resolution:	1 km
Unambiguous Velocity:	48 m/s
Wind Speed:	6 classes

Services. Its characteristics are indicated in Table 1.7. Although the USSR flagship Akademik Korolyov is expected to operate a 10 cm Doppler radar, no characteristics of this radar are available.

The Doppler radar data will not be transmitted in real-time. Data collection and management is the responsibility of the agencies sponsoring the radars, who should be consulted for conditions of availability.

#### 1.4.6 Satellites

Satellite data include digital data from the geostationary GMS and polar orbiting NOAA and DMSP satellites. The University of Wisconsin will be the satellite data center. The table below shows the satellite data availability.

	GMS	NOAA	DMSP
Availability	Hourly	2/day/satellite	2/day/satellite
VIS	IMAGER	AVHRR	OLS
IR	IMAGER	AVHRR	OLS
Microwave	N/A	N/A	SSM/I
Soundings	N/A	TOVS	SSM/I

The TOVS soundings will be available to the experiment through GTS. In the post-experiment mode, the University of Wisconsin will do a post-processing of the cloud-drift winds. The SSM/I images from DMSP will be available at JTWC.

#### 1.5 Data Streams

The TCM-90 data streams (i.e., flow diagrams in Figs. 1.4 - 1.8) for each of the data programs should assist in the analysis of the data management plan and assist the Data Manager during the field program. In addition to the data program streams, a project operations overview flow diagram (Fig. 1.9) has been provided. This is helpful in understanding the relationships between the operations, forecast and data management centers.

The only data program not represented in the data streams is the Doppler radar data. The responsible agencies, listed in Section 1.4.5, will collect and disseminate these data sets.

#### 1.6 Data Sets and Products

The data management strategy of TCM-90 and concurrent experiments includes the production of data sets and products that complement and summarize the data sets. These products will include the quick-look analyses from the Experiment Operations Center, a Data User's Guide and the Intensive Observation Period report in the second section of this report.

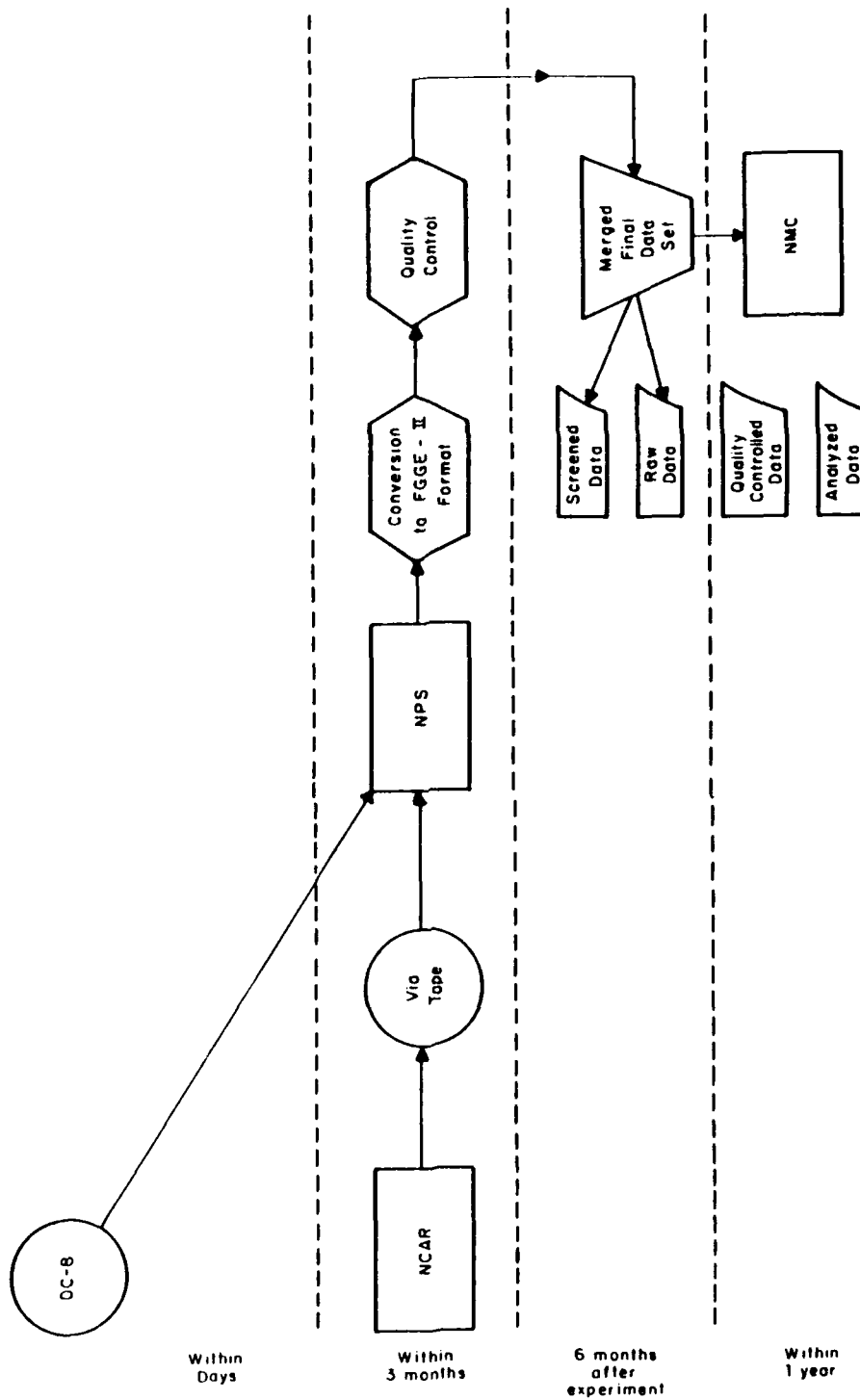


Figure 1.4 Aircraft data stream

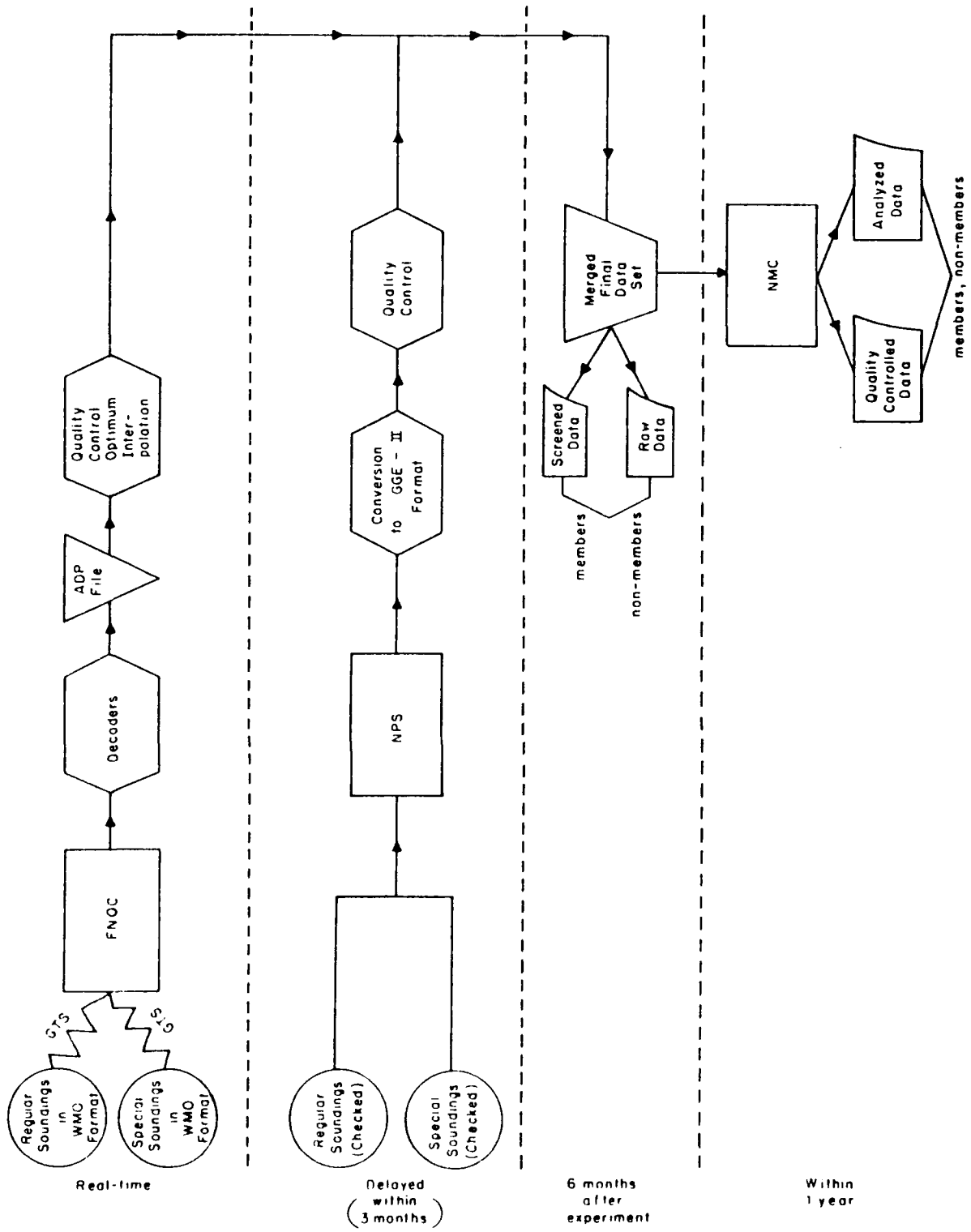


Figure 1.5 Regular and special site upper-air data.



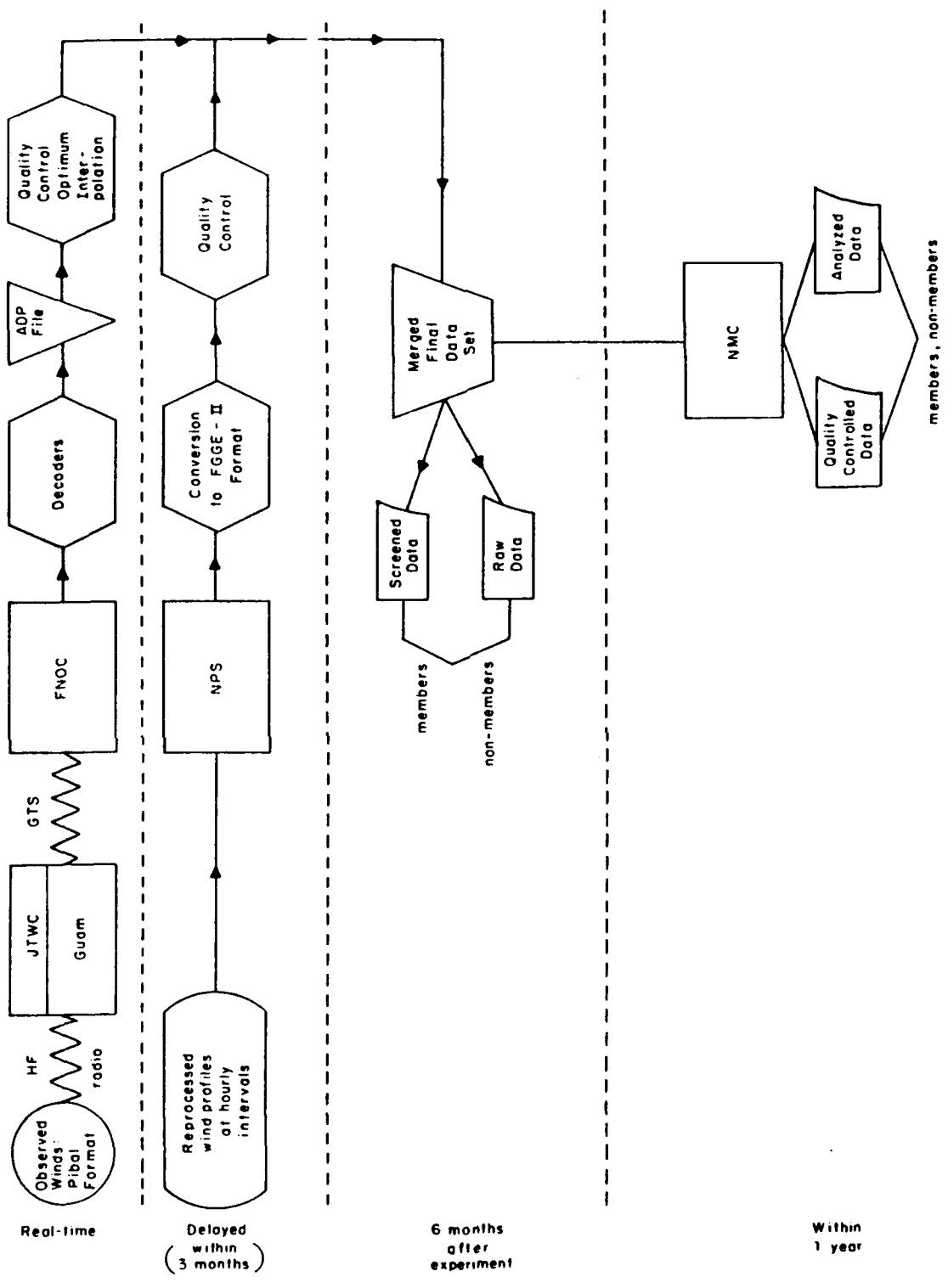


Figure 1.6 Radar wind profiler data stream.

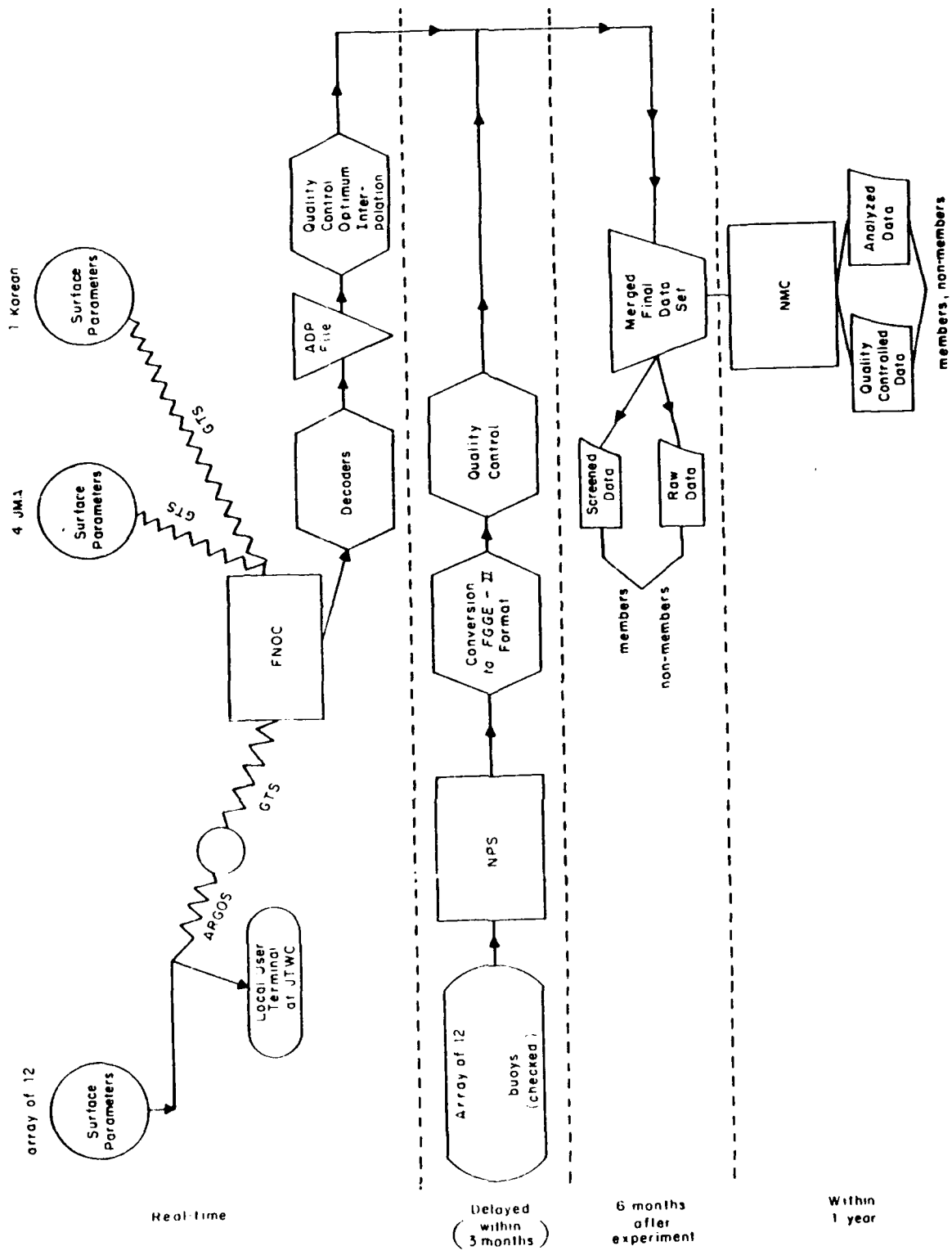


Figure 1.7 Drifting buoy data stream.

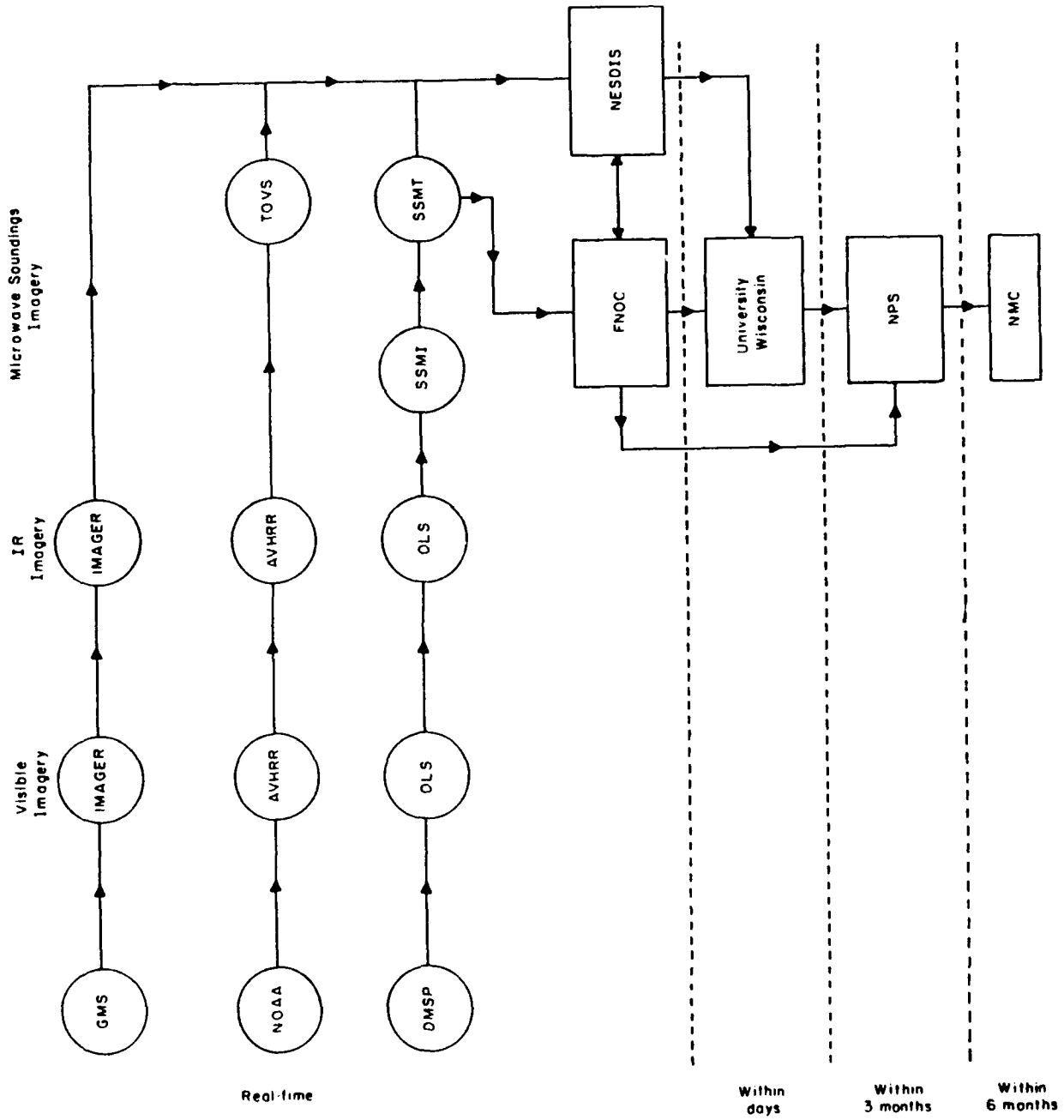


Figure 1.8 Satellite data stream.

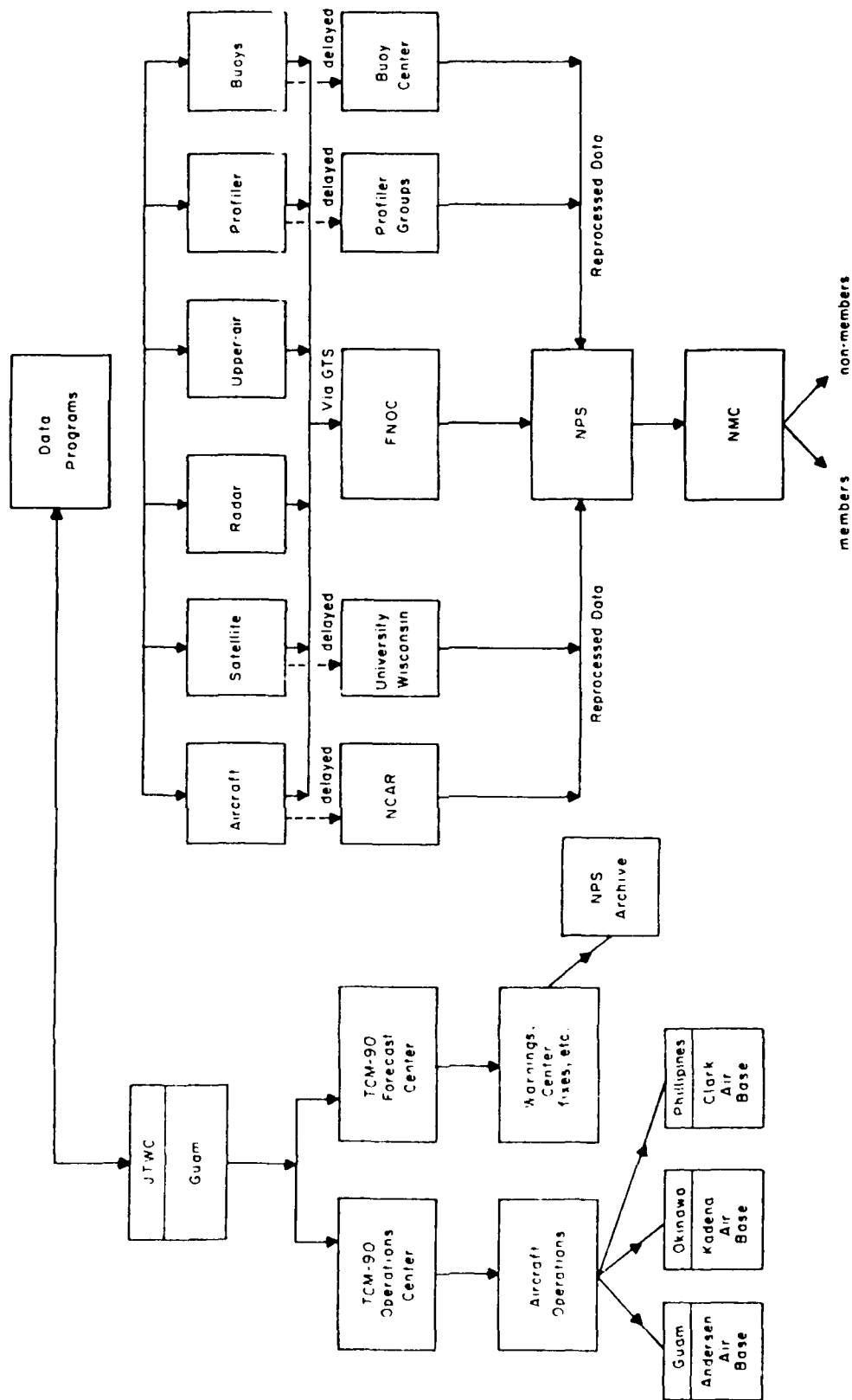


Figure 1.9 TCM-90 project operations overview.

### 1.6.1 Experiment Operation Center products

A daily record of the major meteorological events during TCM-90 will be available from the Experiment Operation Center. Subjective analyses at the gradient level and at 200 mb will be archived at 12-h intervals. Subjective sea-level pressure analyses will be prepared at 00 UTC each day, and 6-h plots of all ship and buoy surface reports will be prepared during IOP's. Selected computer analyses of 500 mb or Deep-Layer Mean fields will be collected.

Mosaics of 00 UTC VIS and IR images and 12 UTC IR images will be prepared within the Equator to 45°N between 110°E and 180°E. A standard enhancement will be used on both the VIS and IR imagery to highlight regions of deep convection. Images of particularly interesting circulation features will also be collected.

Working best tracks from the Automated Tropical Cyclone Forecast (ATCF) system will be available (see next section on the IOP summaries). Forecast tracks from JTWC, OTCM, CLIPER, CSUM and other objective aids also will be available.

### 1.6.2 Data User's Guide

The Data User's Guide will include descriptions of the data programs, their respective data sets, formats, availability and responsible agency. Additional information will include aircraft, instrumentation descriptions, directory of regular and special upper-air sites, buoy deployment sites and a list of participating ships.

### 1.7 Data Users/Organizations

Some researchers will utilize the real-time data and other groups will utilize the final analyses. An example of the real-time data users are the operational centers, such as the TCM-90 operations and forecast centers, the aircraft operations centers and the data program centers. The users of the final analyses will include Members and non-Members, who consist of experiment participants/organizers and non-participant researchers, respectively. Members include the ONR participants from the U.S. and Australia, the TYPHOON Committee members and the Taiwan and USSR participants. With respect to data exchanges of the final analyses, complete data sets will be made available first to Members and then to non-Members on a delayed basis. Table 1.8 is a tentative list of TCM-90 participants and their requested observations.

	Holland	Vinichenko	Frank	Volton	McTill	Mathon	Portno	Carl	Gray	Smith	Yamasaki	Guard	Kamaga	Williams	Schroder	Rurthara	Reichmann	Chan	Wang	Chan	Chang	Pa
Rawinschie	X				X				X		X	X										
Screened observations									X													
Checked observations	X	X	X	X	X				X					X	X	X			X		X	
Final grid point analyses	X	X	X	X	X	X	X	X	X	X	X			X	X	X	X	X	X	X	X	X
Quick-look analyses		X				X			X	X	X	X		X			X	X	X	X	X	
Synoptic description			X			X			X		X	X		X			X	X	X	X	X	
Satellite imagery		X	X	X	X	X			X	X	X	X		X	X	X	X	X	X	X	X	X
Hard copy		X	X	X					X	X	X			X	X	X	X	X	X	X	X	X
Digital		X	X	X	X				X						X	X	X	X	X	X	X	X
Radar wind profiler	X		X		X				X		X			X	X				X			
Aircraft flight level observations	X	X	X	X	X				X		X	X		X	X	X	X	X	X	X	X	X
Drifting buoy									X		X				X							
Dropwindsondes	X		X	X	X				X	X	X	X		X	X	X	X	X	X	X	X	X

Table 1.3 TCM-90 Participant Requested Observations

## II. Intensive Observation Period (IOP) Summaries

<u>IOP</u>	<u>Beginning Time</u>	<u>Termination Time</u>
1	12 UTC 8 August	00 UTC 10 August
2	12 UTC 15 August	12 UTC 17 August
3	00 UTC 18 August	00 UTC 20 August
4	12 UTC 5 September	00 UTC 8 September
5	00 UTC 13 September	12 UTC 14 September
6	00 UTC 15 September	12 UTC 16 September
7	00 UTC 17 September	00 UTC 19 September

An Intensive Observation Period (IOP) for TCM-90 was called when a severe tropical cyclone was expected to provide data within the SPECTRUM domain and was expected to provide data to study one of the hypotheses listed in the Introduction. The TCM-90 stations (as well as the TYPHOON-90 and TATEX stations) could begin special soundings at 06 UTC or 18 UTC on shorter notice than the SPECTRUM stations. Consequently, the TCM-90 IOP 1 and IOP 4 began 12 h earlier than the corresponding SPECTRUM IOP. Although the TCM-90 stations could continue special soundings for a maximum of 48 h, the SPECTRUM stations could continue for up to 5 days. Thus, IOP's 2 and 3 for TCM-90 were a single IOP for SPECTRUM. Although the target storm for IOP's 2 and 3 was Typhoon Yancy, the data set during IOP 3 captured a sharp left of Tropical Storm Zola. Similarly, IOP's 5, 6 and 7 for TCM-90 were a single IOP for SPECTRUM that terminated a day earlier than for TCM-90. Whereas the target storm for IOP 5 was Typhoon Ed, the target storm for IOP's 6 and 7 was Supertyphoon Flo. Nevertheless, the motion of the early stages of Flo during IOP 5 and of the later stages of Ed during IOP's 6 and 7 provide additional case studies.

More details on these storms and hypotheses are provided in the individual summaries below. Notice in the summary table on the next page that all of the IOP's involved an interaction with an adjacent ridge circulation. Thus, the description of the interaction processes and how and when this interaction occurs is expected to be a prime research topic. Interactions with adjacent synoptic features were involved in many of the cases. Embedded mesoscale circulation features during early formation stages of several of the storms led to uncertainties in the initial storm direction and speed. The TATEX cases included Yancy and Dot in IOP's 3 and 4.

<u>IOP</u>	<u>Storm</u>	<u>Hypothesis</u>
1	Winona	Interaction with ridge to east
2-3	Yancy	Interaction with subtropical ridge Outer wind structure effects on motion Interaction with orography Embedded mesoscale circulations in early stage motion
3	Zola	Interaction with ridge to east Tropical Upper Tropospheric Trough (TUTT) effect Embedded mesoscale circulations in early stage motion
4	Dot	Interaction with subtropical ridge Embedded mesoscale circulations in early stage motion
5	Ed	Interaction with orography Interaction with a monsoon trough
6	Flo-Ed	Interaction with ridge to the north Embedded mesoscale circulation in early stage motion
7	Flo-Ed	Interaction with monsoon trough Interaction with midlatitude trough during recurvature Interaction with ridge to east TUTT effect

Several interesting cases occurred just prior to TCM-90 or in the interval between the two phases. Although the data sets will be reduced without the ship soundings or the enhanced land rawinsondes, these cases will provide a contrast with the TCM-90 cases. A partial list of these cases follows:

<u>Storm</u>	<u>Interesting aspect</u>
Vernon	Poleward formation, subsequent southeast track Interaction with ridge to east and north TUTT effect
Tasha	Acceleration to north
Abe	Embedded mesoscale circulation in early stage motion
Becky	Interaction with ridge Interaction with orography Interaction with ridge Interaction with orography
Cecil	Midget storm Northward motion followed by southward motion



Data system notes:

1. As indicated in Table 1.1, only the NASA DC-8 aircraft participated in TCM-90. Partial data sets were obtained in IOP's 4 and 5 and complete dropwindsonde sets were collected in IOP's 6 and 7.

2. The planned radar wind profiler deployments on Iwo Jima and Minami Daito Jima were not possible due to logistics difficulties and lack of frequency approvals, respectively. A rawinsonde team was present on Iwo Jima beginning 15 August as a substitute observing system. The installation of the Kadena, Okinawa profiler was slightly delayed so that observations were not obtained until 14 August. This profiler acquired an excellent data set as Typhoon Abe passed to the south and west of Okinawa, and continued to operate after IOP 7 when Typhoon Gene passed west of Okinawa. A radar wind profiler was not available for installation at Clark AB, Philippines. A special rawinsonde team was placed at Clark to augment the soundings to a 3-h schedule during IOP's and a 6-h schedule between IOP's. This team switched to Cubi Point, Philippines on 15 August because of interference with LORAN signals at Clark AB. The times at which the MRI and Kyoto profilers (mentioned in Table 1.4) are not known.

3. The U.S. ship was at 20°N, 146°E only during the first week of August.

4. A rawinsonde team from Monash University provided complete soundings at Saipan (91232) throughout TCM-90, but they were not received in real-time due to communication problems. The hourly radar wind profiler observations at Saipan were transmitted each 6 h in a PIBAL format.

5. Based on the real-time data collection, the Laoag (98223) and Legaspi (98444) stations in the Philippines began transmitting in IOP 4. Evidently no observations were made at Davao in the Southern Philippines.

6. The eleven successfully deployed drifting buoys transmitted data at times of polar orbiter passages that averaged about four messages per day.

7. The satellite summaries (prepared by Chris Velden) in the IOP descriptions below are the reports within the domain Equator - 50°N and 110°E - 160°E in 24-h periods. The satellite wind vectors are the operational estimates. Separate retrievals by the University of Wisconsin will be made in the above domain during IOP's. The Geostationary Meteorological Satellite (GMS) VIS (daytime only) and IR imagery is hourly, except that special 30-minute imagery is collected four times a day for cloud-drift wind calculations.

Summary

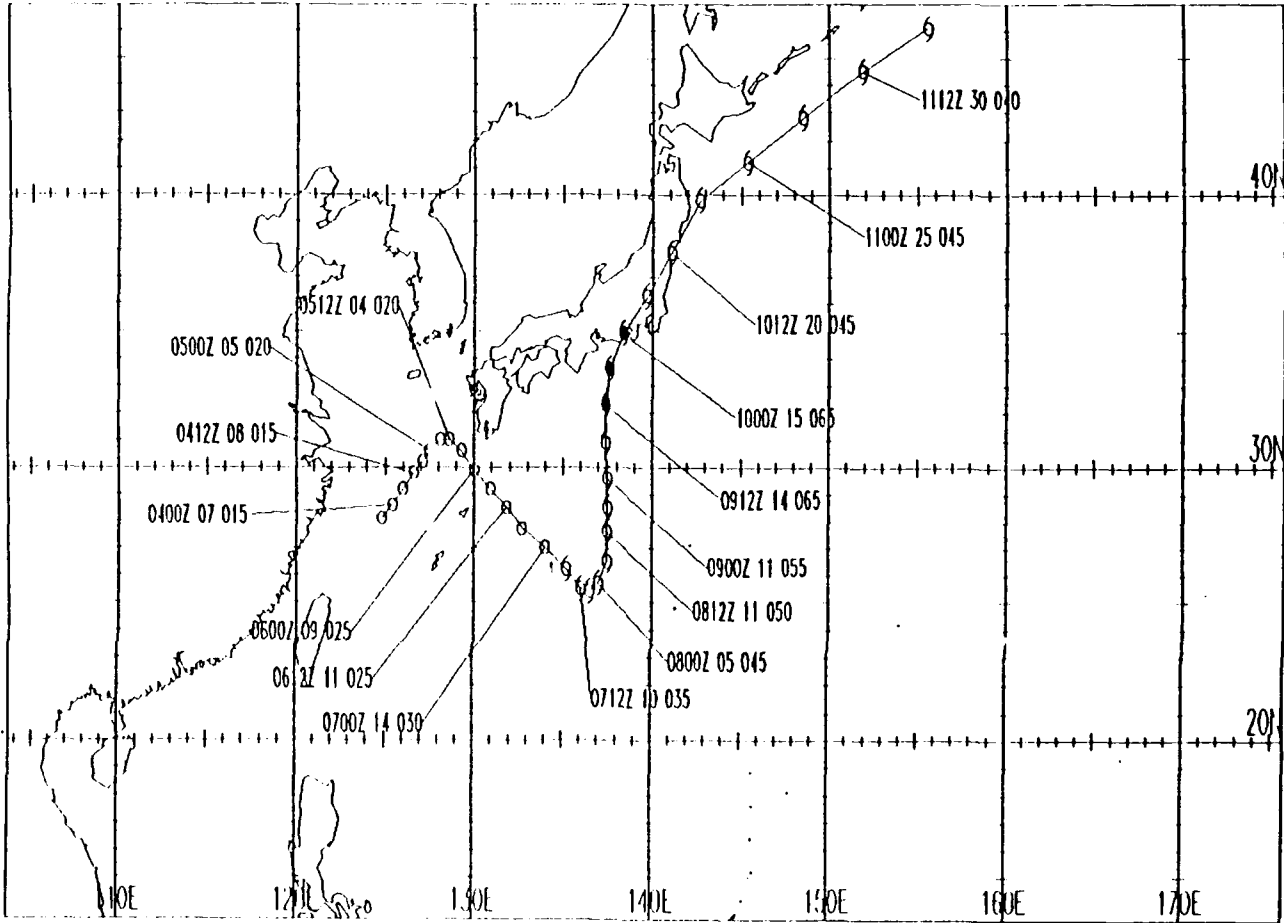
Winona (12W) was a rather unusual tropical cyclone both in terms of genesis location and movement. The cyclone formed in the monsoon trough, which was displaced well north of its normal location, and was not expected to develop much beyond a minimum tropical storm. The southeastward movement during the first few days of its lifetime (Fig. 2.1) was almost directly opposite the direction expected from climatology. Most of the objective aids predicted a turn to the north too soon. This case appears to be a good example of the interaction between a tropical cyclone, the deep monsoon southwesterlies and the subtropical ridge. The movement of Winona towards the north and northeast at the later stages was apparently in response to the approach of a midlatitude trough from the northwest, which should also be of some interest to TCM-90 researchers.

Synoptic Discussio.

The genesis of Winona can be traced to the remnants of TS Tasha (10 W) over eastern China. Enhanced convection became prevalent in the monsoon trough over the East China Sea as the low pressure area associated with the remnants of Tasha (10 W) moved out to sea around 00 UTC 4 August. This area of convection tracked eastward initially. The convection organized rather slowly as most of the low-level southwesterlies were feeding into the circulation of Typhoon Vernon (11 W) which was to the east-northeast. The cloud system center began moving southeastward along the edge of the deep monsoon southwesterlies at around 12 UTC 5 August. Rapid development was not anticipated as the 200 mb winds were unidirectional from the north over the system.

At 00 UTC 7 August, the system was near the axis of the 200 mb ridge (Fig. 2.2) and an exposed low-level circulation center could be identified to the north of the convection from the visible satellite imagery. A ship about 400 km south of the center reported a southwesterly wind of 35 kt. JTWC upgraded the system to Tropical Storm Winona at 06 UTC 7 August. The movement continued to be east-southeast and most objective forecast aids predicted a sharp turn to the north within 48 h. The 500 mb analysis at 00 UTC 7 August (Fig. 2.3) has Winona embedded in a complex flow pattern with Vernon (11 W) to the northeast and anticyclonic circulations to the southwest and southeast. A weak cyclonic circulation is also evident over eastern China. An extended alert for an Intensive Observing Period (IOP) beginning at 18 UTC 8 August was initiated in view of the unusual track of Winona and the possible interaction between Winona and the anticyclones.

Figure 2.1 Working best track of Typhoon Winona (12 W) from 00 UTC 4 August to 18 UTC 11 August 1990. Positions at 6-h intervals are shown for the tropical depression (circles) tropical storm (open cyclone symbols) and typhoon (closed cyclone symbols). The labels indicate day and hour (Z), the translation speed (kt) and maximum wind speed (kt).



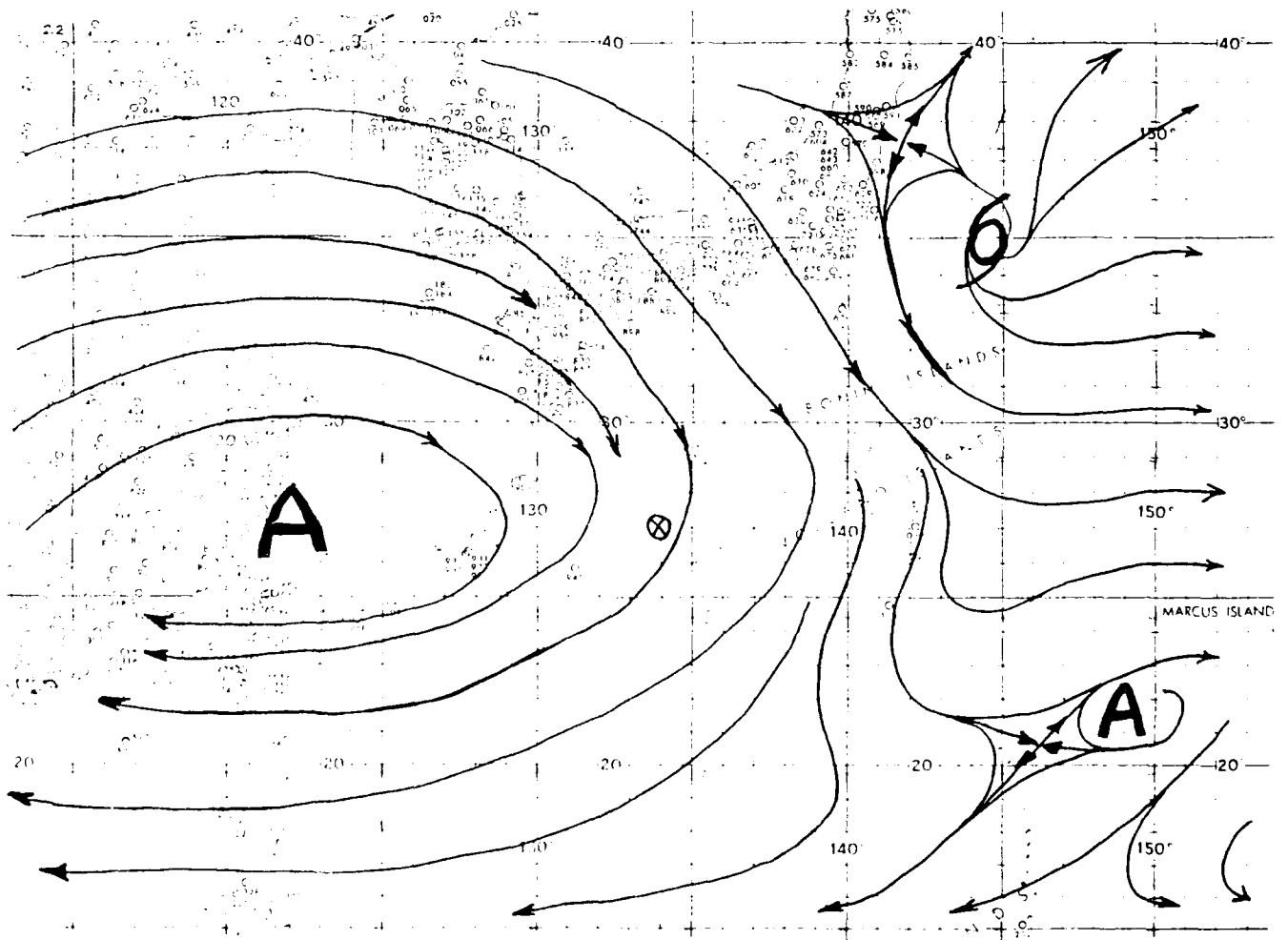


Figure 2.2 Streamlines at 200 mb at 00 UTC 7 August with TD 12 W (Winona) near  $27^{\circ}\text{N}$ ,  $134^{\circ}\text{E}$  and TS Vernon  $34^{\circ}\text{N}$ ,  $144^{\circ}\text{E}$ .

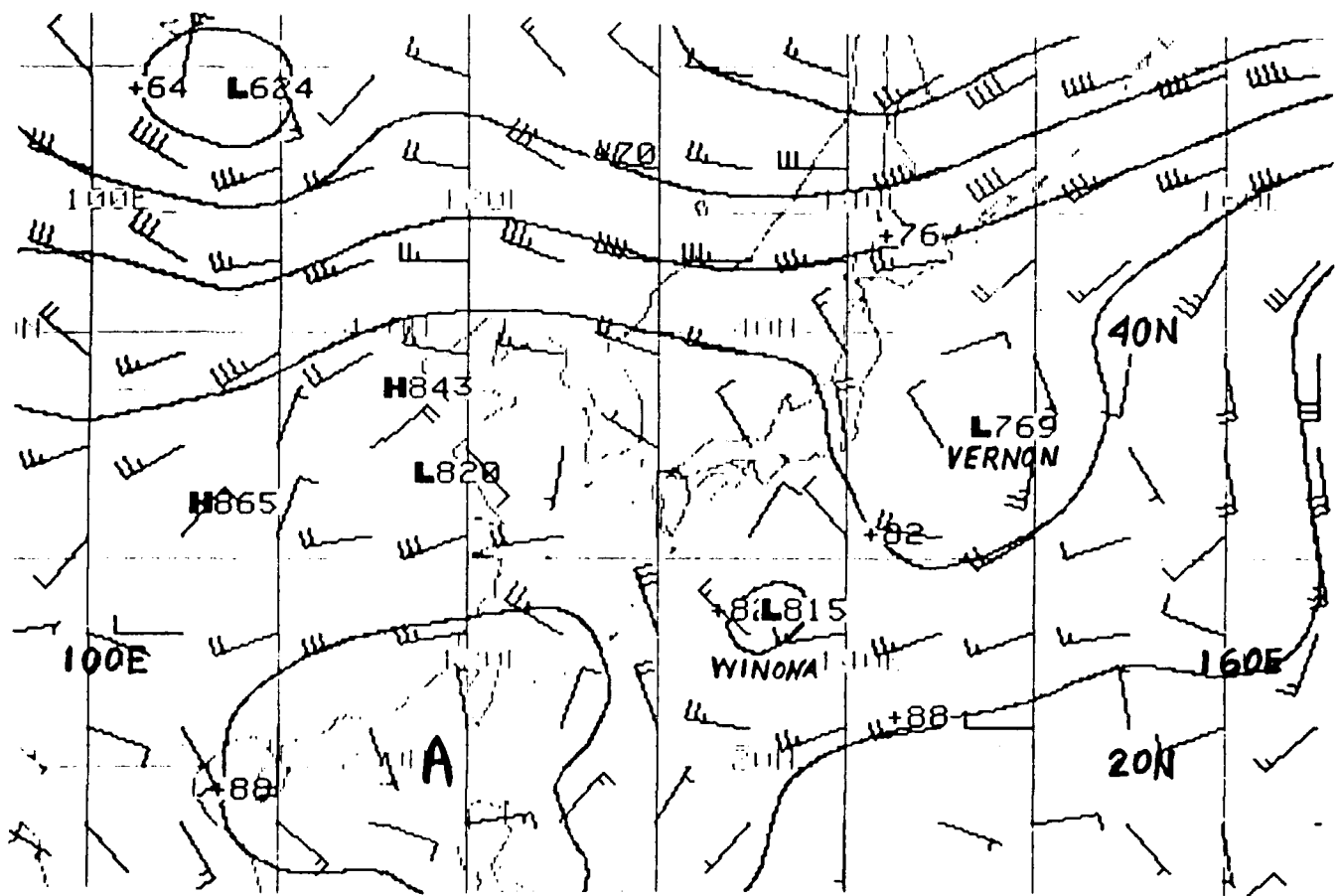


Figure 2.3 FNOG 500 mb wind (kt) and height (5xxx m) analysis at 00 UTC 7 August.

By 00 UTC 8 August, Winona had intensified slightly with maximum winds near the center estimated to be around 45 kt. The 500 mb flow (Fig. 2.4) has the anticyclone that was originally to the south of Winona now to the southeast, while Vernon (11 W) has continued to track northeastward. The cyclonic circulation over eastern China has also moved to the East China Sea. At this time, Winona had slowed down to around 4 kt and turned sharply to the north, as predicted by most objective aids. Further intensification was also expected as the 200 mb flow had possible outflow channels toward the northeast and southwest (Fig. 2.5). An IOP to be started at 12 UTC 8 August was confirmed for TCM-90, TYPHOON-90 and TATEX. However, SPECTRUM was unable to initiate an IOP so quickly and their IOP did not begin until 00 UTC 9 August.

At 00 UTC 9 August, the 500 mb anticyclonic circulation in the FNOC analysis that was previously to the east of Winona was located to the northeast (Fig. 2.6). One hypothesis is that the northward migration and expansion of this anticyclone was concomitant with the northward movement of Winona. This may have been a result of the enhancement of the anticyclonic circulation to the right side of Winona (looking in the direction of movement) due to the development of a wavenumber 1 asymmetry, similar to Hypothesis I of TCM-90. It is also possible that the anticyclone developed to the north and northeast of Winona in response to the rapid deepening of the extratropical cyclone near the Kamchatka Peninsula. Another feature on Fig. 2.6 is that the cyclonic circulation over the East China Sea had merged with the westerlies at this time. The objective forecast aids consistently predicted Winona to move north, make landfall over southern Japan and then recurve towards the northeast. However, TY Vernon and TS Steve had previously turned to the right in a similar situation.

Winona indeed maintained a northward track and intensified to a typhoon around 21 UTC 9 August as an outflow channel continued to be available to the northeast. The visible image at 23 UTC 9 August had a well-defined circulation with evidence of an eye. As landfall was anticipated, the IOP was terminated at 00 UTC 10 August.

After landfall, Winona weakened and began to accelerate towards the northeast. Winona was embedded in the westerlies at 12 UTC 10 August and moved northeastward at around 25 kt.

#### Data Coverage

Many logistics and communication problems had been resolved during the first week of TCM-90. A summary of the upper-air coverage (near real-time) is given in Table 2.1. Data system notes 3, 4 and 5 above apply to the upper air coverage. Sample coverage maps during a regular synoptic time (Fig. 2.7) and an off-time (Fig. 2.8) are provided to indicate the distributions of upper air observations.

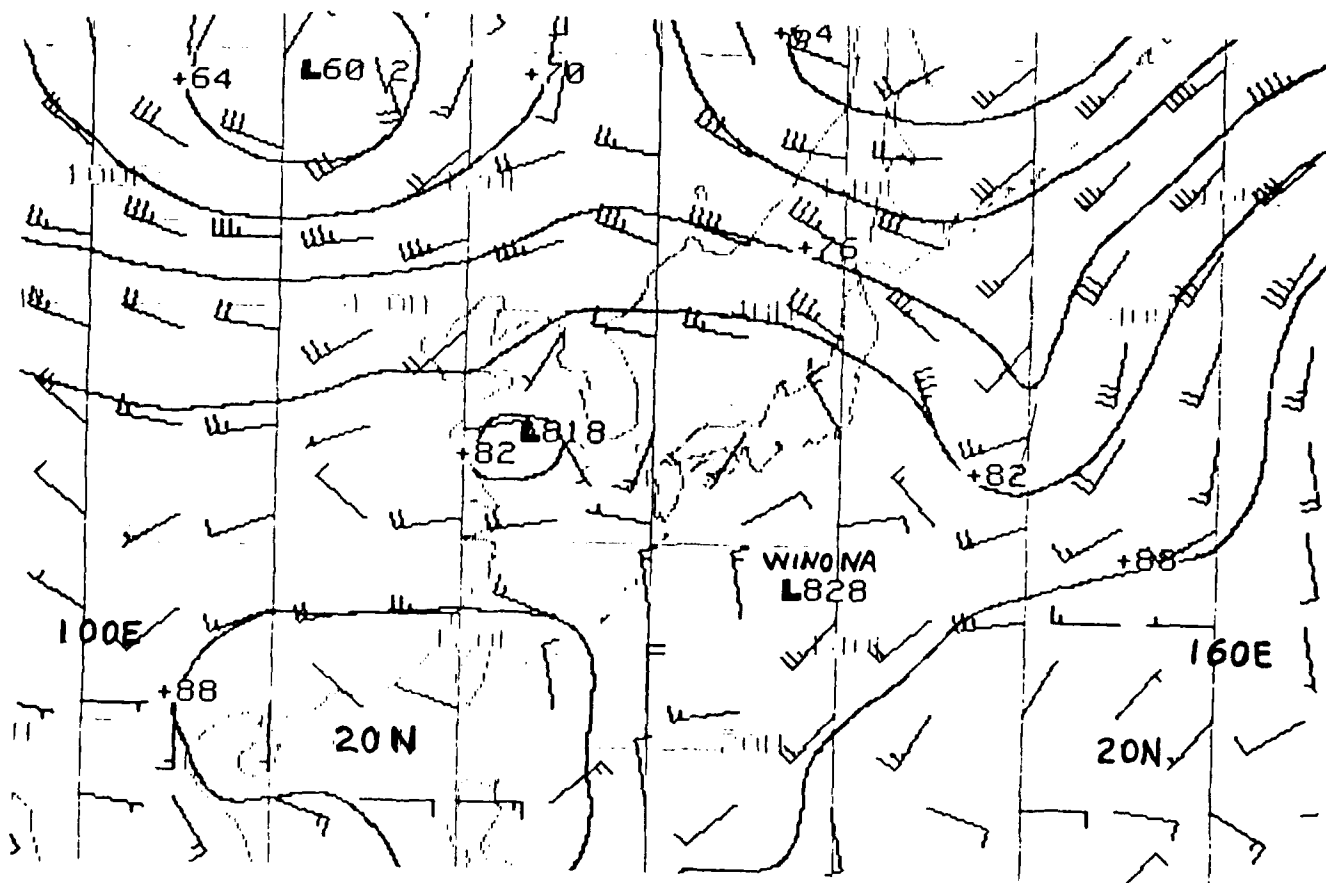


Figure 2.4 500 mb wind and height analysis at 00 UTC 8 August with TS Winona near 26°N, 137°E.

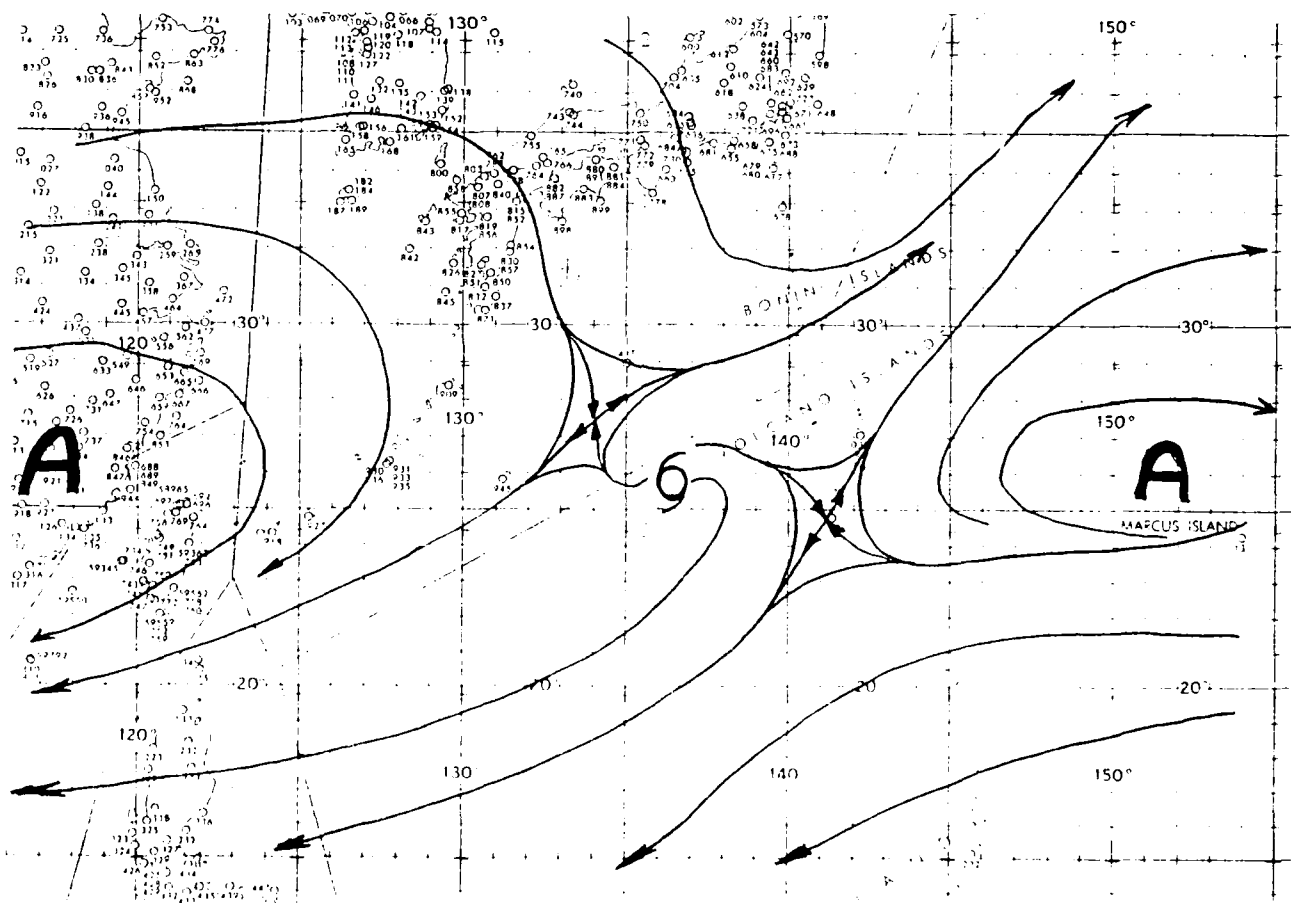


Figure 2.5 Streamline analysis at 200 mb at 00 UTC 8 August.



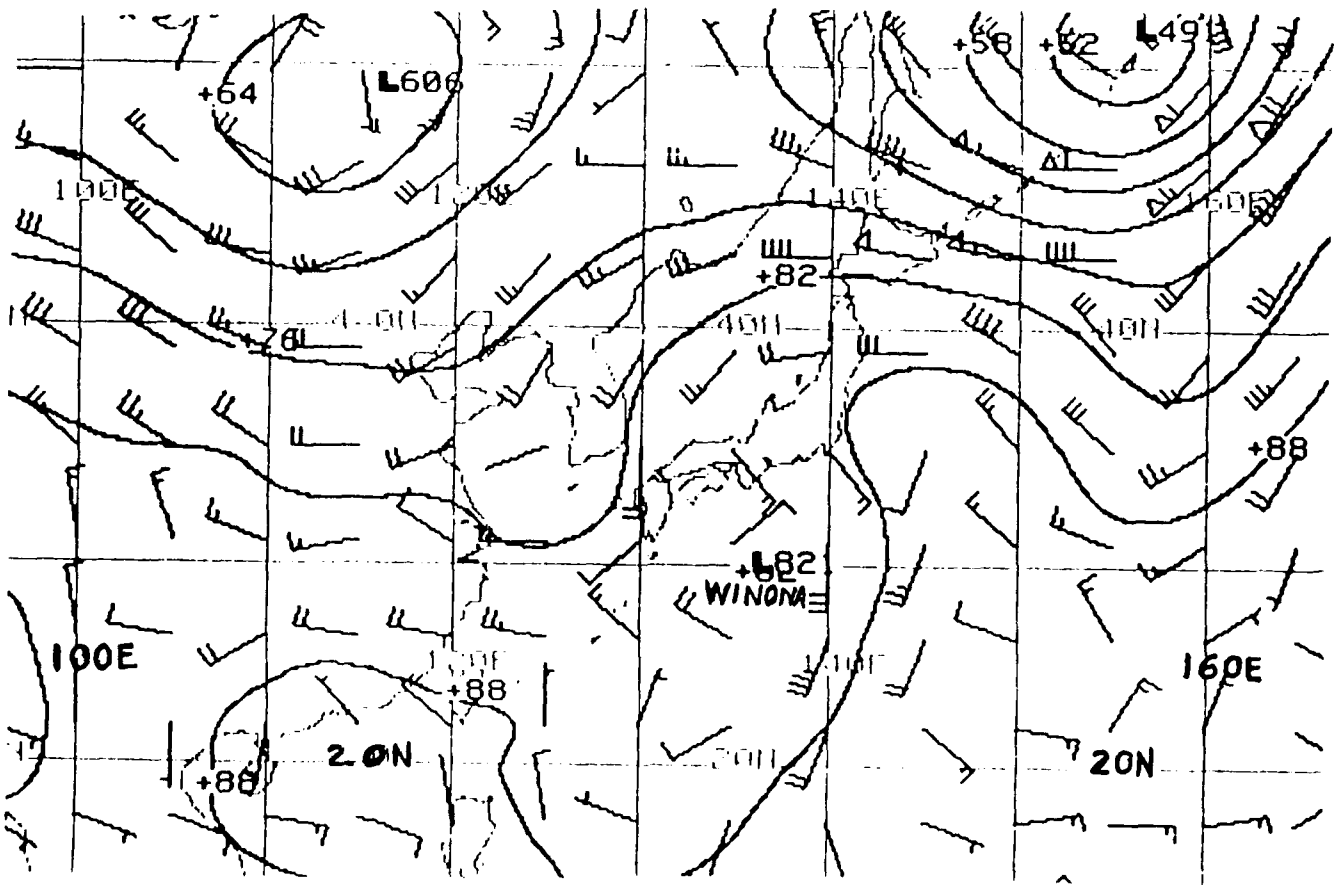


Figure 2.6 500 mb wind and height analysis at 00 UTC 9 August with severe TS Winona near 30°N, 137°E.

IOP-1, 90080812 - 90081000, TY WINONA

NO.	STATION	0808		0809				0810
		12	18	00	06	12	18	00
BLOCK 45 (HONG KONG)								
1	45004	X		X	X	X	X	X
BLOCK 47 (KOREA)								
2	47122	X	X	X	X	X	X	X
3	47138	X		X	X	X	X	X
4	47158	X		X	X	X	X	X
5	47185	X		X	X	X	X	X
BLOCK 47 (JAPAN)								
6	47582	X		X	X	X	X	X
7	47590	X		X	X	X	X	X
8	47600	X		X	X	X	X	X
9	47678	X		X	X	X	X	X
10	47744	X		X	X	X	X	X
11	47778	X		X	X	X	X	X
12	47807	X		X	X	X	X	X
13	47827	X		X	X	X	X	X
14	47909	X		X	X	X	X	X
15	47918	X		X	X	X	X	X
16	47936	X		X	X	X	X	X
17	47945	X		X	X	X	X	X
18	47971	X		X	X	X		X
19	47991	X		X	X	X		X
BLOCKS 48,96 (HAILAND, MALAYSIA)								
20	48327	X		X		X	X	X
21	48407			X	X	X	X	X
22	48455	X		X		X	X	X
23	48568	X		X		X	X	X
24	48615	X		X		X		X
25	48648	X		X		X		X
26	96413	X		X		X		X
27	96471	X		X		X		X

Table 2.1 Upper-air soundings during IOP 1.

*IOP-1 (continued)*

NO.	STATION	0808		0809				0810
		12	18	00	06	12	18	00
BLOCKS 54,57,58,59 (PEOPLE'S REPUBLIC OF CHINA)								
28	54857	X		X		X	X	X
29	57083	X		X	X	X	X	X
30	57494	X		X	X	X	X	X
31	57972	X		X	X	X	X	X
32	58150	X		X	X	X	X	X
33	58457	X		X	X	X	X	X
34	58847	X		X	X	X	X	X
35	59316	X		X	X	X	X	X
36	59758	X		X	X	X	X	X
37	59981	X		X		X	X	X
BLOCK 98 (PHILIPPINES)								
38	98223							
39	98327	X	X	X	X	X		X
40	98426							
41	98444							
42	98646			X	X	X		X
43	98753							
44	98851							
BLOCK 91 (PACIFIC ISLANDS, NATIONAL WEATHER SERVICE)								
45	91217	X	X	X	X	X	X	X
46	91232	X	X	X	X	X	X	X
47	91334	X	X	X	X	X	X	X
48	91338	X		X		X		X
49	91408	X	X	X		X		X
50	91413	X	X	X	X	X	X	X
BLOCK 47 (IWO JIMA)								
51	47000							
BLOCK 46 (TAIWAN)								
52	46692	X		X	X	X	X	X
53	46699	X		X		X		X
54	46734				X	X		X
55	46747	X				X		
56	46759							
57	46780							
58	46810					X		X
SHIPS								
1	FR11	X	X	X	X	X	X	X
2	FR11	X	X	X	X	X	X	X
3	UHQS	X	X	X	X	X	X	X
4	UMAY	X	X	X	X	X	X	X
5	IBOX			X	X	X	X	X
6	ICCN							

TOTAL NUMBER = 194

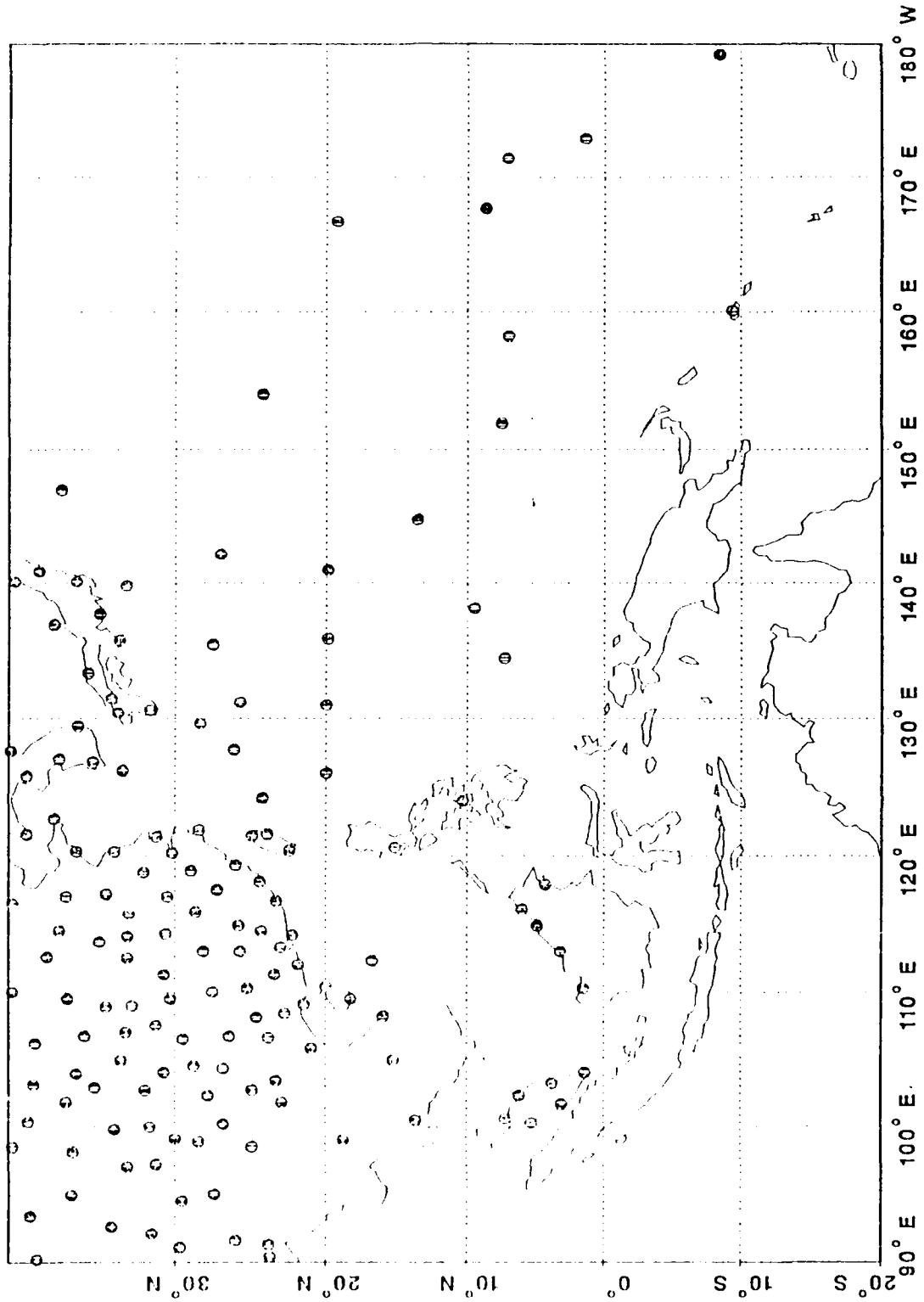


Figure 2.7 Coverage of upper-air soundings during a regular synoptic time of 00 UTC 9 August.

TOTAL NUMBER = 50

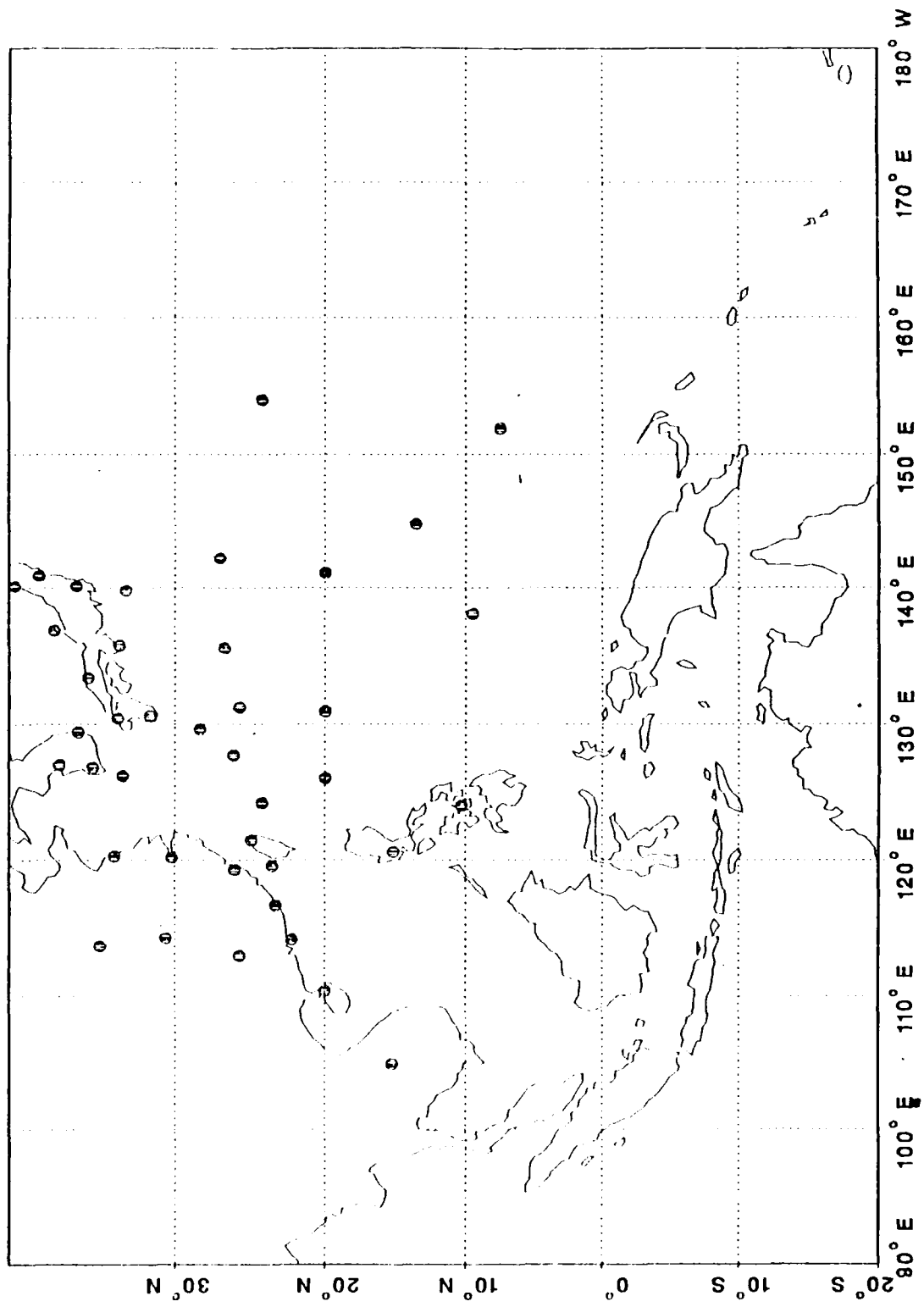


Figure 2.8 Coverage of upper-air soundings during an off-time period of 06 UTC 9 August.

The drifting buoy observations were received via the Local Users Terminal only. Transmission via the Global Telecommunication System (GTS) began at 18 UTC 9 August.

The preliminary satellite archive summary (see data coverage note 7 above) indicates some gaps on 9 August because the National Environmental Satellite Information Service (NESDIS) computer was down for several hours. Attempts are being made to recover the lost soundings and winds.

Satellite Soundings (# reports in 24 hours)

	8 August	9 August
NOAA10	1564	1495
NOAA11	1630	1634
DMSP8	569	411
DMSP9	486	344

Satellite Winds (# vectors)

	8/8	8/9	8/10
00 UTC	188	184	145
06	195		
12	149		
18	120	011	

Satellite Imagery

8/8	8/9
All GMS	All GMS
22 UTC NOAA10 pass	10 & 22 UTC NOAA10 passes
17 UTC NOAA11 pass	04 & 17 UTC NOAA11 passes

Summary

The working best track for Typhoon Yancy (13W) is shown in Fig. 3.1. The cyclone formed near  $10^{\circ}\text{N}$ , well east of the TCM-90 domain, and initially moved northward before following a westward, and then west-northwest track. Typhoon intensity was reached near 12 UTC 16 August, and maximum intensity of around  $45 \text{ m s}^{-1}$  (90 kt) occurred just east of Taiwan near 18 UTC 18 August. Yancy was a very large storm. At one stage, secondary bands of convection contained winds in excess of  $25 \text{ m s}^{-1}$  up to 700 km equatorward of the storm center and strong winds extended a further 1500 km.

Although the track was generally towards the northwest, it contained a number of interesting features. For example, the interaction with the subtropical ridge, especially during the passage of a midlatitude trough, is of considerable interest. The interaction with Taiwan produced a most interesting and unusual movement of the surface circulation down the western edge of the mountains.

Formation

The synoptic situation on 00 UTC 14 August is shown by the gradient-level and 200 mb analyses in Fig. 3.2. Typhoon Yancy developed near the axis of a strong monsoon trough that had been the major synoptic feature in the western North Pacific Ocean during the previous ten days. Moist convection had persisted in the trough during this time, with the center of activity consolidating towards the central and eastern parts of a broad monsoon trough that developed between  $130^{\circ}$  and  $150^{\circ}\text{E}$ . Maximum winds in this trough exceeded  $15 \text{ m s}^{-1}$  before a distinct core had developed.

A divergent upper-level flow persisted over the development region (Fig. 3.2b) with outflow both to the west and to the east. A strong, but narrow and shallow, TUTT lay along the northern edge of the convective cloud region and contributed to the sharp boundary in the satellite imagery. Several small cells formed, moved westward and dissipated in this region. The 500 mb subtropical ridge lay almost zonally along  $25^{\circ}$ - $28^{\circ}\text{N}$ .

Several potential circulation centers formed during the early development phase, and were associated with embedded, mesoscale convective clusters and apparent upper-level circulation centers. The northward track shift during 12 August (Fig. 3.1) was associated with the development of a dominant circulation center as Yancy finally formed near the trough axis.

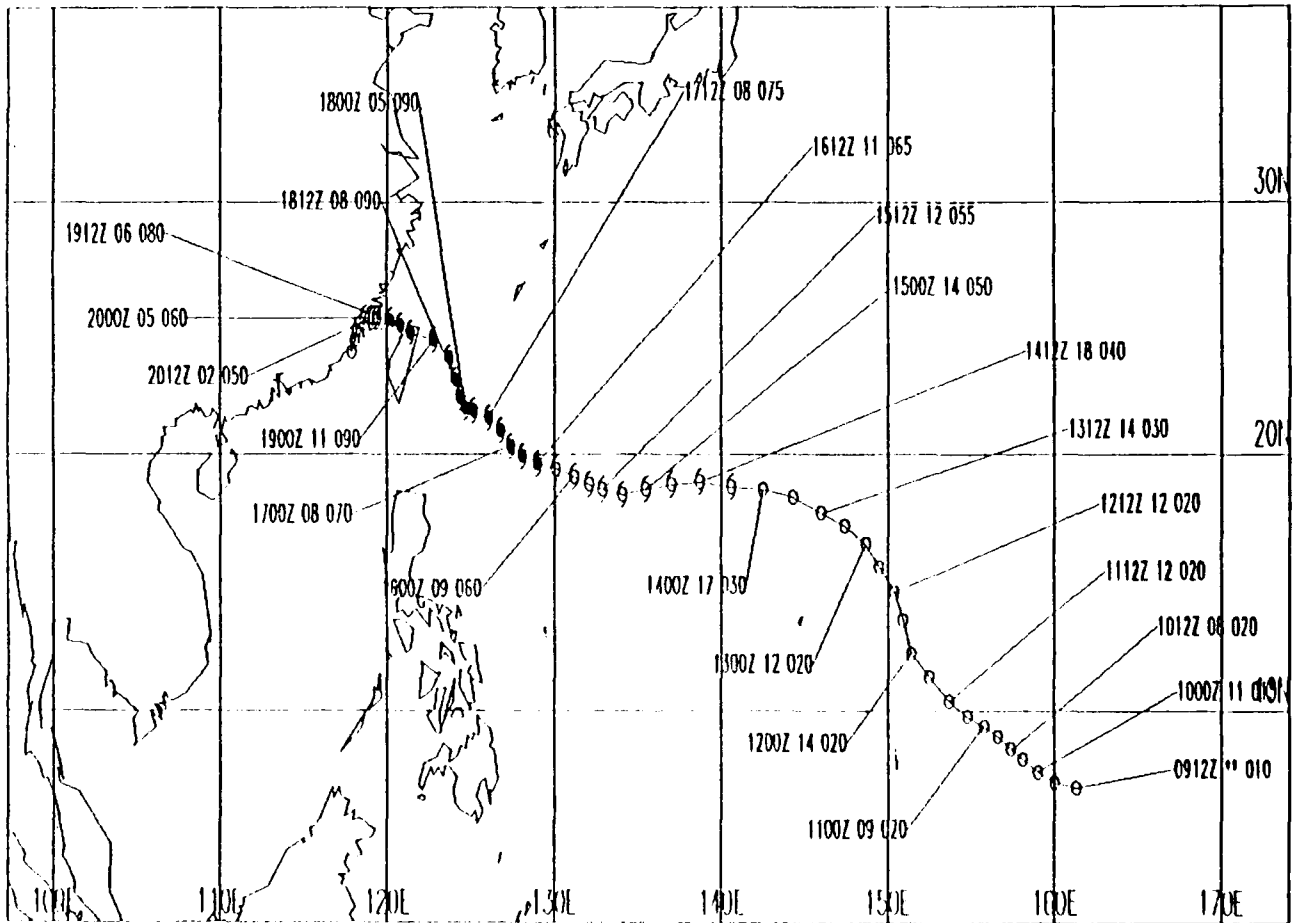


Figure 3.1 Working best track of Typhoon Yancy from 00 UTC 11 August to 00 UTC 22 August. Symbols are the same as in Fig. 2.1



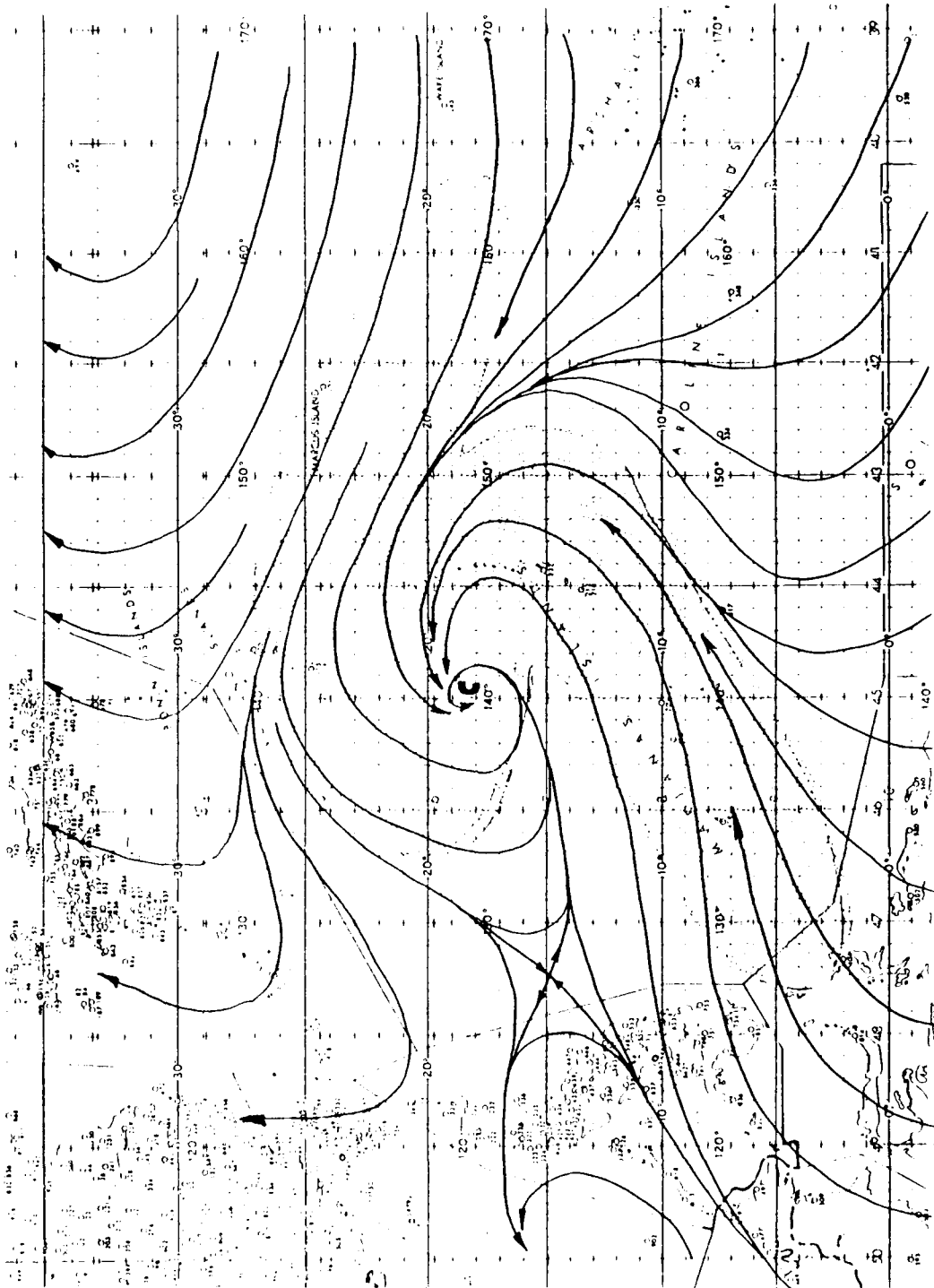


Figure 3.2 Streamline analyses for 00 UTC 14 August at the gradient level. Winds of greater than  $15 \text{ m s}^{-1}$  are stippled.

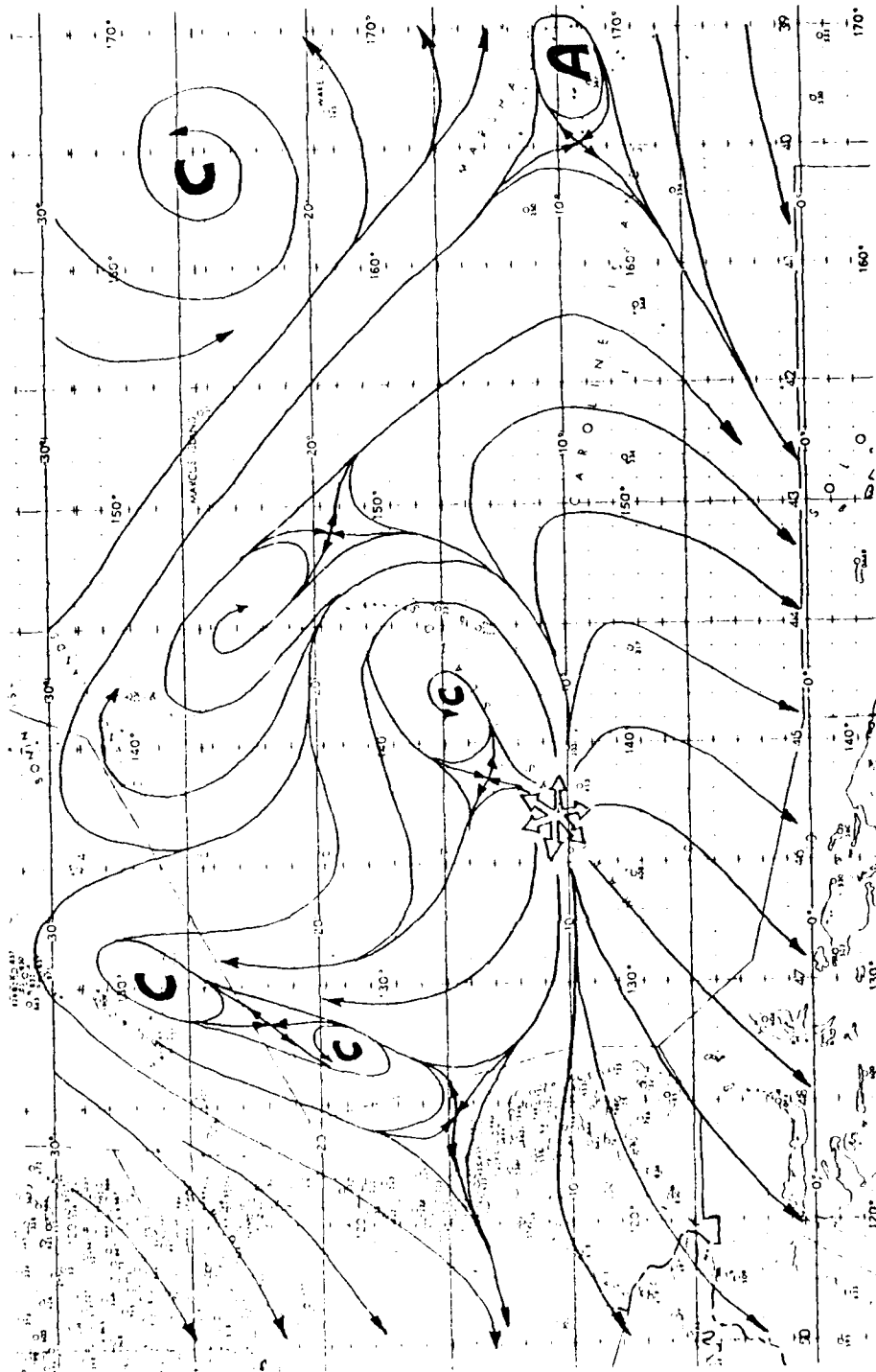


Figure 3.2b Streamline analysis for 00 UTC 14 August at 200 mb.

### Development

By 00 UTC 15 August, Yancy had developed a distinct low-level circulation center on the poleward side of the monsoon cloud mass. This dislocation was attributed to strong upper-level flow from the north and east that apparently inhibited rapid development at this time. A strongly divergent flow became established over the storm on 17 August, with outflow branches into the equatorial easterlies and into the major TUTT cell described in Fig. 3.2b. Relatively rapid deepening to maximum intensity followed. Weakening and decay were directly attributable to the close track past the Taiwan mountains. A slow final decay stage followed landfall in the Yangtze valley.

A significant feature of Typhoon Yancy is that the system formed within a large monsoonal trough (Fig. 3.1). As a result, Yancy was a very large cyclone that seemed to increase in size as it moved westward (Fig. 3.3).

### Movement

During the formation stage, the movement of Yancy was erratic as mesoscale systems developed, decayed and then were replaced by new systems. The overall monsoon trough seemed to move westward during this time. The early northward movement in Fig. 3.1 was probably a result of redevelopment of the circulation within the northern convective regime, rather than an advective movement of one system.

A 48-h period of rapid westward movement followed as the cyclone developed to typhoon strength. The seemingly simple, westward track belies the forecast difficulties that were experienced. During the night of 16 August, the center became very difficult to locate under a central cloud mass. One option that was vigorously debated was that Yancy would turn towards a short-wave trough in the westerlies and recurve. The guidance from numerical models also was ambivalent. Whereas the European Centre for Medium-range Weather Forecasts (ECMWF) and the Japan Meteorological Agency global models moved Yancy northward, the One-way influence Tropical Cyclone Model (OTCM) maintained a westward track. The cyclone also executed a mesoscale oscillation as it moved past Taiwan. Although not resolved on the general track in Fig. 3.1, the low-level circulation in Yancy moved southward along the western coast of Taiwan for several hours before redeveloping under the westward-moving midlevel circulation.

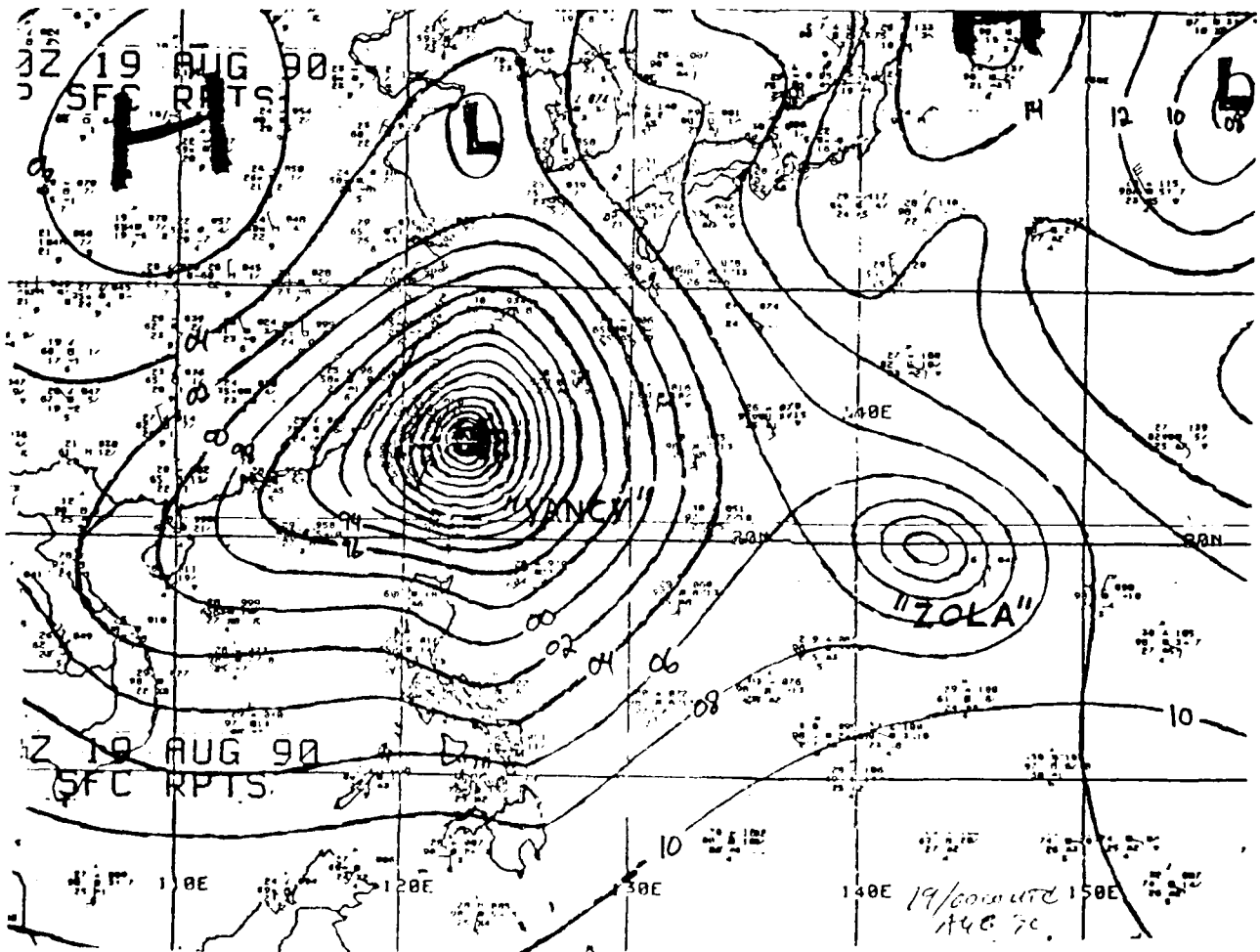


Figure 3.3 Mean-sea-level pressure (mb) analysis by M. Lander for 00 UTC 19 August that indicates the large horizontal extent of Typhoon Yancy and the trailing circulation that would become Typhoon Zola.

## Hypotheses and Research Aspects

1. Interactions with the subtropical ridge. The rapid westward movement of Yancy was evidently associated with the strong subtropical ridge that was maintained on its poleward side. During August 16, a short-wave midlatitude system was moving eastward and an apparent break in the ridge developed poleward of the cyclone (Fig. 3.4). The detailed interactions that occurred could provide valuable information as to why such cyclones fail to recurve. This case should provide a test of the TCM-90 hypothesis on the westward extension of the subtropical ridge induced by interaction with tropical cyclones.

2. Cyclone outer structure. Previous research has shown that the motion of a tropical cyclone is quite sensitive to details in its outer wind structure. Typhoon Yancy was very large and had strong flows in the southwesterly monsoon and in the trade easterlies. These strong winds seemed to be generated in situ, rather than result from external surges. Further study is recommended on the mechanisms that led to this structure and the impact on the cyclone motion. A key question is the fraction of the rapid translation that was due to propagation versus advective components.

3. Interaction with Taiwan. The major deviation of the track during interaction with Taiwan was captured with detailed conventional, Doppler radar and profiler observations by TATEX. Analysis of these data should further improve knowledge of the effects of obstacles on tropical cyclone motion.

## Data Coverage

A summary of the upper-air coverage is given in Table 3.1. Data system notes 3, 4 and 5 above apply to the upper-air coverage. Maps of the coverage are similar to Figs. 2.7 and 2.8.

The radar wind profiler at Kadena, Okinawa was operational during this IOP. Real-time transmission of the Saipan wind profiler observations each 6 h had begun.

The preliminary satellite archive summary (see data coverage note 7 above) is given below. No GMS imagery was collected at the Australian Bureau of Meteorology due to a mainframe failure.

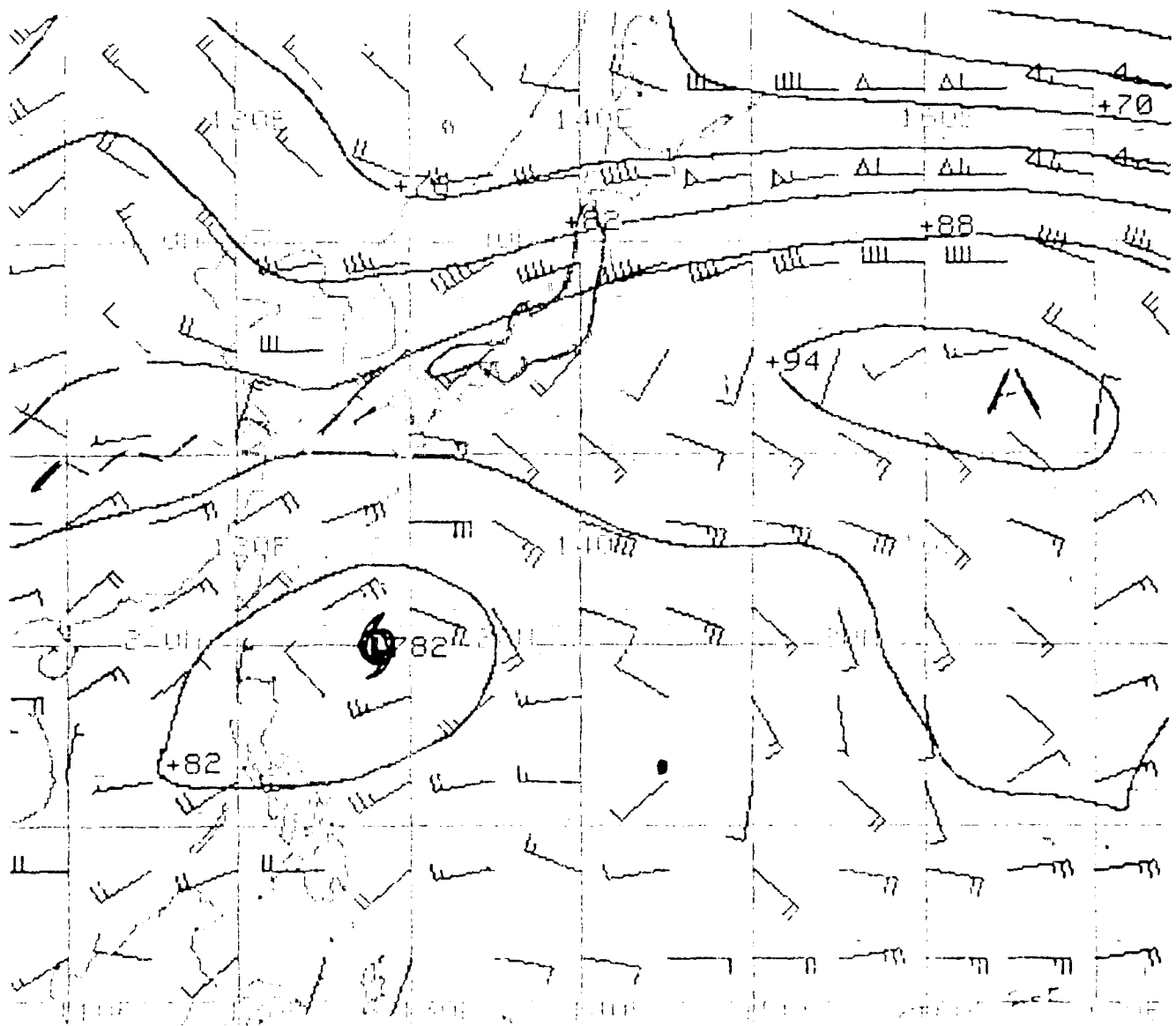


Figure 3.4 NOCAPS 500 mb analysis for 12 UTC 16 August that indicates the midlatitude short-wave trough and the break in the subtropical ridge. Heights are in decameters and each full wind barb is 10 kt (5 m s<sup>-1</sup>).

*IOP-2, 90081512 - 90081712, TY YANCY*

NO.	STATION	0815		0816				0817		
		12	18	00	06	12	18	00	06	12
BLOCK 45 (HONG KONG)										
1	45004	X	X	X	X	X	X	X	X	X
BLOCK 47 (KOREA)										
2	47122	X	X	X	X	X	X	X	X	X
3	47138	X	X	X	X	X	X	X	X	X
4	47158	X	X	X	X	X	X	X	X	
5	47185	X	X	X	X	X	X	X	X	X
BLOCK 47 (JAPAN)										
6	47582	X	X	X	X	X	X	X	X	X
7	47590	X	X	X	X	X	X	X	X	X
8	47600	X	X	X	X	X	X	X	X	X
9	47678	X	X	X	X	X	X	X	X	X
10	47744	X	X	X	X	X	X	X	X	X
11	47778	X	X	X	X	X	X	X	X	X
12	47807	X	X	X	X	X	X	X	X	X
13	47827	X	X	X	X	X	X	X	X	X
14	47909	X	X	X	X	X	X	X	X	X
15	47915	X	X	X	X	X	X	X	X	X
16	47936	X	X	X	X	X	X	X	X	X
17	47945	X	X	X	X	X	X	X	X	X
18	47971	X		X	X	X		X		X
19	47991	X		X	X	X		X	X	X
BLOCKS 48,96 (THAILAND, MALAYSIA)										
20	48327	X		X	X	X	X	X	X	X
21	48407	X	X	X	X	X	X	X	X	X
22	48455	X	X	X	X	X	X	X	X	X
23	48568	X	X	X	X	X	X	X	X	X
24	48615	X		X	X	X		X	X	X
25	48648	X		X	X	X		X	X	X
26	96413	X		X	X	X		X		X
27	96471	X			X	X		X	X	X

**Table 3.1** Upper-air soundings during IOP 2.

*IOP-2 (continued)*

NO.	STATION	0815		0816				0817		
		12	18	00	06	12	18	00	06	12
BLOCKS 54,57,58,59 (PEOPLES REPUBLIC OF CHINA)										
28	54857	X	X	X	X	X	X	X	X	X
29	57083	X	X	X	X	X	X	X	X	X
30	57494	X	X	X	X	X		X	X	X
31	57972	X	X	X	X	X	X	X	X	X
32	58150	X	X	X	X	X	X	X	X	X
34	58457	X	X	X	X	X	X	X	X	X
34	58847	X	X	X	X	X	X	X	X	X
35	59316	X	X	X	X	X	X	X	X	X
36	59758	X	X	X	X	X	X	X	X	X
37	59981	X	X	X	X	X	X	X	X	X
BLOCK 98 (PHILIPPINES)										
38	98223									
39	98327	X		X		X	X	X	X	X
40	98426						X	X		X
41	98444									
42	98646		X	X	X	X	X	X	X	X
43	98753									
44	98851									
BLOCK 91 (PACIFIC ISLANDS, NATIONAL WEATHER SERVICE)										
45	91217	X	X	X	X	X	X	X	X	X
46	91232	X	X	X	X	X	X	X	X	X
47	91334	X	X	X	X	X	X	X	X	X
48	91348	X		X		X		X		X
49	91408	X		X	X	X	X		X	
50	91413	X	X	X	X	X	X	X	X	X
BLOCK 47 (IWO JIMA)										
51	47000	X			X	X		X		X
BLOCK 46 (TAIWAN)										
52	46692	X		X	X	X	X	X	X	X
53	46699	X		X		X		X		X
54	46734	X		X	X	X	X	X	X	X
55	46747	X		X		X		X		X
56	46759									
57	46780									
58	46810					X				
SHIPS										
1	IRIH	X	X	X	X	X	X		X	X
2	IRH	X		X		X	X	X	X	X
3	UIQS	X	X	X	X	X	X	X	X	X
4	UMAY	X	X	X	X	X	X	X	X	X
5	JBOA				X	X	X	X	X	X
6	JCCX	X	X	X	X	X	X	X	X	



Satellite Soundings (# reports in 24 hrs)

	8/15	8/16	8/17
NOAA10	985	1290	1308
NOAA11	1070	1284	1306
DMSP8	567	593	601
DMSP9	697	717	419

Satellite Winds (# vectors)

	8/15	8/16	8/17
00 UTC		198	166
06			
12		120	112
18	41	77	

Satellite Imagery

8/15	8/16	8/17
No GMS	No GMS	No GMS
17 UTC NOAA11 pass	10 UTC NOAA10 pass	10 UTC DMSP8 pass
09 UTC DMSP8 pass	05 & 17 UTC NOAA11 passes	
	22 UTC DMSP8 pass	

Summary

Intensive Observation Period (IOP) 3 from 00 UTC 18 August to 00 UTC 20 August was initiated to capture the movement of Typhoon Yancy (13W) as it approached Taiwan. However, Tropical Storm Zola (14W) was developing to the southeast of Guam during this period. Because TS Zola made a sudden and unpredicted left turn (Fig. 4.1), it should provide an excellent case study of the processes that caused the change in direction. Interaction with a Tropical Upper-Tropospheric Trough (TUTT) occurred during this period. Interaction with an adjacent ridge may have played an important role in the left turn during IOP 3 and the subsequent track to the northwest and then later in the recurvature. Unfortunately, an IOP could not be called during the recurvature period because the USSR ships had begun the transit to replenish and the SPECTRUM group did not consider it to be a suitable case. Nevertheless, 12-h observations will be available in most of the domain and some 6-h observations are available from the Japanese stations in the path of Typhoon Zola.

Formation

The first indication of the formation of a tropical low at the surface became evident at 00 UTC 15 August to the southeast of TY Yancy. This low center near  $5^{\circ}\text{N}$ ,  $155^{\circ}\text{E}$  was embedded in the monsoon trough. Northeasterly winds at 200 mb over the system were approximately  $15\text{ m s}^{-1}$  (30 kt). A cloud cluster was evident in the satellite imagery to the southwest of an active region of monsoonal convective activity. The Naval Operational Global Atmospheric Prediction System (NOGAPS) 500 mb analysis had a weak cyclonic circulation near  $18^{\circ}\text{N}$ ,  $161^{\circ}\text{E}$  with about  $10\text{ m s}^{-1}$  (15-20 kt) easterlies northward to the subtropical ridge around  $32^{\circ}\text{N}$ . This circulation was evident prior to the development of the surface circulation. Based on the satellite imagery, indications of development prior to detection of the surface circulation were poor as only widespread convective activity was expected.

On 16 August, strong monsoonal convection was occurring to the south of the low-level circulation center near  $18^{\circ}\text{N}$ ,  $144^{\circ}\text{E}$ . Divergent flow existed at 200 mb above the system. By 2330 UTC 16 August, TD 14W (Zola) was at  $15.9^{\circ}\text{N}$ ,  $143.5^{\circ}\text{E}$  while Typhoon Yancy was near  $20^{\circ}\text{N}$ ,  $127^{\circ}\text{E}$ . A small deep convective cloud blob was located on the northwest tip of a slightly curved convective cloud band. This band was on the eastern side of a highly convective cloud mass. Since no central dense overcast was present, the Dvorak T number was 1.0. A marked outflow channel toward the southwest at 200 mb was present about 7 deg. lat. west-southwest of TD 14W (Zola). The 500 mb flow over the system had strengthened to  $7\text{ m s}^{-1}$  (15 kt) from the southwest while the ridge axis remained near  $33^{\circ}\text{N}$ .

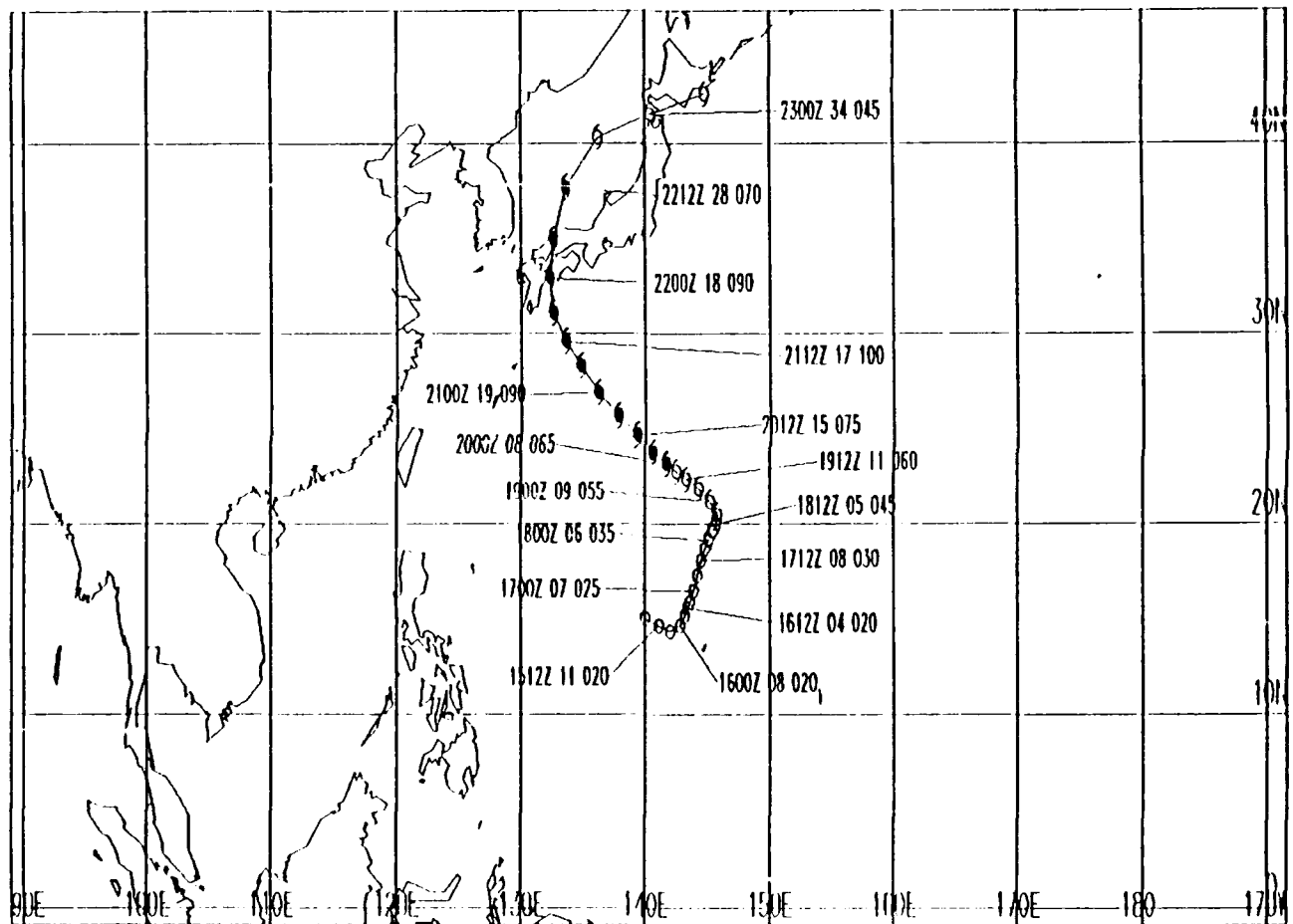


Figure 4.1 Working best track of Typhoon Zola between 06 UTC 15 August and 00 UTC 23 August 1990. Symbols are the same as in Fig. 2.1.

Slow intensification of TD 14W (Zola) was expected as the low-level circulation center was adjacent to the deep convection. The displacement of the low-level circulation center from the deep convection was possibly due to the vertical shear on the western side.

At 00 UTC 18 August, TD 14W (Zola) was given a Dvorak T 1.5. Outflow from the TD appeared to be enhanced due to the presence of a TUTT almost due north near  $28^{\circ}\text{N}$ . As development continued, TD 14W (Zola) was upgraded to a Tropical Storm (TS) at 06 UTC 18 August. The  $15\text{--}25\text{ m s}^{-1}$  (30-50 kt) winds associated with a monsoon surge to the south and west of TS Zola appeared to have been drawn closer to the system. By 00 UTC 19 August, the maximum winds were estimated to be  $27\text{ m s}^{-1}$  (55 kt). The circulation around Zola was much smaller than that associated with Typhoon Yancy (see Fig. 3.3). During 19 August, the deep convection associated with Zola began to be separated from an east-west band of deep convection to the south of the system. A warm spot in the night-time infrared imagery indicated a possible eye formation. Zola was upgraded to typhoon status at 00 UTC 20 August when it had a ragged and poorly defined eye. As Zola intensified through the day, the cloud signature became more concentric. The TUTT cell may have contributed to the intensification by enhancing the outflow.

### Motion

One of the common problems for the forecaster is to determine an accurate position and initial motion vector during the early stages of development. This is especially true when several mesoscale circulations are embedded in a monsoon trough. Following the diurnal convection maximum (early morning), a different circulation center may become dominant. Positioning on the new system may lead to a sharp change in speed and direction, which then establishes a fictitious persistence vector. Such an event occurred on 16 August when a new position was estimated to be near  $13^{\circ}\text{N}$ ,  $143^{\circ}\text{E}$  (Fig. 4.1).

The 500 mb steering flow on 16 August indicated the system should move to the north-northeast. Since the subtropical ridge was around  $33^{\circ}\text{N}$ , nothing was evident to impede this storm track. Between 17 and 18 August, a midlatitude trough had moved from the Japan Sea to the east of Japan, but the southern extent of the trough was limited by the subtropical ridge. Another factor on 18 August was the monsoon surge to the south and west of Zola. Thus, a northeastward motion seemed reasonable.

By 00 UTC 19 August, it became evident that TS Zola had executed a sharp left turn (Fig. 4.1). Zola was centered at  $21.2^{\circ}\text{N}$ ,  $145.6^{\circ}\text{E}$  and moving toward  $320$  deg. at  $4.5\text{ m s}^{-1}$  (9 kt). Such a change to a northwest track might be associated with the strengthening of the ridge to the north (Fig. 3.3). The question for the researcher is what led to the sudden track change. The objective track forecast aids were not helpful in anticipating

the left turn. The question for the forecaster was whether this was a short-term change that would be followed quickly by a resumption of the northeastward track (and thus produce a "small S" track). The alternative was that the period of northwestward track would continue for some time before the storm recurved toward the northeast (a "big S" track). That is, it is important for the forecaster to understand what caused the left turn, and whether this condition would continue the northwest track for a short time or a long time.

By 20 August, it seemed clear that Zola would continue on a northwest track for at least another 24 h. Zola was expected to accelerate due to a stronger steering flow. After about 48-72 h, a more northward track was expected around the western flank of the 500 mb ridge. The forecast aids supported this scenario with a predicted recurvature near 32°N. As indicated above, an IOP was not called to capture this stage with 6-h observations.

### Hypotheses

The key question during IOP 3 was the cause of the sharp left turn of TS Zola around 20°N. Interaction with the adjacent ridge appears to be one alternative. Another alternative is a change from a steering flow associated with the monsoon trough to one associated with the low-latitude ridge. It is uncertain whether the intensification of the tropical cyclone had any effect during the left turn. The subsequent acceleration of the storm to the northwest following the turn is also believed to be associated with an interaction between the tropical cyclone and the adjacent ridge.

An interaction with a TUTT cell may have contributed to the intensification of Zola. The role of the TUTT cell in the left turn of the track and in the subsequent acceleration to the northwest are less clear.

### Data Coverage

This IOP is a continuation of IOP 2 with a gap at the 18 UTC 17 August for the TCM-90, but a continuous IOP for SPECTRUM. Consequently, the data coverage in Table 4.1 is similar to Table 3.1.

The Bureau of Meteorology mainframe failure prevented any GMS imagery collection. In addition, a lightning strike caused a power outage at the University of Wisconsin on the afternoon of 18 August that continued through 19 August. Efforts are in progress to replace the satellite wind and polar-orbiter imagery.

Table 4.1 Upper-air soundings during IOP 3.

*IOP-3, 90081800 - 90082000, TY YANCY, TY ZOLA*

NO.	STATION	0818				0819				0820
		00	06	12	18	00	06	12	18	00
BLOCK 45 (HONG KONG)										
1	45004	X	X	X	X	X	X	X	X	X
BLOCK 47 (KOREA)										
2	47122	X		X	X	X	X	X	X	X
3	47138	X		X	X	X		X	X	X
4	47158	X		X	X	X		X	X	X
5	47185	X		X	X	X		X	X	X
BLOCK 47 (JAPAN)										
6	47582	X		X	X	X		X	X	X
7	47590	X		X	X	X		X	X	X
8	47600	X		X	X	X		X	X	X
9	47678	X		X	X	X		X	X	X
10	47744	X		X	X	X		X	X	X
11	47778	X		X	X	X		X	X	X
12	47807	X		X	X	X		X	X	X
13	47827	X		X	X	X		X	X	X
14	47909	X		X	X	X		X	X	X
15	47918	X		X	X	X		X	X	X
16	47936	X		X	X	X		X	X	X
17	47945	X		X	X	X		X	X	X
18	47971	X		X		X		X		X
19	47991	X		X		X		X		X
BLOCKS 48,96 (HILAND, MALAYSIA)										
20	48327	X	X	X	X	X		X	X	X
21	48407	X	X	X	X	X		X	X	X
22	48455	X	X	X	X	X		X	X	X
23	48568	X	X	X	X	X		X	X	X
24	48615	X		X	X	X		X	X	X
25	48648	X		X	X	X		X		X
26	96413	X		X	X	X		X		X
27	96471	X		X	X	X		X	X	X

Table 4.1 Upper-air soundings during IOP 3, continued.

NO.	STATION	0818				0819				0820
		00	06	12	18	00	06	12	18	00
BLOCKS 54,57,58,59 (PEOPLE'S REPUBLIC OF CHINA)										
28	54857	X		X	X	X		X	X	X
29	57083	X	X	X	X	X		X	X	X
30	57494	X	X	X	X	X		X	X	X
31	57972	X	X	X	X	X		X	X	X
32	58150	X	X	X	X	X		X	X	X
33	58457	X	X	X	X	X		X	X	X
34	58847	X	X	X	X	X		X	X	X
35	59316	X	X	X	X	X		X	X	X
36	59758	X	X	X	X	X		X	X	X
37	59981	X		X	X	X		X	X	X
BLOCK 98 (PHILIPPINES)										
38	98223									
39	98327	X		X		X		X		X
40	98426									
41	98444									
42	98646	X		X	X	X		X	X	X
43	98753									
44	98851									
BLOCK 91 (PACIFIC ISLANDS, NATIONAL WEATHER SERVICE)										
45	91217	X	X	X		X	X	X	X	X
46	91232	X	X	X	X	X		X		X
47	91334	X				X		X		X
48	91348	X		X		X		X		X
49	91408	X		X		X		X		
50	91413	X		X		X		X		X
BLOCK 47 (IWO JIMA)										
51	47000	X		X	X	X	X			
BLOCK 46 (TAIWAN)										
52	46692	X		X	X	X		X	X	X
53	46699	X		X	X	X		X		X
54	46734	X		X	X	X		X		X
55	46747	X		X				X	X	
56	46759									
57	46780									
58	46810							X		X
SHIPS										
1	FR11	X		X	X	X	X	X	X	X
2	FR11	X	X	X	X	X	X	X	X	X
3	CHQS	X	X	X	X	X	X	X	X	X
4	UNLAY	X	X	X	X	X		X	X	
5	BROA	X		X	X	X		X	X	X
6	CCX	X			X	X		X	X	X

Satellite Soundings (# reports in 24 hrs)

	8/18	8/19
NOAA10	1698	1322
NOAA11	1418	1299
DMSP8	352	447
DMSP9	665	536

Satellite Winds (# vectors)

	8/18	8/19	8/20
00 UTC	149		159
06	138		
12			
18		84	

Satellite Imagery

	8/18	8/19
No GMS		No GMS
No NOAA or DMSP		No NOAA or DMSP



### Summary

Dot (18W) formed in the vicinity of Saipan, reached tropical storm intensity on 4 September and steadily intensified to a maximum intensity of 35-40 m s<sup>-1</sup> (75 kt) on 7 September. The initial track was west-southwestward (Fig. 5.1). After reaching tropical storm intensity, Dot turned to the northwest and maintained a nearly straight track to landfall on central Taiwan. Translation speeds varied between 5 and 8 m s<sup>-1</sup>.

The major features of interest to the experiment were: the sustained northwestward track, during which the subtropical ridge continued to develop westward; and the development and maintenance of a sharp TUTT shearline just poleward of the convection associated with Dot.

### Formation

Dot formed near 15°N just equatorward of a region of strong tradewinds and poleward of a convergence between moderate equatorial easterly and westerly flows (Fig. 5.2a). Whereas the strong tradewind flow preceded cyclone formation, the equatorial westerly flow seemed to develop in situ. Divergent upper-tropospheric flow was analyzed over the region and a sharp TUTT was just poleward (Fig. 5.2b). This TUTT was clearly evident from the sharp poleward edge of the developing convective cluster.

### Development

After reaching tropical storm strength on 4 September, Dot developed steadily to a maximum intensity of around 35-40 m s<sup>-1</sup> (75 kt) early on 7 September. At this stage, Dot was a medium-sized typhoon (Fig. 5.3a) and extensive southwesterly monsoonal flow had developed on its equatorward side.

A sharp TUTT remained to the north of the typhoon (Fig. 5.3b) and was associated with the marked cloud-free zone in the satellite imagery. Although a TUTT preceded the development of Dot, it was apparent that significant interactions were occurring between the two systems. One possible mechanism is that the TUTT moved to, or developed in, the region of sustained subsidence from the tropical convective mass.

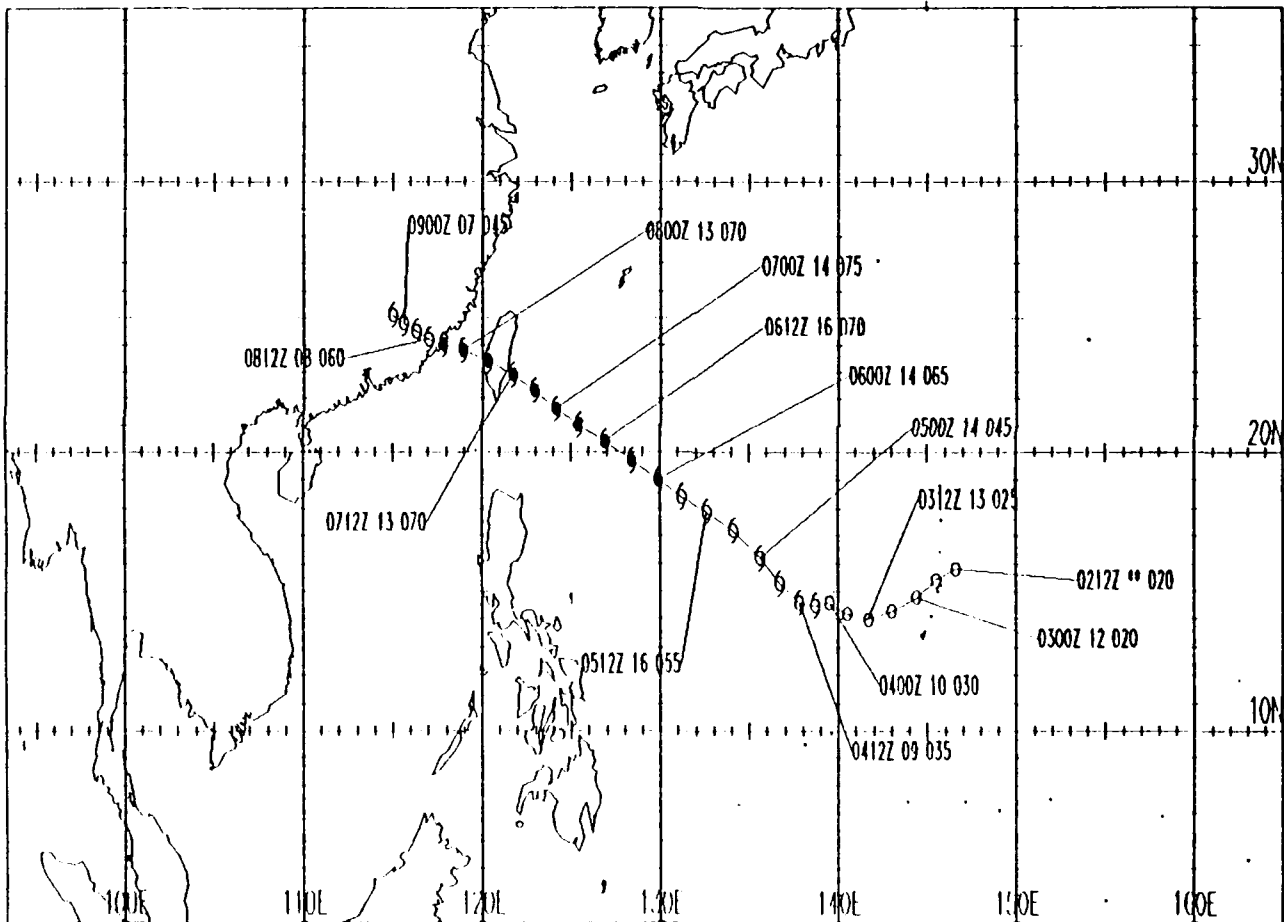


Figure 5.1 Working best track of typhoon Dot between 12 UTC 2 September and 18 UTC 7 September. Symbols are the same as in Figure 2.1.

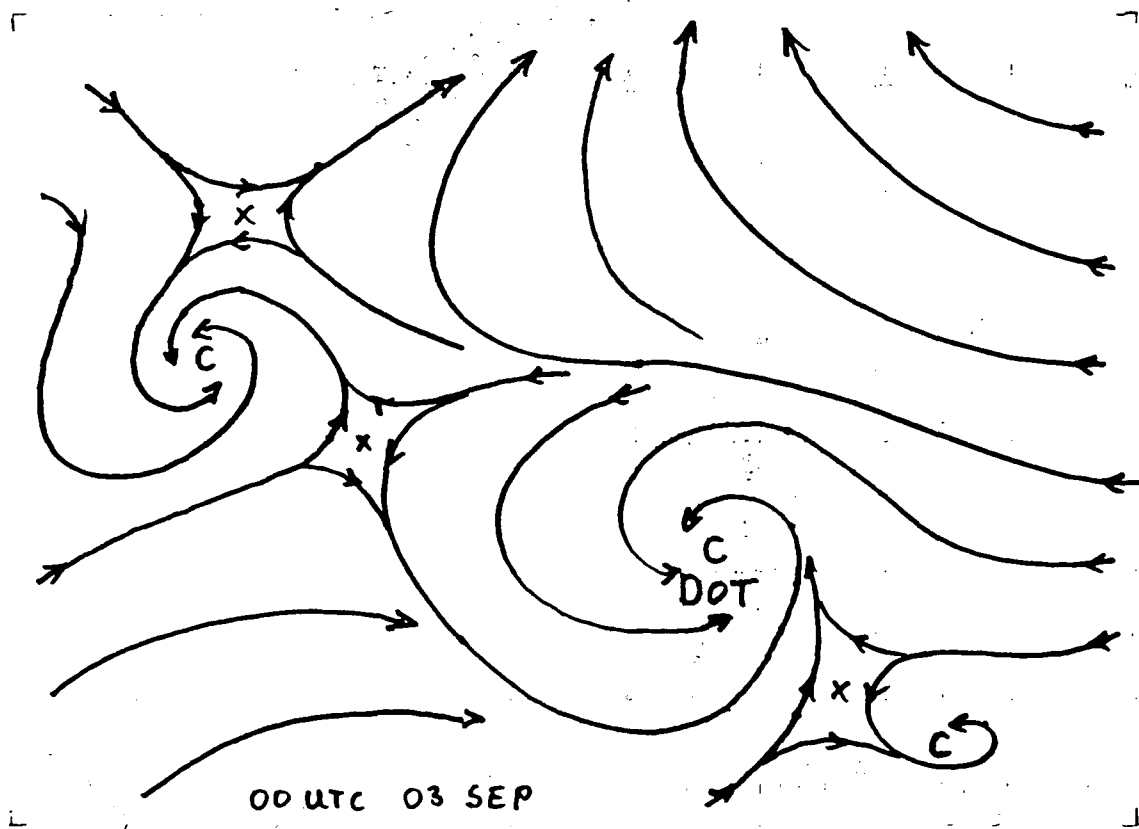


Figure 5.2a Streamline analyses for 00 UTC 3 September at the gradient level. Winds of greater than  $15 \text{ m s}^{-1}$  are stippled.

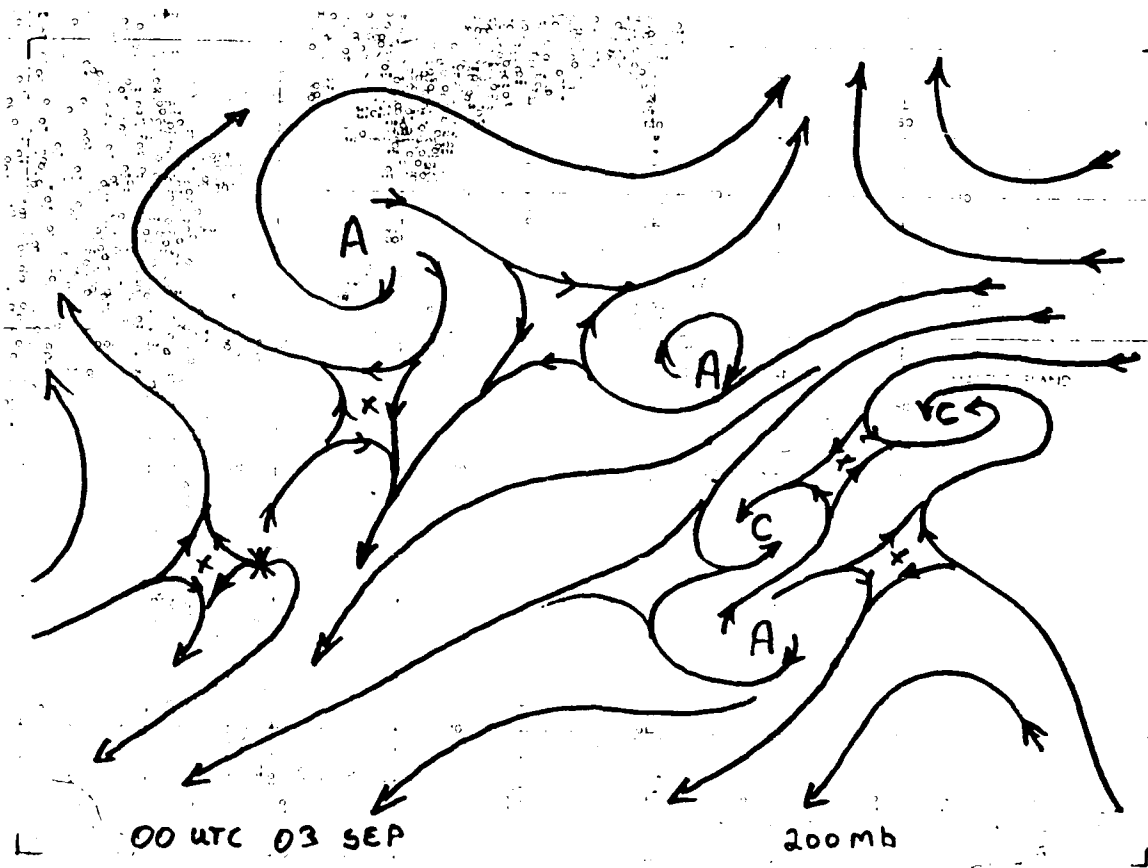


Figure 5.2b Streamline analysis for 00 UTC 3 September at 200 mb.

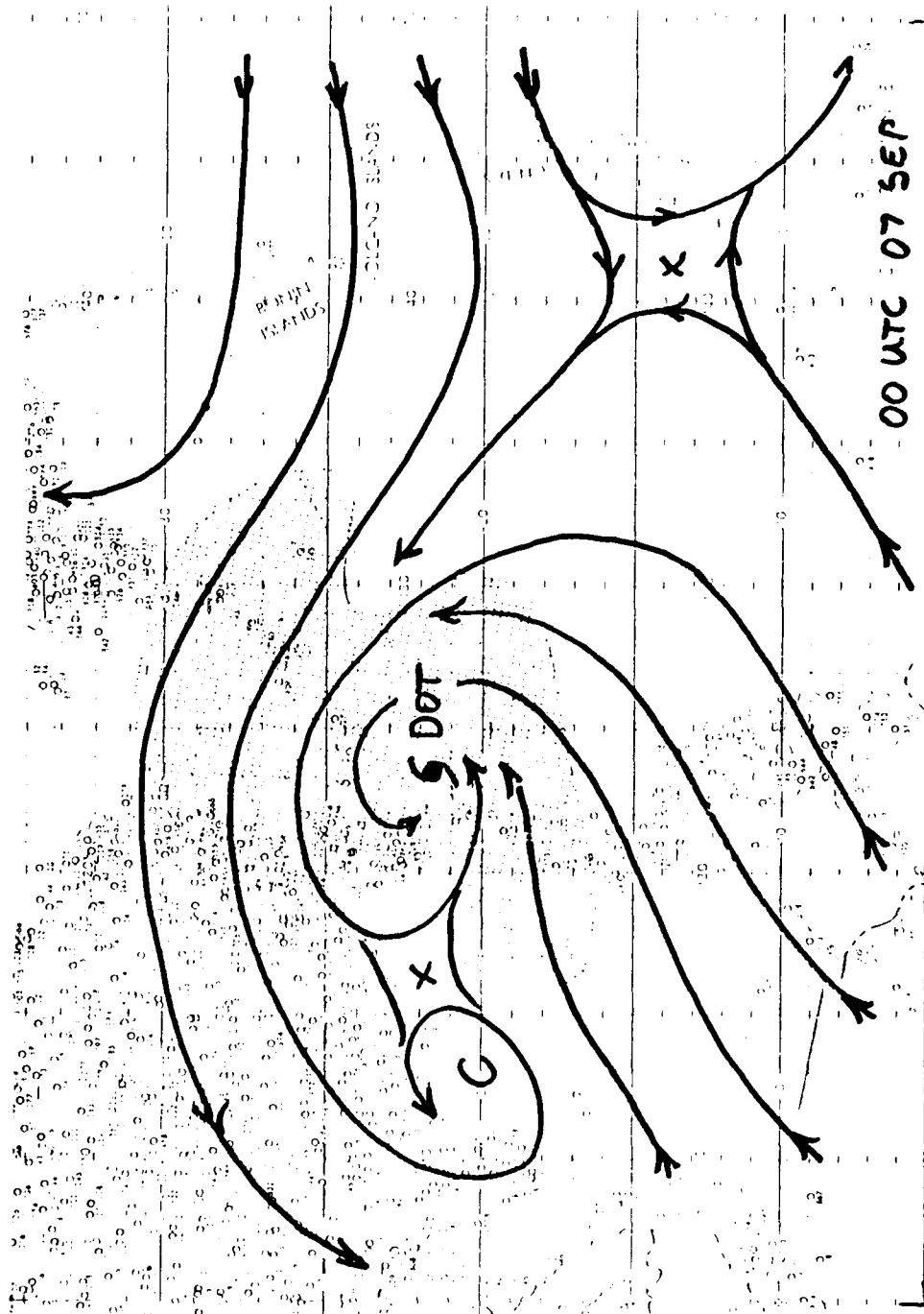


Figure 5.3a Streamline analyses for 00 UTC 7 September at the gradient level. Winds of greater than  $15 \text{ m s}^{-1}$  are stippled.

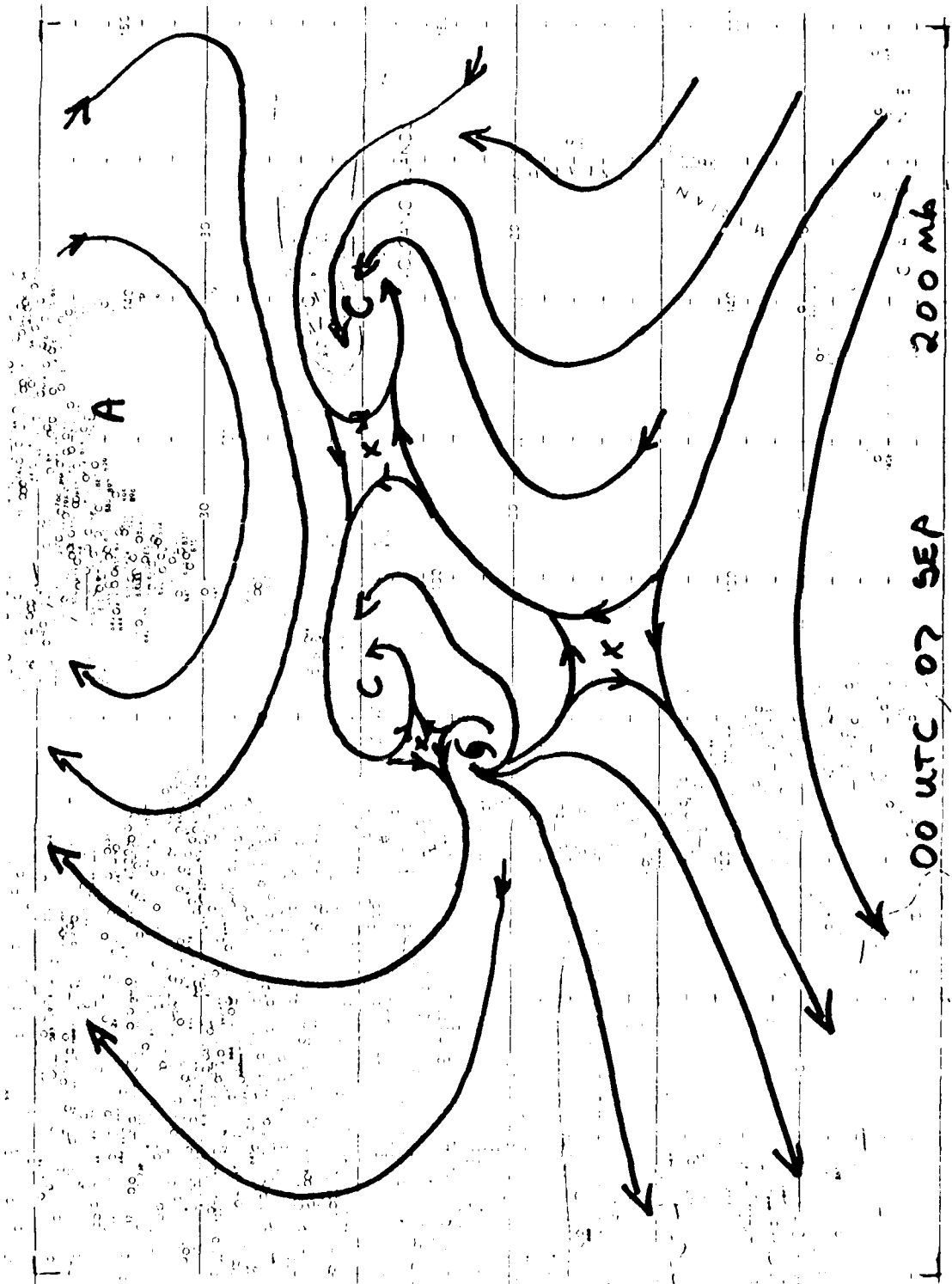


Figure 5.3b Streamline analysis for 00 UTC 7 September at 200 mb.

Dot weakened slightly as it approached Taiwan. A major disruption of the circulation followed as the typhoon moved towards and across central Taiwan during the evening of 7 September. Dot then moved into central and southern China, where it remained as a significant rain depression for several days.

### Movement

It was quite difficult to position the center of the circulation during the period before Dot reached typhoon strength. As a result, the track details during this period are subject to considerable uncertainty. Strong convective clusters tended to develop on the southeast side of the cyclone, rapidly rotate around the center, and decay on the northwest side. It is likely that the circulation center oscillated significantly in response to the development and movement of these clusters.

During 4 September, a midlatitude trough developed northwest of Dot and moved westward (Fig. 5.4a). This event generated considerable discussion among the TCM-90 participants as to whether the typhoon would recurve. Most of the numerical models predicted recurvature or a significant northward movement. However, the subtropical ridge extended steadily westward and maintained a nearly constant orientation relative to the typhoon (Fig. 5.4 b and c), which continued to move steadily northwestward (Fig. 5.1).

### Hypotheses and Research Aspects

1. Interaction with the subtropical ridge. The major feature in the steady westward motion of Dot was the concomitant westward development of the subtropical ridge. A detailed examination of this interaction is necessary to define the underlying mechanisms. In this case, it also is of considerable interest to understand why the midlatitude trough had little effect on the ridge extension.

2. Interaction with the TUTT. The apparently symbiotic relationship between the typhoon and the TUTT was fascinating. Detailed study of this relationship should improve overall understanding of how the environment and the storm mutually adjust.

### Data Coverage

This IOP following a break period after the completion of the first phase. The stations at Laoag (98232) and Legaspi (98444) in the Philippines became active in this IOP (Table 5.1). Notice that the SPECTRUM group did not start their IOP until 00 UTC 6 September and continued through to 00 UTC 8 September. Due to a failure in communications, the Pacific Island stations 91217, 91334, 91408 and 91413 also did not make a sounding at 18 UTC 5 September. Consequently, the TCM-90 IOP was extended

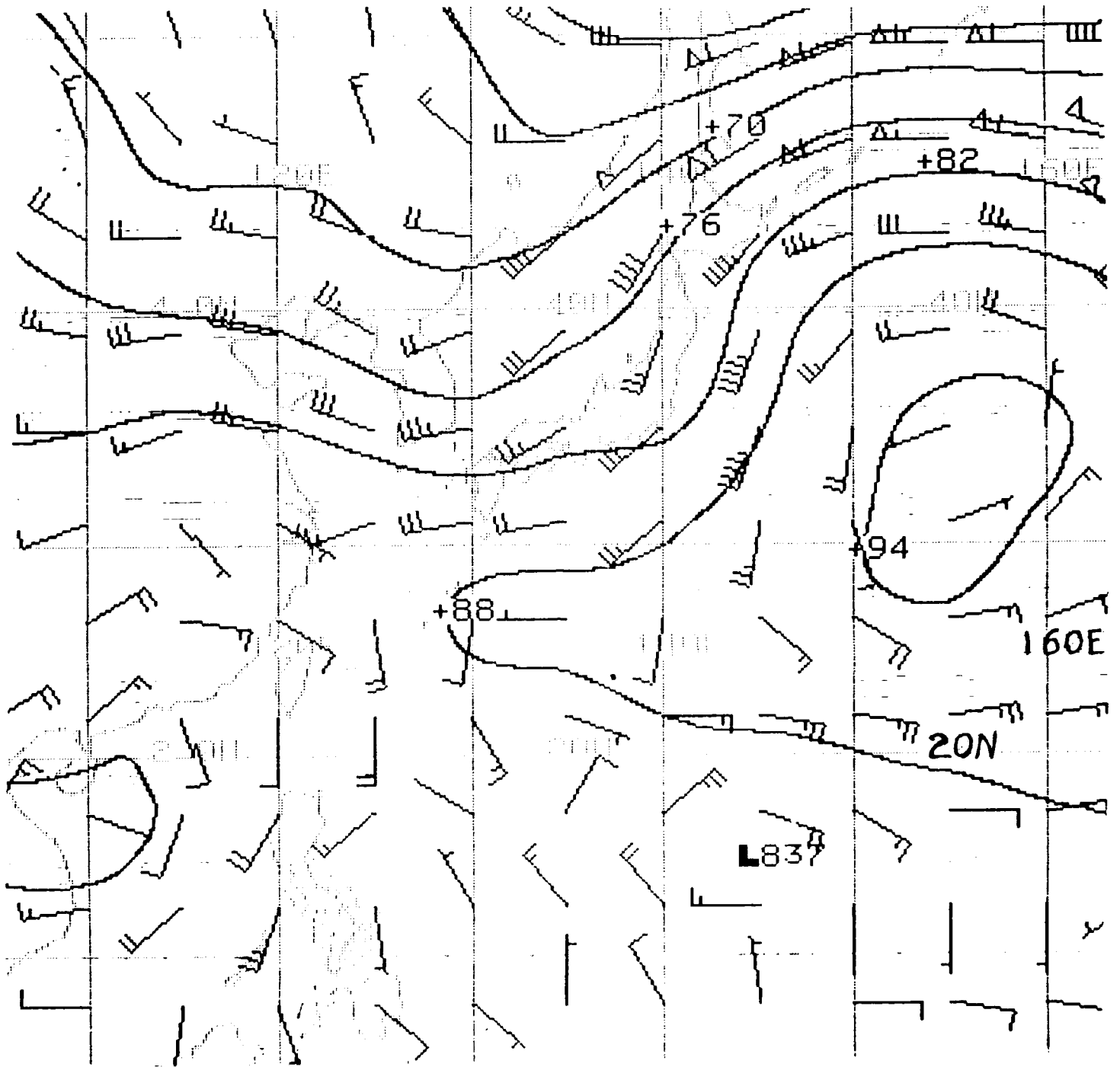


Figure 5.4a Analysis of the 500 mb winds and geopotential height fields (88 represents 5880 m) for 00 UTC on a) 3 September.



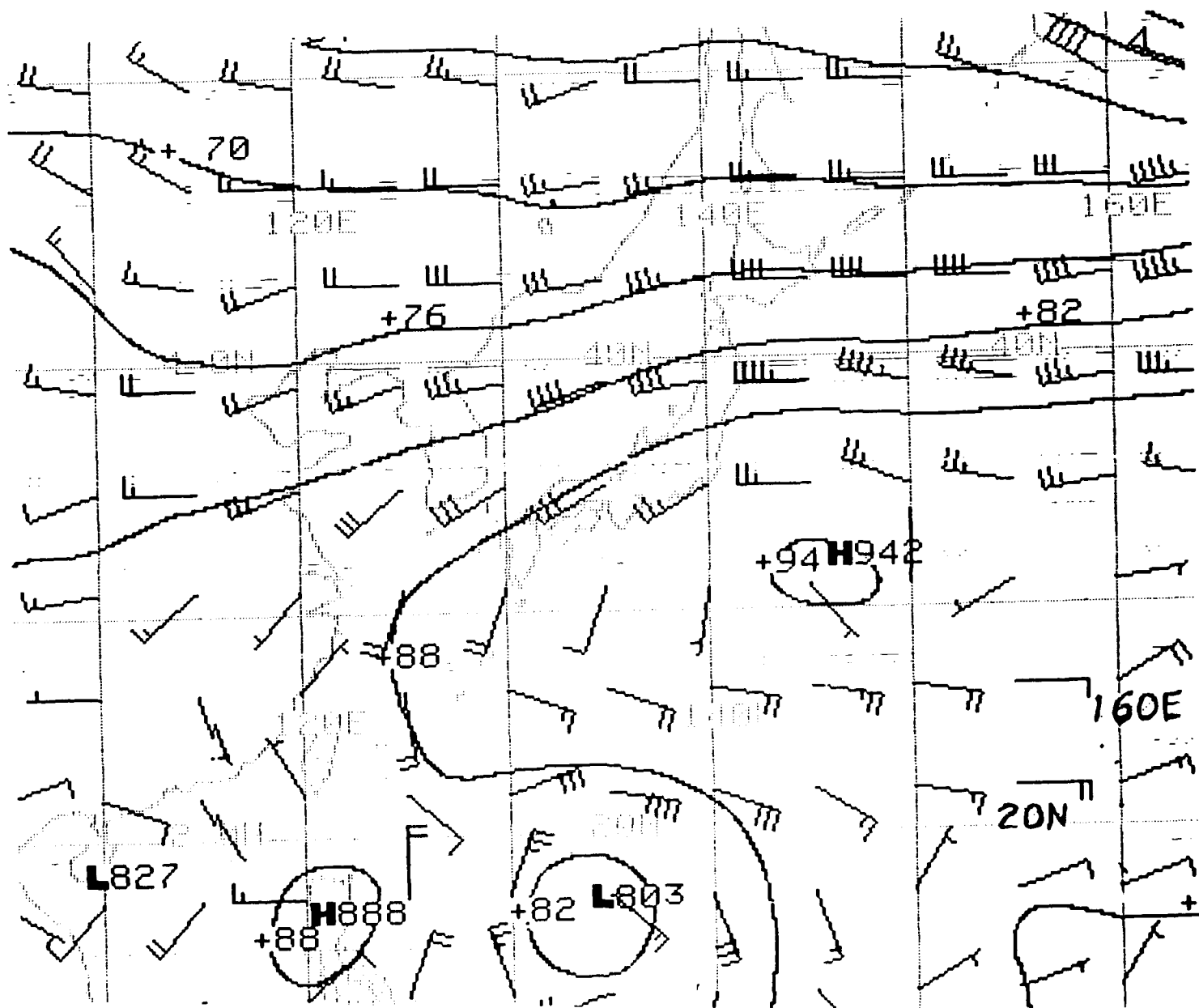


Figure 5.4b Analysis at 500 mb and geopotential height fields (88 represents 5880 m) for 00 UTC 5 September.

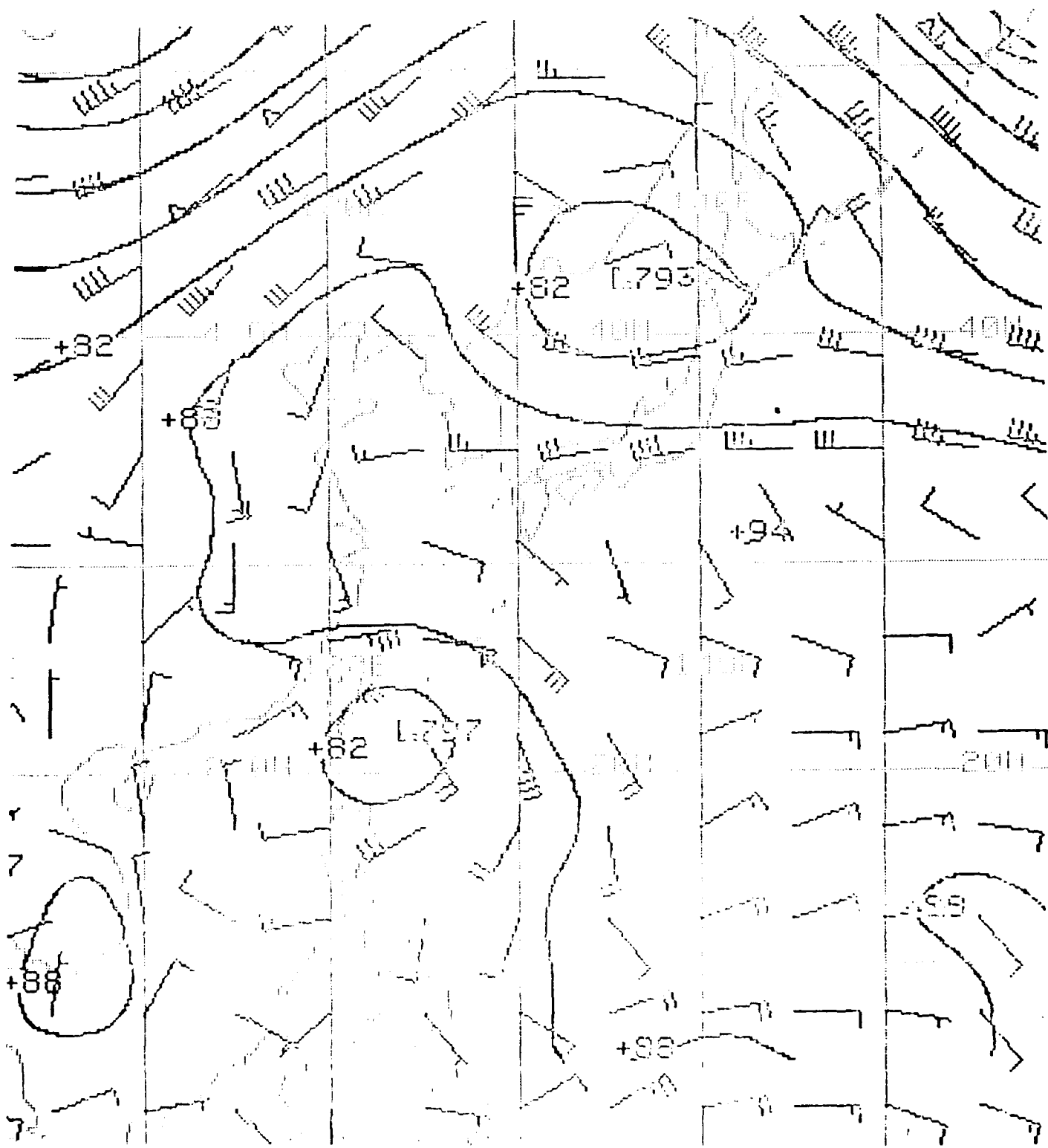


Figure 5.4c Analysis of 500 mb and geopotential height fields (88 represents 5880 m) for 00 UTC 7 September.

Table 5.1 Upper-air soundings during IOP 4.

*IOP-4, 90090512 - 90090800, TY DOT*

NO.	STATION	0905		0906				0907				0908
		12	18	00	06	12	18	00	06	12	18	00
BLOCK 45 (HONG KONG)												
1	45004	X	X	X	X	X	X	X	X	X	X	X
BLOCK 47 (KOREA)												
2	47122	X	X	X	X	X	X	X	X	X	X	X
3	47138	X		X	X	X	X	X	X	X	X	X
4	47158	X		X	X	X	X	X	X	X	X	X
5	47185	X		X	X	X	X	X	X	X	X	X
BLOCK 47 (JAPAN)												
6	47582	X	X	X	X	X	X	X	X	X		
7	47590	X		X	X	X	X	X	X	X	X	X
8	47600	X		X	X	X	X	X	X	X	X	X
9	47678	X		X	X	X	X	X	X	X	X	X
10	47744	X		X	X	X	X	X	X	X	X	X
11	47778	X		X	X	X	X	X	X	X	X	X
12	47807	X		X	X	X	X	X	X	X	X	X
13	47827	X		X	X	X	X	X	X	X	X	X
14	47909	X		X	X	X	X	X	X	X	X	X
15	47918	X		X	X	X	X	X	X	X	X	X
16	47936	X		X	X	X	X	X	X	X	X	X
17	47945	X		X	X	X	X	X	X	X	X	X
18	47971	X		X	X	X		X	X	X		X
19	47991	X		X	X	X		X	X	X		X
BLOCKS 48,96 (THAILAND, MALAYSIA)												
20	48327	X		X	X	X	X	X	X	X	X	X
21	48407	X		X	X	X	X	X	X	X	X	X
22	48455	X		X	X	X	X	X	X	X	X	X
23	48568	X		X	X	X	X	X	X	X	X	X
24	48615	X		X	X	X		X		X	X	
25	48648	X	X	X		X		X		X	X	X
26	96413	X		X		X		X			X	
27	96471			X		X		X		X	X	X

*IOP-4 (continued)*

NO	STATION	0905		0906				0907				0908
		12	18	09	06	12	18	00	06	12	18	00
BLOCKS 51, 52, 58, 59 (PEOPLE'S REPUBLIC OF CHINA)												
28	54857	X		X	X	X		X	X	X	X	X
29	57083	X		X	X	X		X	X	X	X	X
30	57494	X		X	X	X		X	X	X	X	X
31	57972	X		X	X	X		X	X	X	X	X
32	58150	X		X	X	X		X	X	X	X	X
34	58457	X		X	X	X		X	X	X	X	X
34	58847	X		X	X	X		X	X	X	X	X
35	59316	X		X	X	X		X	X	X	X	X
36	59758	X		X	X	X		X	X	X	X	X
37	59981	X		X	X	X		X	X	X	X	X
BLOCK 98 (PHILIPPINES)												
38	98223			X		X		X	X			X
39	98327	X		X		X				X		X
40	98426		X								X	
41	98444	X		X	X	X	X	X		X	X	X
42	98646			X	X		X	X	X	X	X	X
43	98753											
44	98851											
BLOCK 91 (FACIFIC ISLANDS, NATIONAL WEATHER SERVICE)												
45	91247	X		X	X	X	X	X	X	X	X	X
46	91232	X	X	X	X	X	X	X	X	X	X	X
47	91334	X		X	X	X	X	X	X	X	X	X
48	91348	X		X		X		X		X		X
49	91408			X	X	X	X	X	X	X	X	
50	91413	X		X	X	X	X	X		X		X
BLOCK 47 (TWO HIMA)												
51	47000	X		X	X	X		X	X	X	X	X
BLOCK 46 (TAIWAN)												
52	46672	X			X							X
53	46699	X		X		X		X		X		
54	46734	X	X	X	X	X		X	X	X	X	X
55	46747	X		X		X				X	X	X
56	46759											
57	46780											
58	46810	X		X			X					
SHIPS												
1	EPH	X	X	X	X	X	X	X	X	X		X
2	ERU	X	X	X	X	X	X	X	X	X		X
3	ETOS	X	X	X	X	X	X	X	X	X		X
4	ESAY			X	X	X	X	X	X	X		X
5	IBOA	X		X	X	X	X	X		X	X	X
6	ICCN	X		X	X	X	X	X	X	X	X	X

beyond the normal 48-h limit to match the ending of the SPECTRUM IOP. Unfortunately, the four USSR ships did not make a 18 UTC 7 September sounding.

The first NASA DC-8 flight was centered on 00 UTC 6 September. Detailed flight-level winds were obtained along the track south from Okinawa to 17°N, eastward along 17°N south of Dot, northward to 22°N and the westward along 22°N. Only nine dropwindsondes were released because a change in the locations of a LORAN station prevented the system from acquiring the necessary signals to calculate winds. A second DC-8 flight around 00 UTC 7 September into cloud bands east of Typhoon Dot was made only to test TRMM instrumentation.

Satellite Soundings (# reports in 24 hrs)

	9/5	9/6	9/7
NOAA10	1794	1391	1615
NOAA11	1719	1643	1636
DMSP8	473	559	480
DMSP9	562	671	549

Satellite Winds (# vectors)

	9/5	9/6	9/7	9/8
00 UTC		174	213	155
06		102	228	
12	160	134	077	
18	173	179	114	

Satellite Imagery

	9/5	9/6	9/7
All GMS	All GMS	All GMS	
17 UTC NOAA11 pass	09 & 23UTC NOAA11 passes	09 UTC NOAA 10 pass	
09 UTC DMSP8 pass	05 & 18UTC NOAA11 passes	22 UTC DMSP8 pass	
	11 & 22UTC DMSP8 passes		

Summary

Ed (19W) formed east of Guam and tracked westward for nearly two weeks while remaining at or south of about  $20^{\circ}$  N (Fig. 6.1). The distance between the first location in the Marshall Islands and the landfall point in Vietnam was about 6,000 km. Ed was upgraded to tropical depression status (TD 19W) at 00 UTC 9 September, six days after being identified as a distinct region of disturbed weather in the Marshall Islands. Tropical storm intensity was reached during 12 September and Ed became a typhoon on 14 September. The intensity remained near minimal typhoon intensity until Ed weakened near the coast of Vietnam on 18 September.

Although the track was primarily westward, some interesting direction and speed changes occurred (Fig. 6.1). A northward jog from  $13^{\circ}$ N to  $20^{\circ}$ N occurred as it approached Guam during 8 September to 10 September. Following a turn to the left on 10 September, Ed tracked due west for four days while the objective guidance was for a west-northwest track. During this period, the translation speed increased from about 10 kt on 10 September to about 16 kt on 14 September. On 14 September, Ed began an unusual west-southwest heading for two days, which brought Ed to  $16^{\circ}$ N. The translation speed decreased abruptly as this southwestward motion began. After a period of westward motion, Ed began a northwest track nearly parallel to the coast of Vietnam. The translation speed increased 2-3 kt during this period.

A westward extension (or building) of the midtropospheric subtropical ridge apparently contributed to the acceleration of Ed westward along  $20^{\circ}$ N. The unusual southwestward motion was evidently due to advection around a large-scale monsoon trough circulation that also encompassed Typhoon Flo within its circulation. Although it may be coincidental, a high pressure system over mainland China resulted in a 20-30 kt surge of northeasterly winds along the China coast from Shanghai to Hong Kong during this period. Finally, the mountains of North Vietnam evidently contributed to a propagation along the coast.

Five days of nearly continuous IOP observations were collected from 13-19 September, which includes about half of Ed's track. An upper-tropospheric mission north of the center of Ed was also accomplished by the NASA DC-8 on 13 September.

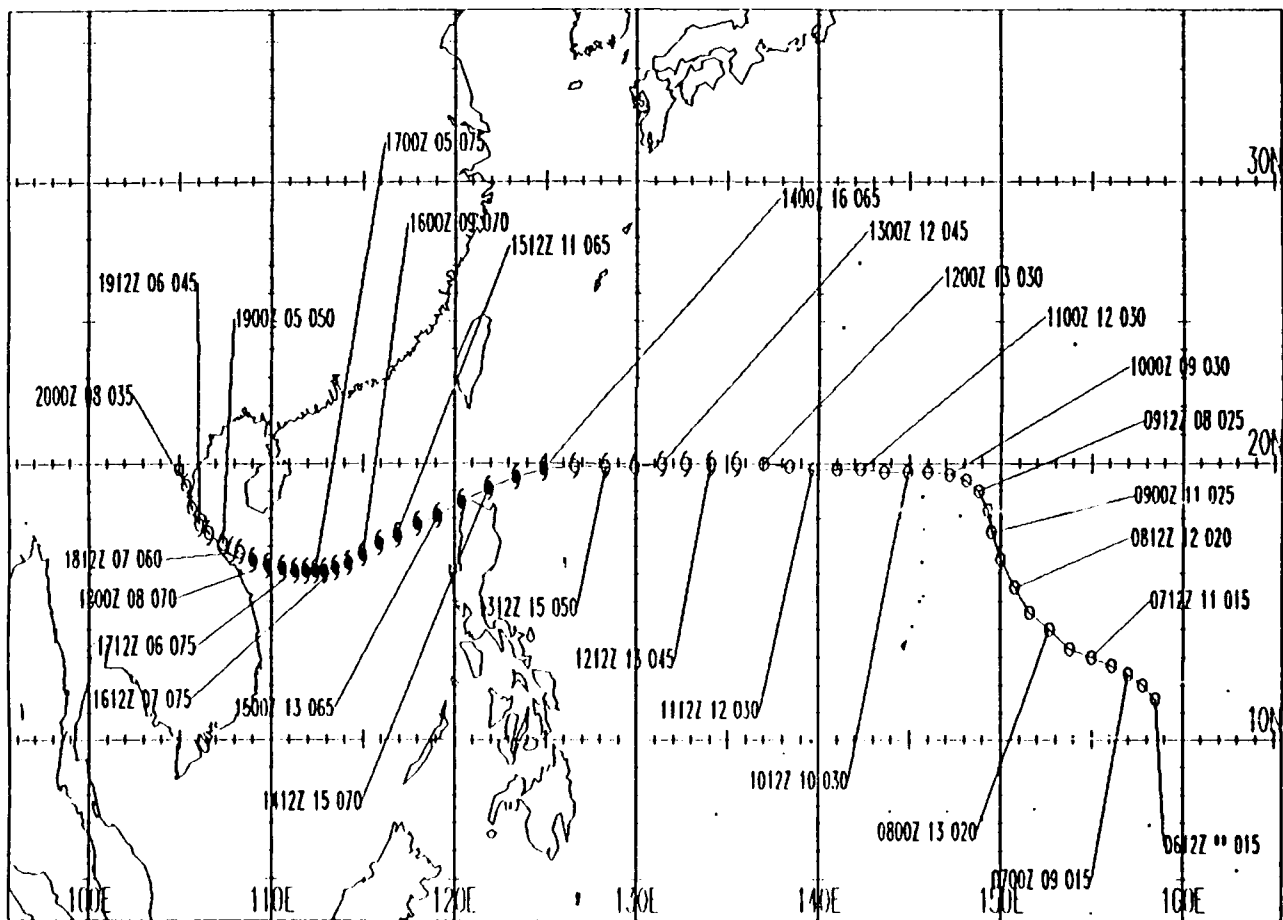


Figure 6.1 Working best track of Typhoon Ed between 12 UTC 6 September and 00 UTC 20 September. Symbols are the same as in Figure 2.1.

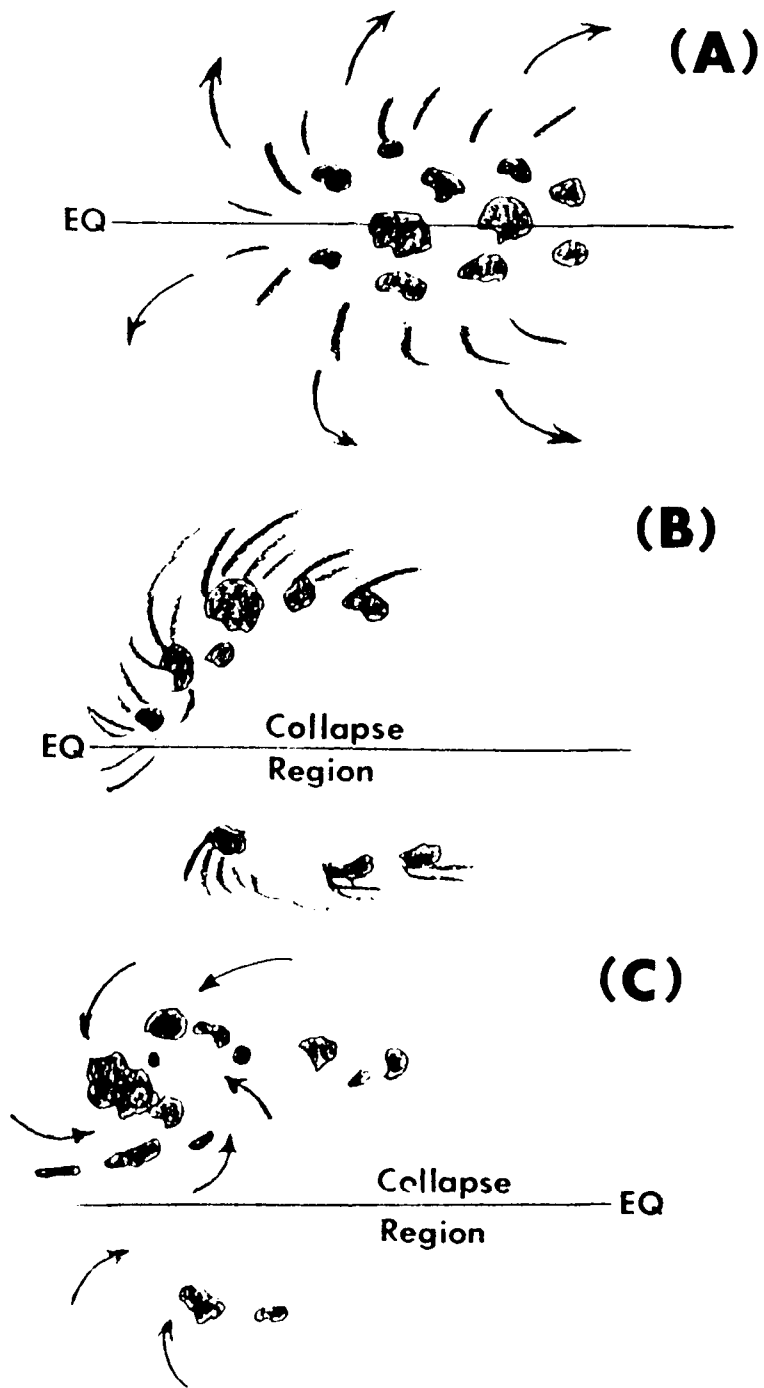


Figure 6.2 Schematic of the evolution of a supercluster of mesoscale convective systems (panel A), the subsequent collapse 24 h later (panel B) and the area of convection that was to become Typhoon Ed.



## Formation

The origins of Ed on 00 UTC 2 September can be traced to the eruption of a supercluster of mesoscale convective systems that expanded to occupy the region  $5^{\circ}\text{S}$  to  $8^{\circ}\text{N}$  between  $165^{\circ}\text{E}$  and the dateline (Fig. 6.2a). About 24 h later, most of the convection near the equator had collapsed (Fig. 6.2b). An area of new convection had developed to the north and northwest of the original supercluster (Fig. 6.2c). This loosely consolidated area of convection tracked westward along  $8^{\circ}\text{N}$ . By 00 UTC 05 September, a weak tropical depression near  $8^{\circ}\text{N}$ ,  $163^{\circ}\text{E}$  was evident from the surface synoptic data, the pattern of cumulonimbus cloud elements and the orientation of cirrus outflow streamers.

During the next two to three days, the depression tracked west-northwestward. By 00 UTC 8 September, a compact cluster of cumulonimbus clouds was about 450 n mi east of Guam. The depression had now reached the eastern periphery of a large-scale monsoon trough circulation that covered the eastern half of the Philippine Sea. Two other cloud clusters within this large monsoon circulation appeared to have the potential to become tropical cyclones. One system was just to the southwest of Guam and the other was centered near  $10^{\circ}\text{N}$ ,  $165^{\circ}\text{E}$ .

During the night of 8 September and throughout 9 September, the pre-Ed cloud cluster jogged northward and became better organized. On 10 September, the surface synoptic data and the motion and alignment of cumulonimbus elements seemed to indicate that the pre-Ed cloud cluster had properties similar to an easterly wave (Fig. 6.3). A Tropical Cyclone Formation Alert (TCFA) was issued at 00 UTC 10 September. The pre-Ed cloud cluster was upgraded to TD 19W at 12 UTC 10 September because the satellite cloud signature included a large cold-topped and centrally-located mesoscale convective system with well-defined curvature and symmetry in the cirrus outflow streamers. Visible satellite imagery during 11 September revealed low-cloud outflow arcs radiating from the central dense cloud mass. Rather large low-cloud velocity displacements can be detected well to the north and northeast of the center (Fig. 6.4) using this technique.

At 06 UTC 12 September, 19W was upgraded to Tropical Storm Ed based upon the continued evolution of the cloud system and synoptic data from the USSR ships along  $20^{\circ}\text{N}$ . During 13 September, TS Ed continued to move west and intensify at a normal rate (about one Dvorak "T" number per day). After Ed became a typhoon on 14 September, a small "donut-shaped" ring of convection formed an eye within the long and convoluted spiral bands (Fig. 6.5). The NASA DC-8 observed this eye feature on radar in a location about 90 n mi south of prior indications of the center based only on satellite imagery.

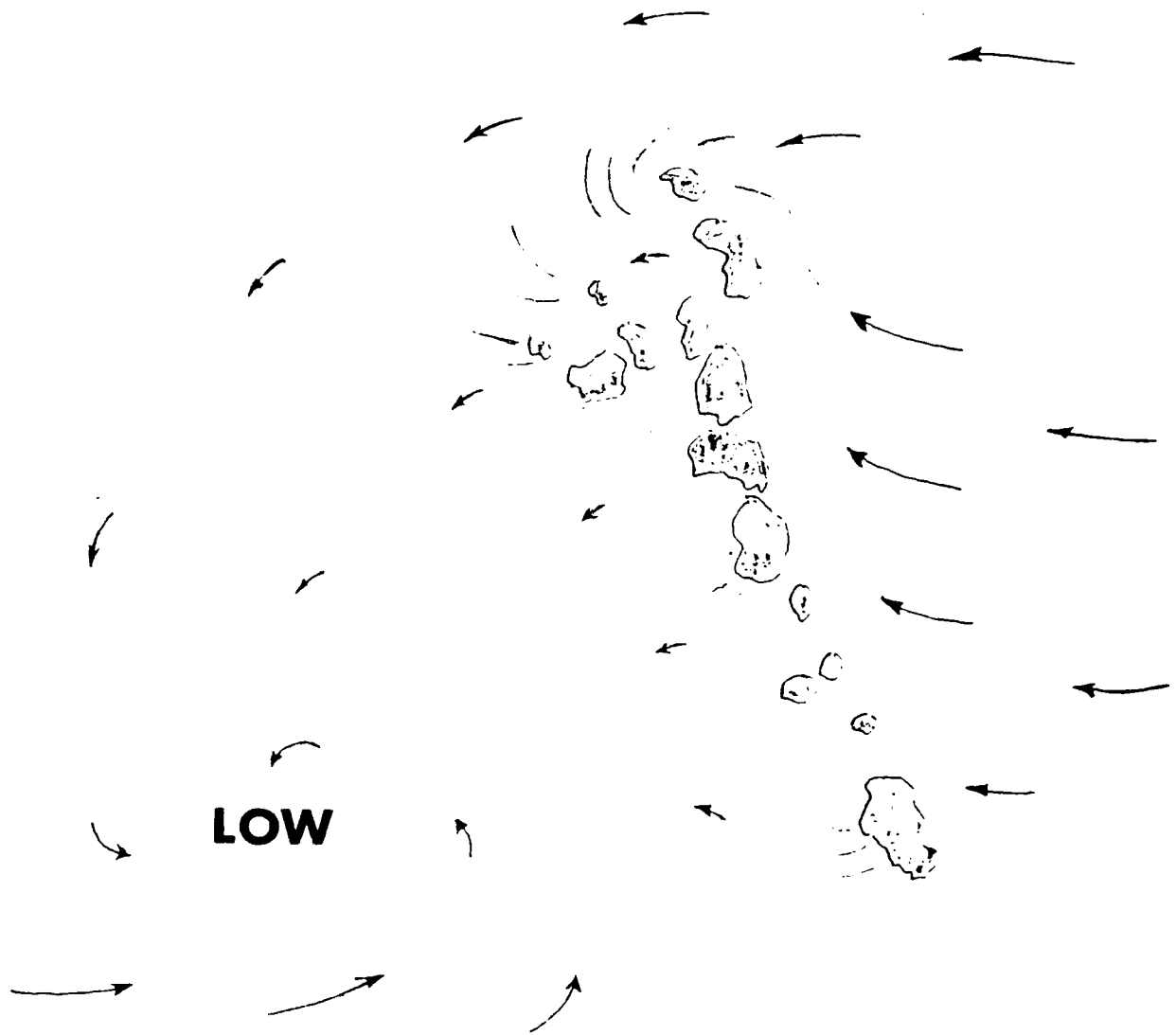


Figure 6.3 Schematic illustration of the wind flow (arrows) and Cb elements relative to the surface low pressure center in the early stages (10 September) of Typhoon Ed.

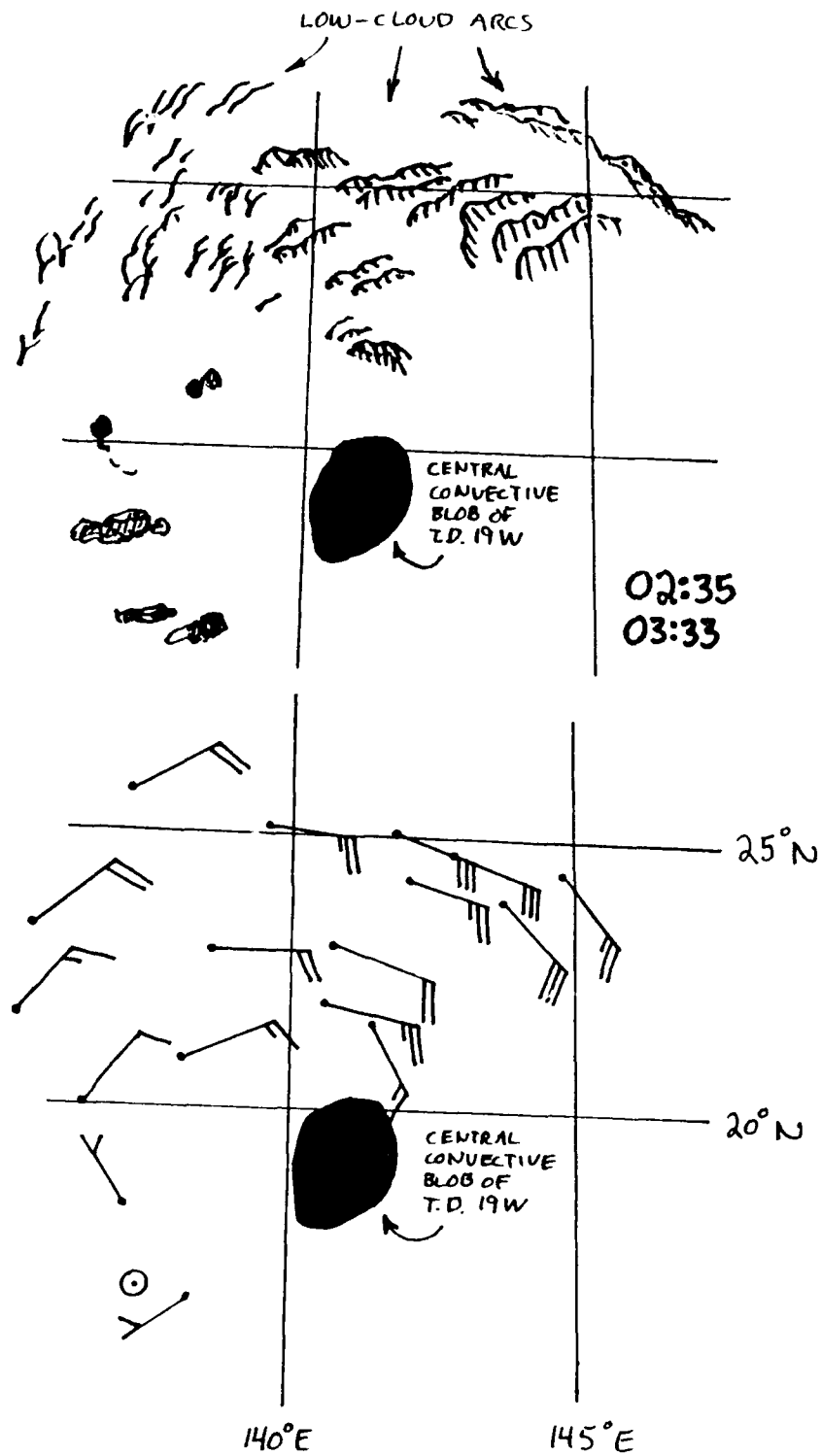


Figure 6.4 Low-level cloud arcs in visible satellite imagery on 11 September. Displacements of these arcs between images are an indication of the wind speeds.

For the rest of its life, Ed would remain a minimal typhoon. The peak intensity of 75 kt ( $37 \text{ m s}^{-1}$ ) was reached as Ed was in the middle of the South China Sea. The structural features that Ed possessed as it became a typhoon (long and convoluted spiral bands, a poorly defined banding eye and at times an independent "donut" eye) were present for most of the time that Ed was a typhoon.

### Movement

The initial motion of the disturbance that was to become Ed was toward the west and could be interpreted as the westward movement of a Rossby-gravity wave induced by an equatorial heat source (Fig. 6.2a). The northwestward track past Guam to  $20^{\circ}\text{N}$  can be attributed to Ed's orbit around the large monsoon trough. A sharp left turn occurred around 18 UTC 9 September (Fig. 6.1). The westward track along  $20^{\circ}\text{N}$  during 11 September was not a smooth translation. Rather, a large cumulonimbus cluster would erupt about every six hours near the center of the tropical depression. This cluster would remain nearly stationary for a few hours, and then a new cluster would erupt farther to the west as the previous cluster decayed. Consequently, the westward motion during this stage appeared to be the result of a sequential popping and decay of large cumulonimbus clusters to the west of the previous cluster. The speed of motion increased steadily from about 10 kt during 10 September to at least 16 kt on 13 September. During this period, Ed was accompanied by two synoptic-scale gyres. A cyclonic gyre to the south could be interpreted as an independent monsoon trough circulation. An anticyclonic gyre to the north appeared to be a westward extension of the subtropical ridge (Fig. 6.6). Both gyres may have been influenced by the storm circulation because the gyres moved westward as Ed moved westward. The westward building of the 500 mb ridge to the north of Ed is consistent with a TCM-90 hypothesis.

Ed's turn toward the southwest after 00 UTC 14 September was clearly depicted in the Bureau of Meteorology Research Centre (BMRC) barotropic model, and presumably was due to an interaction of Ed with the large-scale monsoon trough to the south. In the model, the southwestward turn of Ed into the South China Sea was accompanied by north-northeastward motion of the monsoon trough center, which gradually lost identity as Ed's circulation sheared it apart.

An apparent binary interaction of Ed with Flo might be inferred from 00 UTC 11 September until about 00 UTC 16 September. Ed and Flo seemed to orbit the midpoint between them at a fairly steady angular rate (Fig. 6.7a and 6.7b) at nearly a constant radius of 465 n mi. However, the 930 n mi separation distance is 210 n mi greater than the 720 n mi distance used operationally by the JTWC as the threshold for binary interaction. The alternate hypothesis is that the apparent

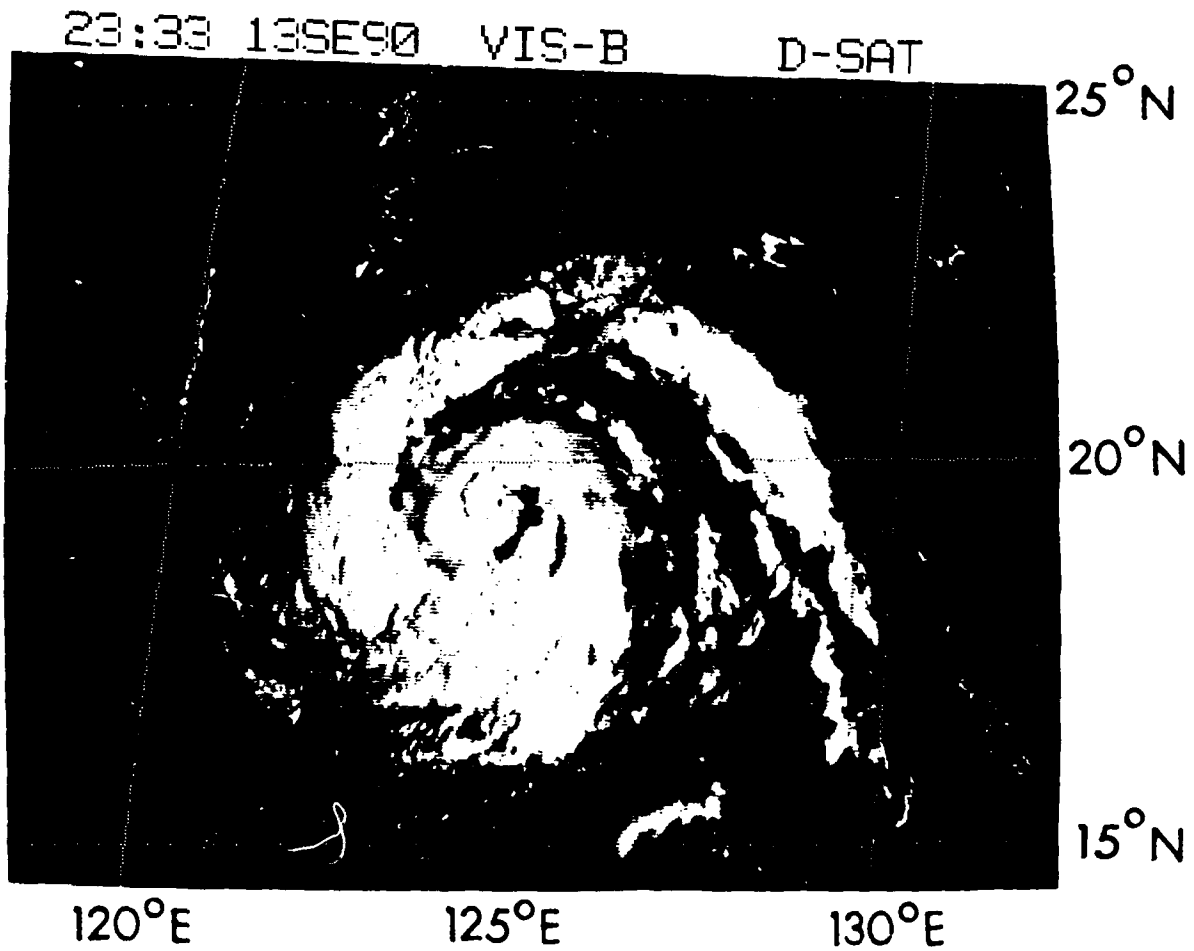


Figure 6.5 Visible satellite imagery at 2332 UTC 13 September with ragged banding around formative eye of Tropical Storm Ed.

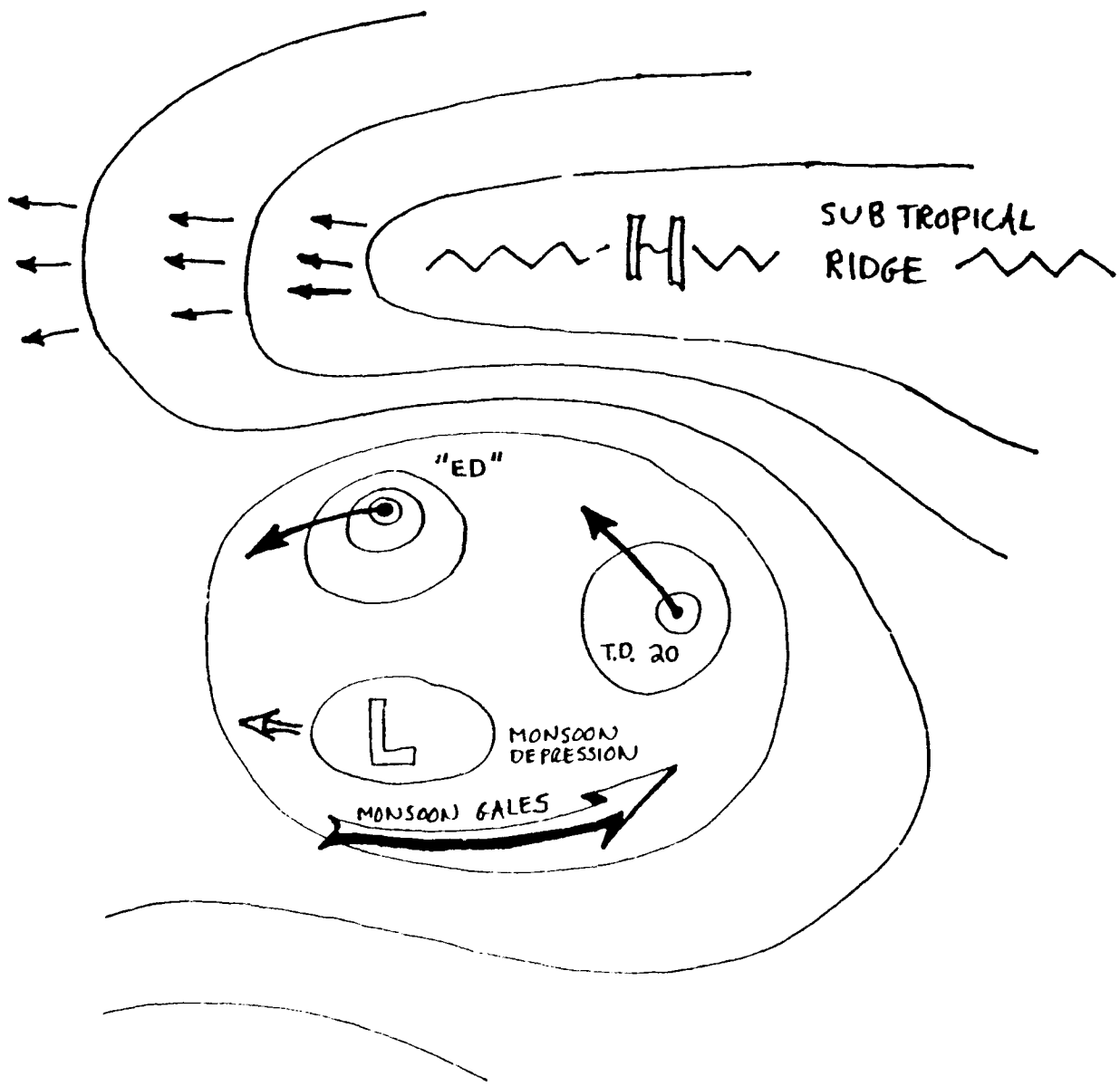


Figure 6.6 Schematic of surface pressure (thin lines) features when Typhoon Ed, TD 20 (pre-Flo) and a monsoon depression co-existed within a large monsoon trough with monsoon gales along the southern boundary (long arrow). The subtropical ridge (zig-zag line) extended to the west during this period.

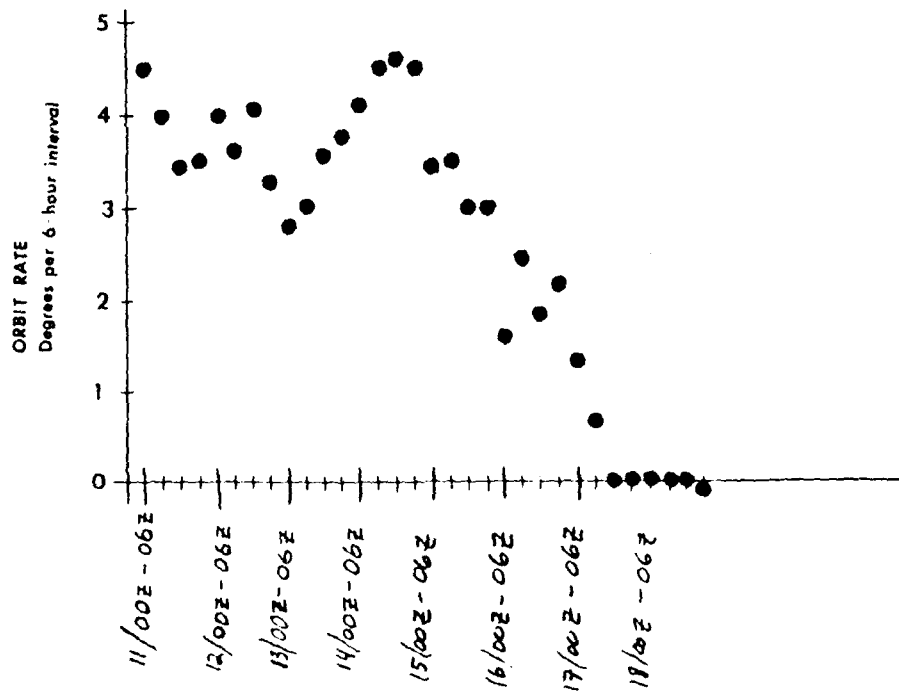
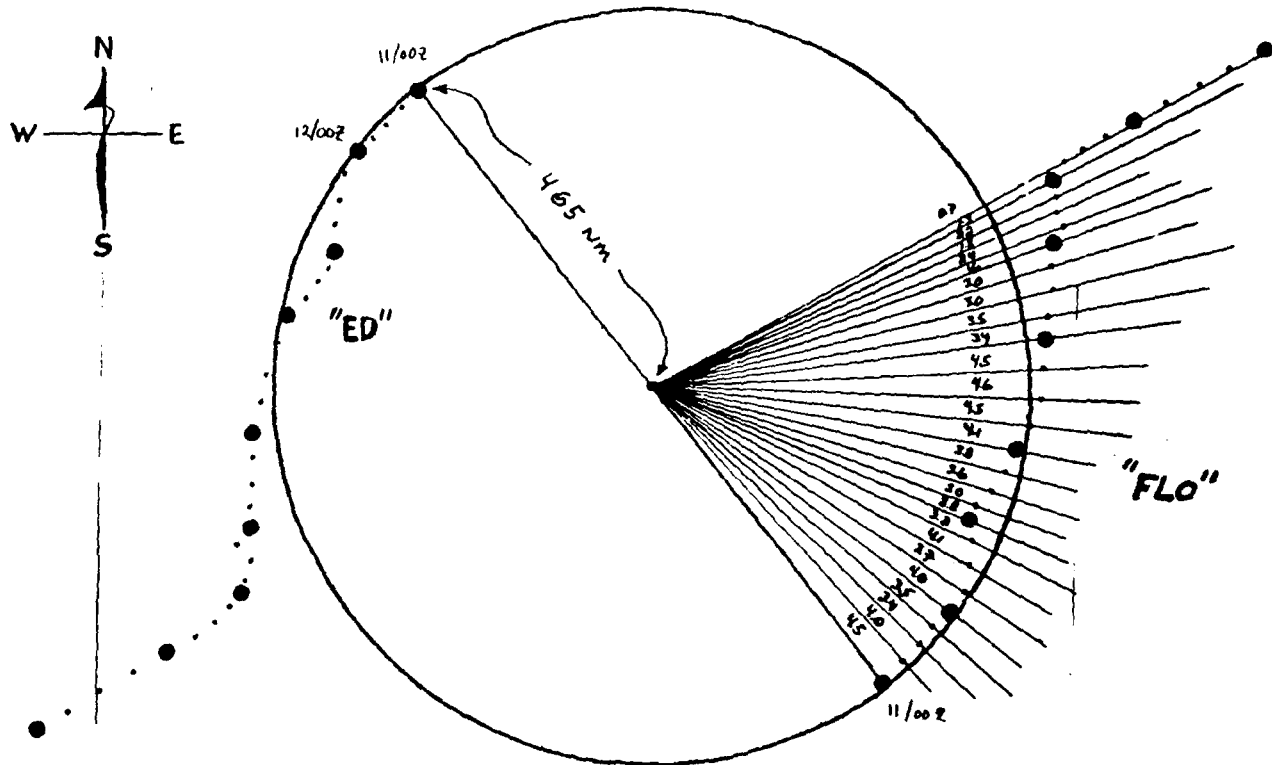


Figure 6.7 (a) Relative motion of tropical cyclones Ed and Flo with respect to the midpoint between the cyclones. Large dots indicate 00 UTC positions and small dots indicate intermediate 6-h intervals. (b) Orbital rate at rotation (degrees per h) with respect to the midpoint.

binary interaction of Flo and Ed was a result of the orbit of both Flo and Ed around the large monsoon trough. After 00 UTC 17 September, the motion of Ed with respect to Flo (Fig. 6.7a) apparently underwent a bifurcation (sudden change in the mode of behavior) or "escape" as the two storms abruptly ceased their mutual orbit and begin to move on diametrically opposed centroid-relative tracks. The alternative interpretation to this binary interaction interpretation is that the two systems were in proximity for a period when both were influenced by the monsoon trough circulation. As Flo became less influenced by this circulation, the apparent binary interaction ceased.

Another factor that may have influenced Ed's southwest motion in the South China Sea was a large high-pressure system over China. Surface pressures rose over mainland China to their highest values of the summer on 14 September following the passage of a migratory midlatitude trough through the region. Elevated geopotential heights also existed in the middle and upper troposphere, as expected with a "warm" high. As Ed approached China, a sharp pressure gradient was established along both the east and south coasts of China. As Ed began on 14 September to turn toward the southwest into the South China Sea (Fig. 6.1), strong (20 to 30 kt) northerly winds were found along the east coast of China from near Shanghai southward through the Taiwan strait. Based upon the forecasts that the mid- and upper-tropospheric geopotential heights over mainland China would remain high, it became increasingly certain that both Ed (and Flo) would not approach the China coast.

As Ed neared the coast of Vietnam on 18 September, it began to turn almost parallel to the coast (Fig. 6.1). Objective aids supported the official JTWC forecast that Ed would track northwestward along the coast. By contrast, the climatology for storms approaching Vietnam indicates that nearly all storms tend to cross the coast rather than parallel the coast.

During the next two days, Ed did indeed track northwestward along the coast of Vietnam while maintaining tropical storm intensity. Debate ensued over the relative contribution of the topography in this track compared to possible changes in the large-scale steering associated with the breakdown of high pressure over China as the midlatitude trough system approached from the northwest.

#### Hypotheses and Research Aspects

1. Interactions with Flo and with the monsoon trough. The motion of Ed around the large monsoon circulation, although not an objective in the original experiment design, seems to have been an important factor in the motion of both Ed and Flo. An investigation of the interactions that occurred, including an apparent orbit of Ed and Flo around a common center, could provide valuable information on the motion of tropical cyclones.



2. Large-scale gyres in the storm environment. One objective of the experiment was the detection of large-scale gyres that arise due to the gradient of absolute vorticity. Asymmetries in the environmental flow around Ed were highly suggestive of an anticyclonic gyre to the north and a cyclonic gyre to the south that tracked westward with Ed. Diagnostic studies should describe the mechanisms involved in the maintenance of these gyres and establish their effect upon the motion of Ed.

3. Interaction with the subtropical ridge. As Ed tracked westward, the subtropical ridge to the north seemed to build westward. Later, as Ed moved southwestward into the South China Sea, a large cell in the subtropical ridge intensified in situ over China. This cell may have played a role in Ed's motion. As with other cases of ridge interactions during TCM-90, the goal will be to determine how much of the changes in the subtropical ridge were induced by the tropical cyclone.

4. Interactions with orography. The study of Ed's motion along the coast of Vietnam must include the possible effects of orography. It is unclear whether Ed's turn to parallel the coast of Vietnam was induced by the terrain or whether it was a manifestation of changes in the large-scale circulation around Ed.

5. Speed changes. Changes of Ed's speed of motion contributed significantly to the JTWC forecast errors for this storm. Real-time integrations of the BMRC barotropic model indicated that the model grid spacing had a significant effect upon the predicted speed of motion. The data collected for Ed should lead to insights on the factors controlling speed of motion.

#### Data Coverage

Generally good upper-air coverage (Table 6.1) continued during IOP 5. Almost 100% of the ship observations were made. A DC-8 flight centered on 06 UTC 13 September found a well-defined radar eye considerably to the south of the expected location (see text above). Unfortunately, the aircraft sustained damage upon landing and was not available for a second flight into Ed.

No NOAA11 satellite imagery was received during this IOP due to McIDAS ingestor problems at the University of Wisconsin. Attempts to retrieve the lost imagery are in progress.

#### Satellite Soundings (# reports in 24 hrs)

	9/13	9/14
NOAA10	1655	1475
NOAA11	1414	1611
DMSP8	549	460
DMSP9	302	727

Satellite Winds (# vectors)

	9/13	9/14
00 UTC		180
06		165
12	160	169
18	136	

Satellite Imagery

9/13	9/14
All GMS	All GMS
	09 & 11 & 23 UTC NOAA10 passes
	09 & 11 UTC DMSP8 passes

Table 6.1 Upper air soundings during IOP 5.

*IOP-5, 90091300 - 90091412, TY ED*

NO.	STATION	0913				0914		
		00	06	12	18	00	06	12
BLOCK 45 (HONG KONG)								
1	45004	X	X	X	X	X	X	X
BLOCK 47 (KOREA)								
2	47122	X	X	X	X	X	X	X
3	47138	X	X	X	X	X	X	X
4	47158	X	X	X	X	X	X	X
5	47185	X	X	X	X	X	X	X
BLOCK 47 (JAPAN)								
6	47582	X	X	X	X	X	X	X
7	47590	X	X	X	X	X	X	X
8	47600	X	X	X	X	X	X	X
9	47678	X	X	X	X	X	X	X
10	47744	X	X	X	X	X	X	X
11	47778	X	X	X	X	X	X	X
12	47807	X	X	X	X	X	X	X
13	47827	X	X	X	X	X	X	X
14	47909	X	X	X	X	X	X	X
15	47918	X	X	X	X	X	X	X
16	47936	X	X	X	X	X	X	X
17	47945	X	X	X	X	X	X	X
18	47971	X	X	X		X	X	X
19	47991	X	X	X		X	X	X
BLOCKS 48,96 (THAILAND, MALAYSIA)								
20	48327	X	X	X	X	X	X	X
21	48407	X	X	X	X	X	X	X
22	48455	X	X	X	X	X	X	X
23	48568	X	X	X	X	X	X	X
24	48615	X	X	X	X	X		X
25	48648	X		X	X	X		X
26	96413	X	X	X	X	X	X	X
27	96471	X	X	X	X	X	X	X

IOP-5 (continued)

NO	STATION	0913				0914		
		00	06	12	18	00	06	12
BLOCKS 54, 57, 58, 59 (PEOPLES REPUBLIC OF CHINA)								
28	54857	X	X	X	X	X		X
29	57083	X	X	X	X	X	X	X
30	57494	X	X	X	X	X		X
31	57972	X	X	X	X	X		X
32	58150	X	X	X	X	X	X	X
33	58457	X	X	X	X	X	X	X
34	58847	X	X	X	X	X	X	X
35	59316	X	X	X	X	X	X	X
36	59758	X	X	X	X	X	X	X
37	59981	X	X	X	X	X		X
BLOCK 98 (PHILIPPINES)								
38	98223	X		X		X		
39	98327	X		X		X		X
40	98426				X		X	
41	98444	X	X	X	X	X	X	X
42	98646	X		X	X	X	X	
43	98753							
44	98851							
BLOCK 91 (PACIFIC ISLANDS, NATIONAL WEATHER SERVICE)								
45	91217	X	X	X		X	X	X
46	91232	X	X	X	X		X	X
47	91334	X		X	X	X	X	X
48	91348	X		X		X		X
49	91408	X		X		X		X
50	91413	X		X		X		X
BLOCK 47 (IWO JIMA)								
51	47000							
BLOCK 46 (TAIWAN)								
52	46692	X	X	X	X	X	X	X
53	46699	X		X		X		X
54	46734	X	X	X	X	X	X	X
55	46747	X		X		X		X
56	46759							
57	46780							
58	46810	X				X		
SHIPS								
1	FRFH	X	X	X	X		X	X
2	FRFF	X	X	X	X	X	X	X
3	UHOS	X	X	X	X	X	X	X
4	UMAY	X	X	X	X	X	X	X
5	IBOX	X	X	X	X	X	X	X
6	ICCX	X	X	X		X	X	X

Summary

Flo (20W) formed southeast of Guam and moved northwestward before recurving south of Japan (Fig. 7.1). The transition from an amorphous cloud mass to a system with cyclonic banding occurred very quickly during the morning of 12 September. Flo passed between Guam and Saipan before developing to tropical storm strength on 13 September. Typhoon strength was reached during 15 September and was followed by a period of rapid intensification to a maximum of about  $70 \text{ m s}^{-1}$  (140 kt) over the next 48 h as Flo approached Okinawa.

Translational speed during the northwestward track varied between  $6$  and  $8 \text{ m s}^{-1}$  (12-16 kt). Flo slowed appreciably to  $3-4 \text{ m s}^{-1}$  (6-8 kt) near recurvature. This slow speed was maintained for two days as Flo drifted northward and then northeastward before accelerating along the Japanese islands ahead of a strong midlatitude trough.

The major features of interest to the experiment were: the initial rapid development and apparent movement around a pre-existing monsoonal depression, as was occurring with Typhoon Ed; and a complex interaction near recurvature between Flo, the subtropical ridge, a developing midlatitude trough, and a deep, intense TUTT cell. Including IOP 5 for Typhoon Ed, five days of nearly continuous IOP data were collected from 13-19 September. Upper-tropospheric missions through and surrounding the supertyphoon also were accomplished by the NASA DC-8 over three consecutive days during recurvature.

Formation

Flo appeared to be the last of a series of typhoons that formed during the disturbed phase of a distinct 30-50 day oscillation. The low-level circulation (Fig. 7.2a) had originally formed as part of a twin vortex pair straddling the equator. In the upper troposphere (Fig. 7.2b), the cluster that was to become Flo was sheared by northeasterly flow around a strong TUTT cell. In the early stages, the surface circulation seemed to lag eastward of the main convective region and at least one redevelopment westward was observed.

The development of Flo to tropical depression stage was rapid and surprising. During the 12 h prior to 06 UTC 12 September, the convective signature changed from an active, but disorganized cluster, to a spiral banded structure and markedly divergent flow over the surface center. Serial soundings were obtained by the radar wind profiler and the radiosonde system at Saipan as Flo passed during 12-13 September. These indicated that Flo was a well-developed, small, warm-cored system at the eastern edge of the large monsoonal circulation and had maximum

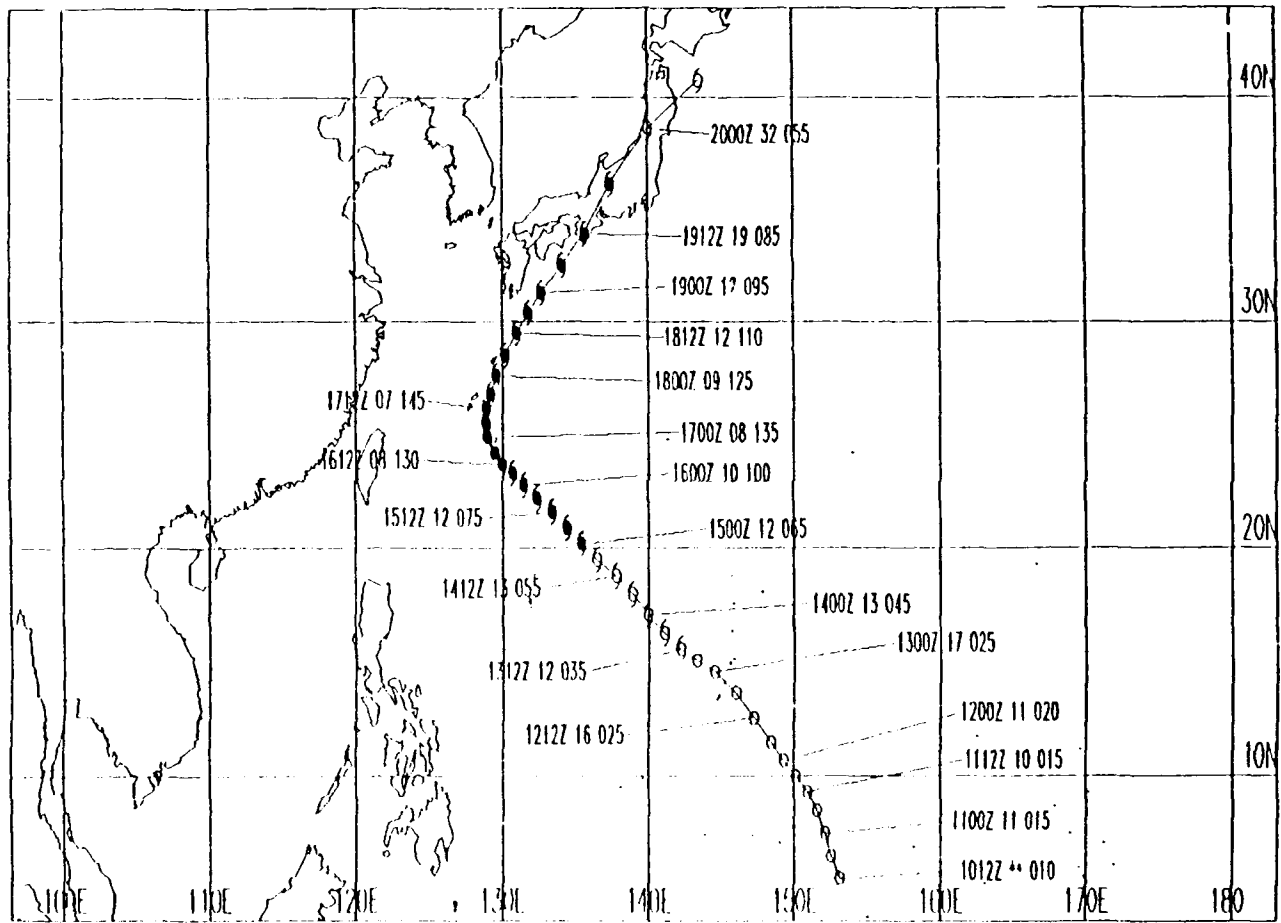


Figure 7.1 Working best track of Supertyphoon Flo between 12 UTC 10 September and 06 UTC 20 September. Symbols are the same as in Fig. 2.1.

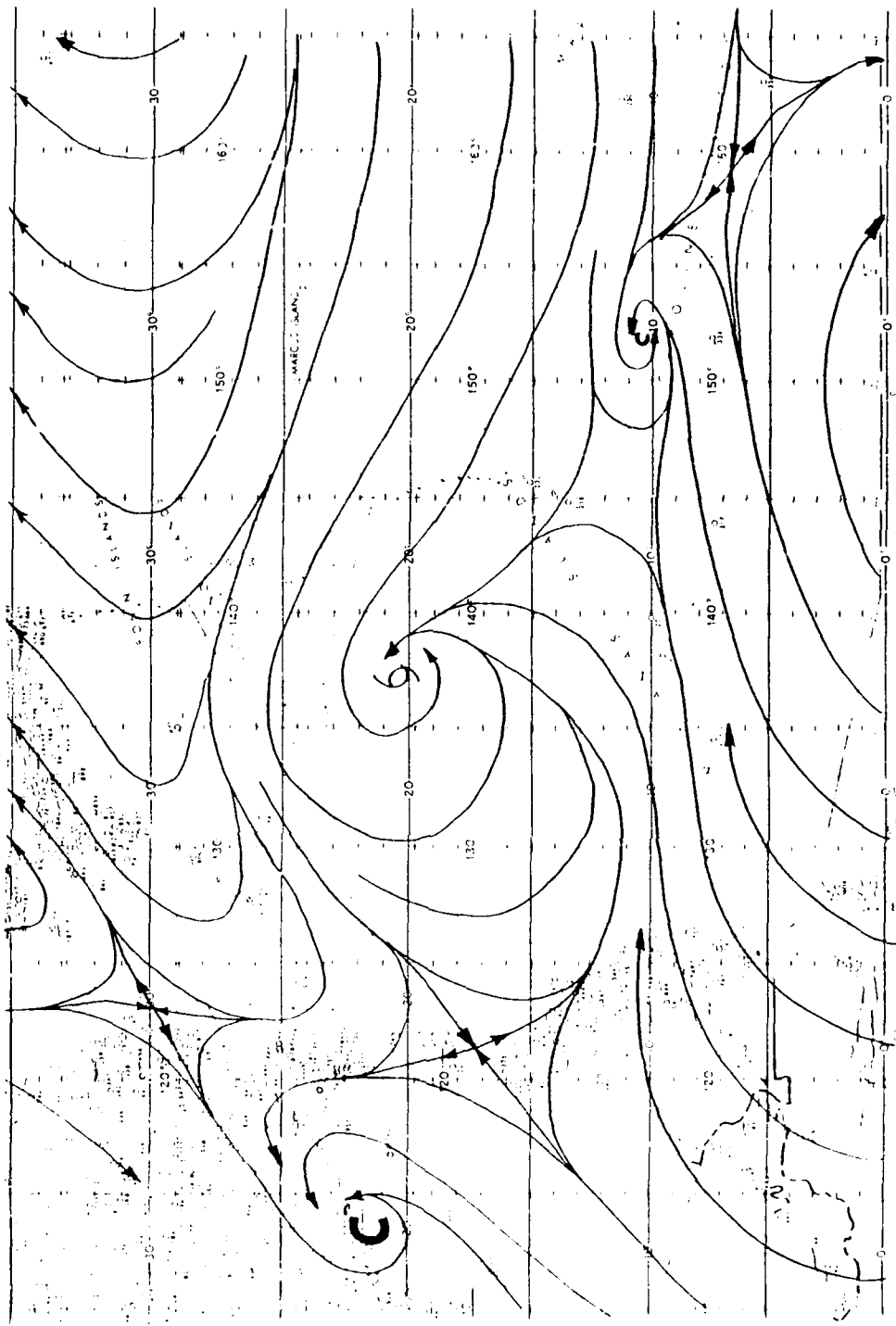


Figure 7.2a Streamline analyses for 00 UTC 12 September at the gradient level. Winds of greater than  $15 \text{ ms}^{-1}$  are stippled.

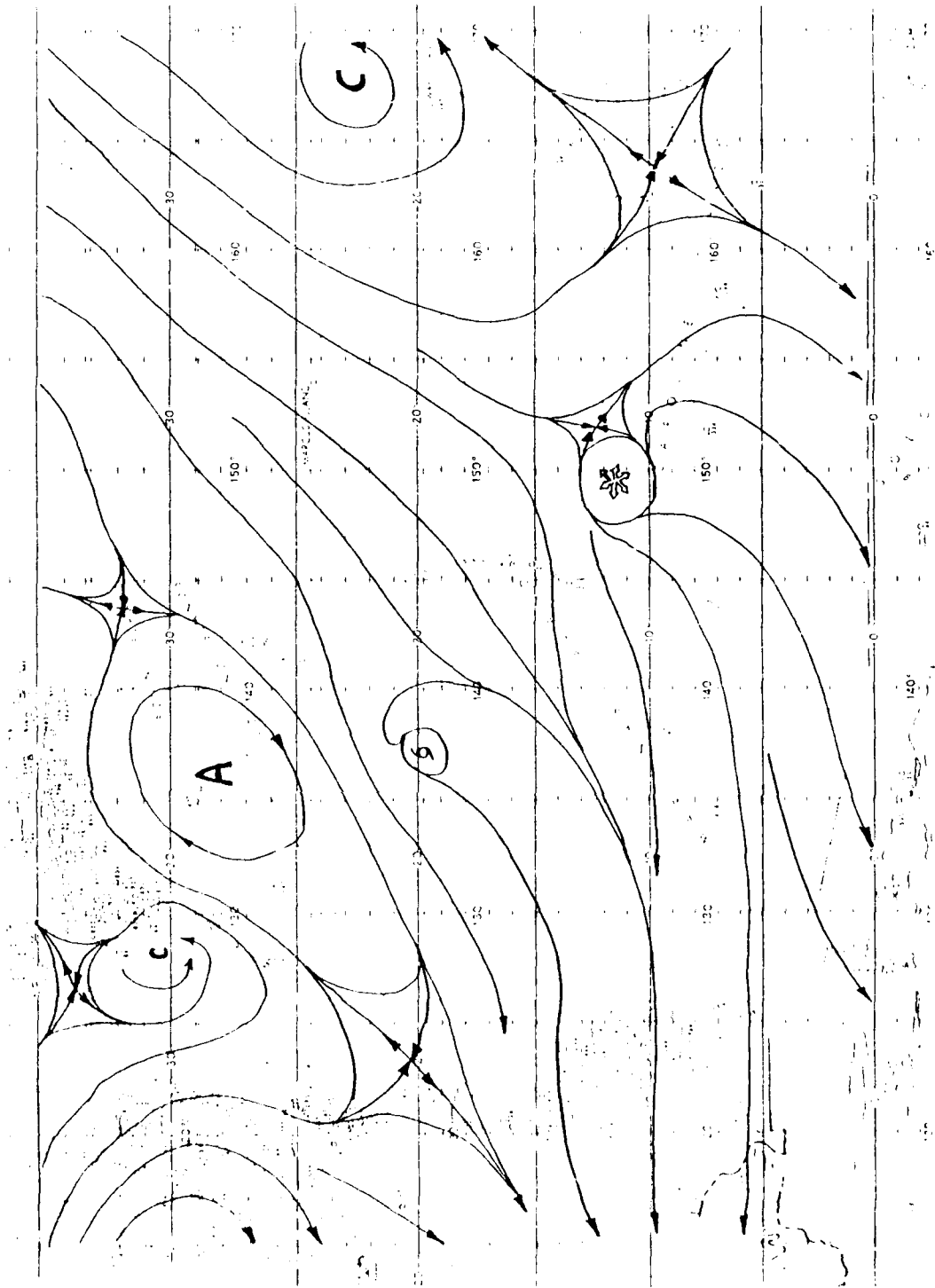


Figure 7.2b Streamline analysis for 00 UTC 12 September at 200 mb.



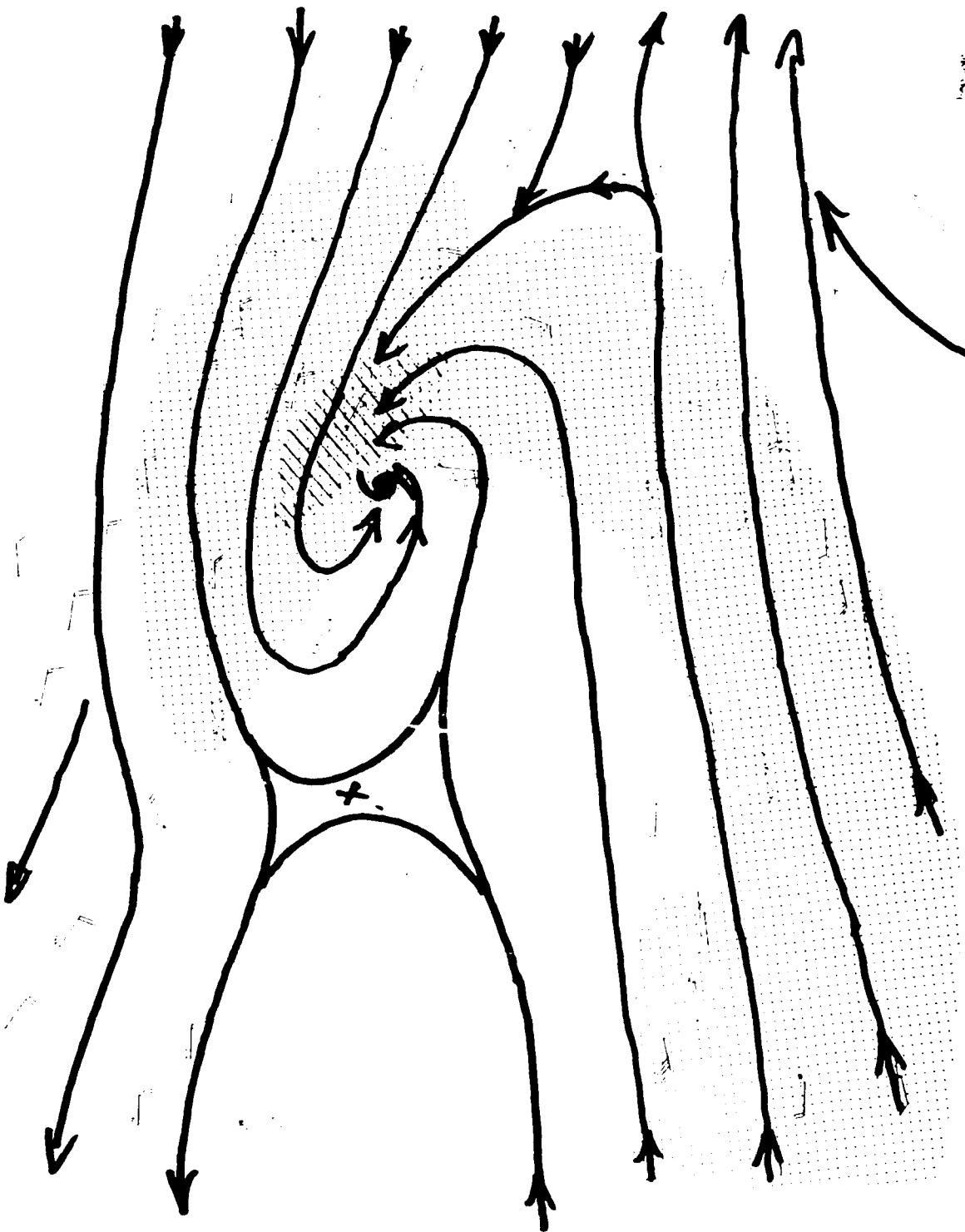


Figure 7.3 Composite analysis for the 36 h beginning at 12 UTC 13 September. Gradient-level winds greater than  $15 \text{ m s}^{-1}$  are stippled and those greater than  $25 \text{ m s}^{-1}$  are hatched.

winds near  $30 \text{ m s}^{-1}$  (60 kt) at 900 mb. However, maximum observed surface winds remained below  $15 \text{ m s}^{-1}$  (30 kt).

Surface and gradient-level winds composited during the 24 h period beginning 12 UTC 12 September (Fig. 7.3) indicate that Flo developed in the shear zone between strong trade easterlies and monsoon westerlies. As with many previous cyclones during TCM-90, the belt of strong monsoon westerlies was well removed from the cyclone core. Analysis of the serial soundings at Saipan indicated that these westerlies hooked around the eastern edge of Flo and ascended to produce a distinct mid-level southerly jet.

### Development

Flo was estimated to reach tropical storm strength at the surface near 12 UTC 13 September. Steady intensification to typhoon strength then followed over the next 36 h. During this time, the cyclone separated from the convection associated with the monsoon westerlies. The TUTT cell (Fig. 7.2b) migrated westward, then orbited to the southwestern flank of the cyclone before decaying. Rapid intensification to supertyphoon strength commenced during the evening of 15 September. This was associated with outflow jets into the midlatitude westerlies, toward a new TUTT cell that was moving westward relative to Flo, and to the southeast.

At the time of maximum intensity (Fig. 7.4a), Flo was a medium-sized typhoon that was well removed from the monsoonal westerlies. In the upper troposphere (Fig. 7.4b), the outflow into the TUTT had ceased (at least at 200 mb), and strong ridging was occurring to the northeast of Flo. The geostationary satellite imagery for 2332 UTC 16 September indicated a classical supertyphoon signature with a clear eye surrounded by a central dense overcast and some spiral bands. Flo was quite close to the developing midlatitude trough at this stage and was connecting to a baroclinic cloud mass over the Japanese islands.

The second DC-8 mission centered around 06 UTC 17 September recorded an uncorrected central pressure of 891 mb from a dropwindsonde and  $55 \text{ m s}^{-1}$  (113 kt) winds at the 190 mb level. Observations from this mission were used to analyze the detailed outflow pattern in Fig. 7.4b. The intense cyclonic flow around the typhoon core had very little direct outflow in evidence. Outflow commenced sharply 300-500 km from the center and an anticyclonic eddy was detected to the southeast.

A rapid decay during 17 September seemed to be associated with development of a new convective ring outside the center followed by a collapse of the eyewall. A DC-8 mission on 18 September observed a pair of convective rings 45 and 55 km from the typhoon center with a crescent-shaped partial eyewall surrounding a tiny eye. Flo remained a major typhoon at landfall on Honshu but then quickly became extratropical.

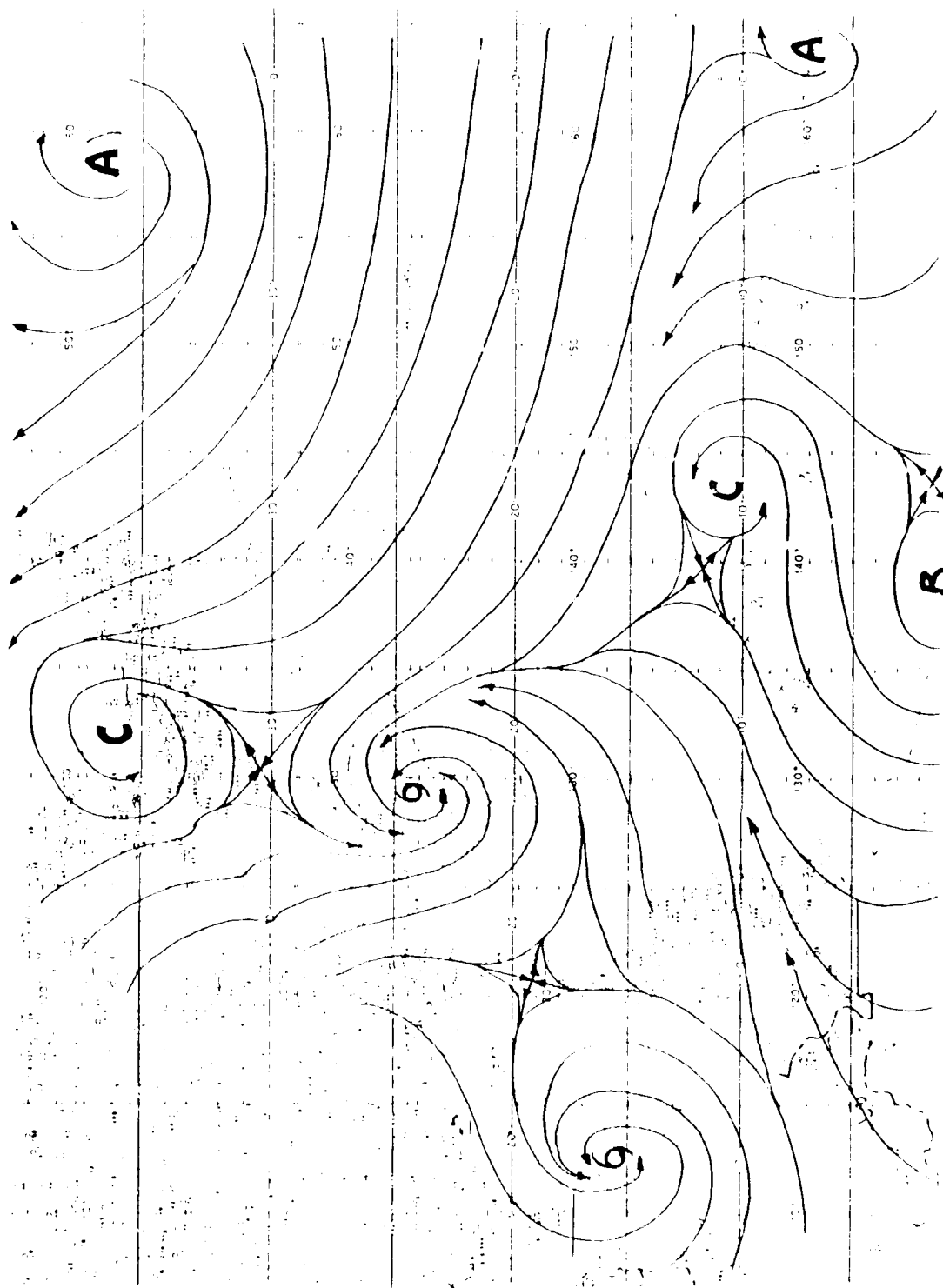


Figure 7.4 Streamline analyses for 00 UTC 17 September at the gradient level. Winds of greater than  $15 \text{ m s}^{-1}$  are stippled.

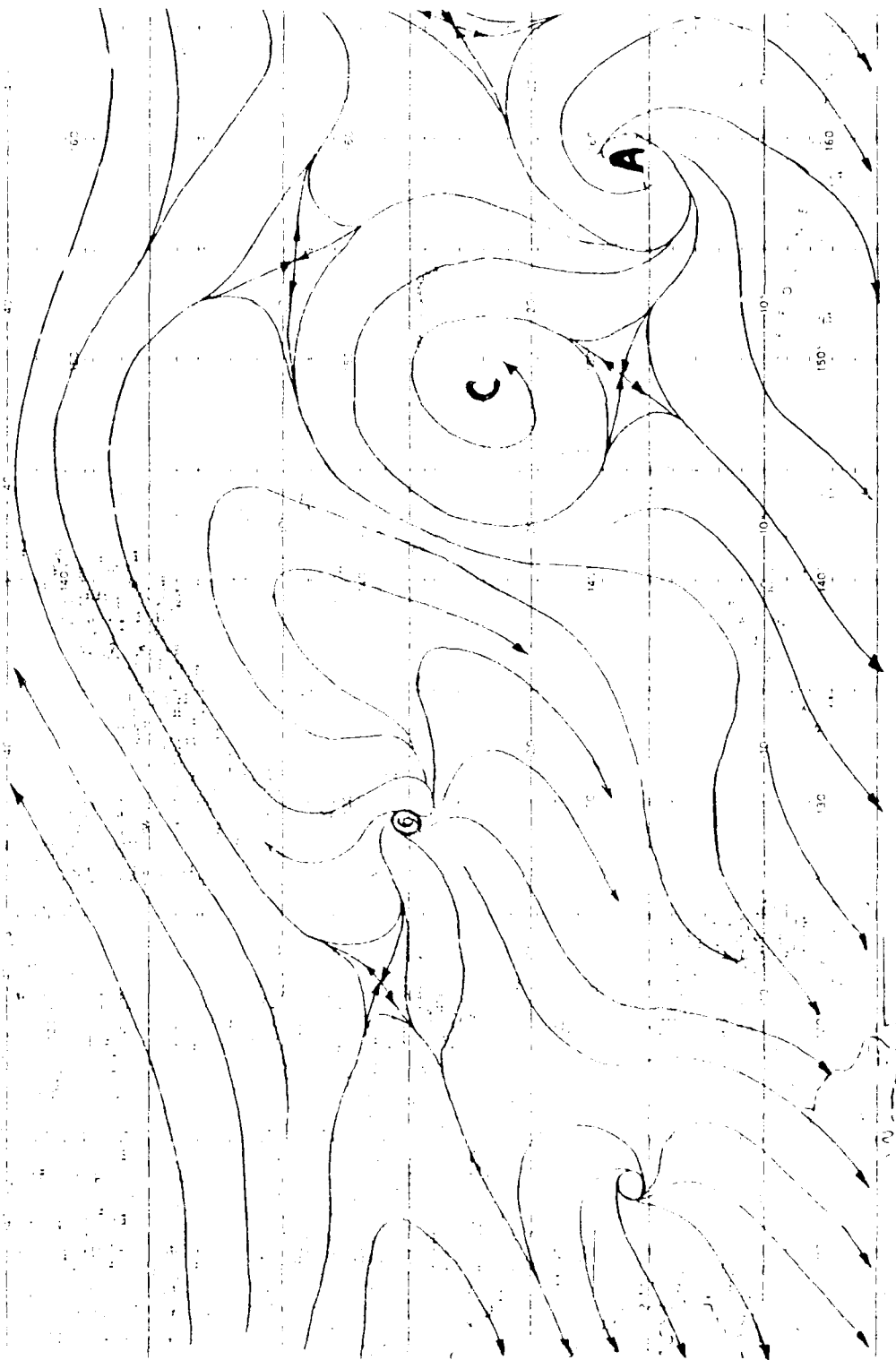


Figure 7.4b Streamline analysis for 00 UTC 17 September at 200 mb.

## Movement

The initial motion of the weak depression that was to become Flo occurred as a sequence of redevelopments toward the convective cluster on its westward side. The northwestward track past Guam and up to 20°N can be attributed to Flo moving around the large monsoonal trough (Fig. 6.6), which also contributed to the westward and southwestward motion of Typhoon Ed. A distinct anticyclonic gyre that is analogous to the gyres in barotropic modelling studies also developed on the east side of Flo in the lower and middle troposphere. The monsoon system appeared to collapse as Flo moved past 20°N and a northwestward track was maintained.

Several interesting, but poorly understood, interactions seemed to contribute to the cyclone movement near the recurvature point. A short wave developed in the midlatitude westerlies (Fig. 7.4b). At the same time, a strong, meridional ridge developed to the east, perhaps due to interactions with the typhoon. Some of the forecast aids indicated that Flo should have been captured and accelerated to the northeast. However, the typhoon maintained a slow northward and northeastward drift, which was consistent with the predictions from several numerical models. Two interactions may have caused this slow recurving motion. The large and intense TUTT cell east of Flo (Fig. 7.4) extended to the surface and moved westward into close proximity with Flo near the recurvature time. The cyclonic circulation around this TUTT cell may have countered the advection by the midlatitude trough. Further, the relative vorticity gradient was oriented from a marked band of anticyclonic vorticity between Flo and the jet axis around the midlatitude trough to the cyclonic vorticity associated with the TUTT cell. Thus, the typhoon propagation associated with this relative vorticity gradient would have a component towards the TUTT cell. On 18 September, this TUTT cell came under the horizontal shearing influence of Flo and rapidly distorted to the north and weakened. Flo then accelerated to the northeast.

## Hypotheses and Research Aspects

1. Interactions with the monsoon circulation. The early motion around the large monsoon circulation was not a hypothesis in the original experimental design. However, the monsoon trough does seem have been an important factor in the motion of both Ed and Flo and appears to be a common process in the western North Pacific region. An investigation of the interactions that occurred, including the development of the anticyclonic gyre to the east and the subsequent collapse of the monsoon system, could provide valuable information on the motion of tropical cyclones in these conditions.

2. Development of the meridional subtropical ridge. The high amplitude meridional ridge that developed while Flo was near recurvature seems to have been associated with the cyclone outflow. Such a ridge interaction was one of the experiment hypotheses and further research could provide further insights into the detailed interactions involved.

3. Interaction between Flo, the midlatitude trough and the TUTT cell. These interactions were the most puzzling and interesting feature of Flo's movement. Although TUTT interaction is one of the experiment hypotheses, the reality was far more complicated than originally thought. This case involved a very large and deep TUTT cell that approached from the southeast and was absorbed into the circulation of Flo. The excellent combination of synoptic and aircraft data provides a unique opportunity for further investigation of the underlying processes.

#### Data Coverage

The upper-air soundings for IOP 6 and IOP 7 are summarized in Tables 7.1 and 7.2 respectively. These IOP's are nearly continuous as only the 18 UTC 16 September soundings were omitted. Similarly, IOP 6 follows directly IOP 5 with only the 18 UTC 14 September soundings omitted. Meanwhile, the SPECTRUM IOP began at the same time as IOP 5 and was continuous for five days until 00 UTC 18 August. Thus, the SPECTRUM stations will be missing on 06 UTC and 18 UTC 18 September. The exceptions are the stations in southern Japan that were being threatened by Supertyphoon Flo during this period. Unfortunately, the JMA ships departed during IOP 6 at the end of their regularly scheduled deployments.

As indicated above, three DC-8 flights were made into Flo on 16, 17 and 18 September. Both the flight-level data and the dropwindsondes make this case an outstanding opportunity for research.

As in IOP 5, the NOAA11 imaging was missed during IOP 6.

#### Satellite Soundings (# reports in 24 h)

	9/15	9/16
NOAA10	1486	1406
NOAA11	1538	1784
DMSP8	592	597
DMSP9	685	661

Satellite Winds (# vectors)

	9/15	9/16
00 UTC	182	142
06	131	202
12	127	
18	130	

Satellite Imagery

9/15	9/16
All GMS 11 UTC NOAA10 pass	All GMS 10 & 12 & 23 UTC NOAA passes 10 & 22 UTC DMSP8 passes

The NOAA11 imagery was resumed on 18 September. Unfortunately, the polar orbiter imagery on 17-18 September includes Flo but not Typhoon Ed along the coast of Vietnam.

Satellite Soundings (# reports in 24 h)

	9/17	9/18
NOAA10	1542	1980
NOAA11	1689	1700
DMSP8	595	446
DMSP9	538	519

Satellite Winds (# vectors)

	9/17	9/18	9/19
00 UTC	139	169	162
06	170	171	
12	130	111	
18	109	085	

Satellite Imagery

9/17	9/18
All GMS 10 & 22 UTC NOAA10 passes 10 & 21 UTC DMSP8 passes	All GMS 06 & 18 UTC NOAA passes 10 UTC DMSP8 pass

Table 7.1 Upper-air soundings during IOP 6.

*IOP-6, 90091500 - 90091612, TY ED, STY FLO*

NO	STATION	0915				0916		
		00	06	12	18	00	06	12
BLOCK 45 (HONG KONG)								
1	45004	X	X	X	X	X	X	X
BLOCK 47 (KOREA)								
2	47122	X	X	X	X	X	X	X
3	47138	X	X	X	X	X	X	X
4	47158	X	X	X	X	X	X	X
5	47185	X	X	X	X	X	X	X
BLOCK 47 (JAPAN)								
6	47582	X	X	X	X	X	X	X
7	47590	X	X	X	X	X	X	X
8	47600	X	X	X	X	X	X	X
9	47678	X	X	X	X	X	X	X
10	47744	X	X	X	X	X	X	X
11	47778	X	X	X	X	X	X	X
12	47807	X	X	X	X	X	X	X
13	47827	X	X	X	X	X	X	X
14	47909	X	X	X	X	X	X	X
15	47918	X	X	X	X	X	X	X
16	47936	X	X	X	X	X	X	X
17	47945	X	X	X	X	X	X	X
18	47971	X		X		X	X	X
19	47991	X		X		X	X	
BLOCKS 48,96 (HEMILAND, MALAYSIA)								
20	48327	X	X	X	X	X	X	X
21	48407	X	X	X	X	X	X	X
22	48435	X	X	X	X	X	X	X
23	48568	X		X		X		X
24	48647	X	X	X		X	X	X
25	48643	X		X	X	X		X
26	96413	X			X	X	X	X
27	96471	X	X	X		X	X	X



Table 7.1 Upper-air soundings during IOP 6 (continued).

NO.	STATION	0915				0916		
		00	06	12	18	00	06	12
BLOCKS 51,57,58,59 (PEOPLES REPUBLIC OF CHINA)								
28	54857	X	X	X	X	X		X
29	57083	X	X	X		X	X	X
30	57494	X	X	X		X		X
31	57972	X	X	X		X	X	X
32	58150	X	X	X	X	X	X	X
33	58457	X	X	X	X	X	X	X
34	58847	X	X	X	X	X	X	X
35	59316	X	X	X	X	X	X	X
36	59758	X	X	X	X	X	X	X
37	59981	X	X	X		X		X
BLOCK 98 (PHILIPPINES)								
38	98223			X				
39	98327	X		X		X		X
40	98426		X	X			X	
41	98444	X	X	X	X	X	X	X
42	98646	X	X	X	X	X	X	X
43	98753							
44	98851							
BLOCK 91 (PACIFIC ISLANDS, NATIONAL WEATHER SERVICE)								
45	91217	X	X	X	X	X	X	X
46	91232	X	X	X	X	X	X	X
47	91334	X		X	X	X	X	X
48	91348	X		X		X		X
49	91408	X		X	X	X	X	X
50	91413	X		X		X	X	X
BLOCK 47 (TWO JIMA)								
51	47000							
BLOCK 46 (TAIWAN)								
52	46692	X	X	X	X	X		X
53	46699	X		X		X		X
54	46734	X	X	X	X	X	X	X
55	46747	X		X		X		X
56	46759							
57	46780							
58	46810		X			X		
SHIPS								
1	ERTH	X	X	X	X	X	X	X
2	ERTH	X	X	X	X	X	X	X
3	UHOS	X		X	X	X	X	X
4	UMAY	X		X	X	X	X	X
5	IBOX	X	X	X	X	X		
6	JCCX	X	X	X				

Table 7.2 Upper-air soundings during IOP 7.

*IOP-7, 90091700 - 90091900, TY ED, STY FLO*

NO	STATION	0917				0918				0919
		00	06	12	18	00	06	12	18	00
BLOCK 45 (HONG KONG)										
1	48004	X	X	X	X	X	X	X	X	X
BLOCK 47 (KOREA)										
2	47122	X	X	X	X	X	X	X	X	X
3	47138	X	X	X	X	X		X		X
4	47158	X	X	X	X	X		X		X
5	47185	X	X	X	X	X		X		X
BLOCK 47 (JAPAN)										
6	47582	X	X	X	X	X	X	X	X	X
7	47590	X	X	X	X	X	X	X	X	X
8	47600	X	X	X	X	X	X	X	X	X
9	47678	X	X	X	X	X	X	X	X	X
10	47744	X	X	X	X	X	X	X	X	X
11	47778	X	X	X	X	X	X	X	X	X
12	47807	X	X	X	X	X	X	X	X	X
13	47827	X	X	X	X	X	X	X	X	X
14	47909	X	X	X	X	X	X	X		X
15	47918	X	X	X	X	X		X		X
16	47936	X		X	X	X		X		X
17	47945	X	X	X	X	X		X		X
18	47971	X	X	X		X		X		X
19	47991	X	X	X		X		X		X
BLOCKS 48,96 (HAINAN, MALAYSIA)										
20	48327	X	X	X	X	X	X	X	X	X
21	48407	X	X	X	X	X	X	X	X	X
22	48455	X	X	X	X	X	X	X	X	X
23	48568	X	X	X	X	X	X	X	X	X
24	48615	X		X	X	X	X	X		X
25	48648	X		X	X	X		X		X
26	96413	X		X	X	X				X
27	96471	X		X	X	X		X		X

Table 7.2 Upper-air soundings during IOP 7 (continued).

NO.	STATION	0917				0918				0919
		00	06	12	18	00	06	12	18	00
BLOCKS 54,57,58,59 (PEOPLES REPUBLIC OF CHINA)										
28	54857	X	X	X	X	X	X	X	X	X
29	57083	X	X	X	X	X	X	X	X	X
30	57494	X	X	X	X	X	X	X	X	X
31	57972	X	X	X	X	X	X	X	X	X
32	58150	X	X	X	X	X	X	X	X	X
33	58457	X	X	X	X	X	X	X	X	X
34	58847		X	X	X	X	X	X	X	X
35	59316	X	X	X	X	X	X	X	X	X
36	59758	X	X	X	X	X	X	X	X	X
37	59981								X	X
BLOCK 98 (PHILIPPINES)										
38	98223					X				
39	98327	X		X		X				X
40	98426				X		X		X	
41	98444	X	X	X	X	X	X	X		X
42	98646	X	X	X						
43	98753									
44	98851									
BLOCK 91 (PACIFIC ISLANDS, NATIONAL WEATHER SERVICE)										
45	91217	X	X	X	X	X	X	X	X	X
46	91232	X	X	X		X		X		X
47	91334	X	X	X	X	X	X	X	X	X
48	91348	X		X		X		X	X	X
49	91408	X		X	X	X	X	X	X	X
50	91413	X	X	X	X	X	X	X	X	X
BLOCK 47 (IWO JIMA)										
51	47000									X
BLOCK 46 (TAIWAN)										
52	46692	X	X	X	X	X	X	X	X	X
53	46699			X		X		X		X
54	46734	X	X	X		X	X	X	X	X
55	46747	X								
56	46759									
57	46780									
58	46810	X					X			
SHIPS										
1	FRFH	X	X	X	X	X	X	X	X	X
2	FRFT	X	X	X	X	X		X	X	X
3	UHOS	X	X	X	X	X		X		X
4	UMAY	X	X		X	X	X	X	X	X
5	HBOA									
6	JCCN									

## References

- Elsberry, R. L., 1989a: ONR Tropical Cyclone Motion Research Initiative: Field Experiment Planning Workshop. Technical Report NPS-63-89-002, Naval Postgraduate School, Monterey, CA 93943, 79 pp.
- Elsberry, R. L., 1989b: ONR Tropical Cyclone Motion Research Initiative: Data assimilation considerations for field experiment analysis. Technical Report NPS-63-89-006, Naval Postgraduate School, Monterey, CA 93943, 64 pp.
- Elsberry, R. L., 1990: International experiments to study tropical cyclones in the western North Pacific. Bull. Amer. Meteor. Soc., 71, 1305-1316.

Distribution List

	No. of Copies
Office of Naval Research (Code 1122MM) 800 North Quincy Street Arlington, VA 22217	1
Dr. Robert L. Haney (Code MR/Hy) Chairman, Department of Meteorology Naval Postgraduate School Monterey, CA 93943-5000	1
Dr. Russell L. Elsberry (Code MR/Es) Department of Meteorology Naval Postgraduate School Monterey, CA 93943-5000	175
Library (Code 0142) Naval Postgraduate School Monterey, CA 93943-5000	2
Research Administration (Code 012) Naval Postgraduate School Monterey, CA 93943-5000	1
Defense Technical Information Center Cameron Station Alexandria, VA 22304-6145	2